MAGNETIC AND STRUCTURAL STUDIES ON SOME d^3 TRANSITIONAL ELEMENT HALIDE COMPLEXES

by

Ian Edward Grey, B.Sc.(Hons.)

Submitted in fulfilment of the requirements
for the
Degree of Doctor of Philosophy

University of Tasmania
Hobart

June, 1969.

This thesis is dedicated

to my parents.

ABSTRACT

In this thesis the results of a study of the magnetic interactions in series of polynuclear complexes of chromium(III), molybdenum(III), and vanadium(II) are reported. These comprise series of compounds of formula $A_3M_2X_9$ (M = Cr(III), Mo(III); X = Cl, Br; A = univalent cation) containing binuclear $[M_2X_9]^{3-}$ entities and the compounds AVX_3 (X = Cl, Br) containing infinite linear chains $(-VX_3-)_n^{1-}$.

Particular emphasis has been placed on the relationship between magnetic properties and the structure of the compounds. In this connection a survey has been made of previous investigations of magnetic interactions in polynuclear transition element complexes. It is evident that there is the need for a study of the variation of magnetic interactions in series of simple polynuclear complexes of closely related structures.

From single crystal and powder x-ray diffraction studies carried out on the $A_3M_2X_9$ system it has been determined that change of the size of cation A results in a change in the metal-metal separation in the binuclear anion. From a combination of the x-ray structural data and magnetic susceptibility measurements the variation of magnetic exchange with change of metal-metal distance has been determined.

Detailed correlations have also been made between the magnetic properties and the proposed structures for the vanadium complexes. The magnetic data on the compounds of formula AVX_3 is consistent with a structural model which involves pairing of vanadium atoms along an infinite chain.

For all the compounds studied it has been possible to obtain useful information on the contributions of the different mechanisms for exchange by a comparison of the magnetic properties of related chloride and bromide complexes. It is concluded that in the molybdenum binuclear compounds, the dominant mechanism for spin-spin coupling is direct exchange between the molybdenum atoms. The various superexchange effects via the bridging halogens contribute no more than 10% of the total exchange. The relative contributions of the ferro- and antiferromagnetic superexchange mechanisms are very dependent on the structure of the binuclear anion. The magnetic interactions in the corresponding chromium complexes are weaker than in their molybdenum analogues by a factor of fifty. The magnetic properties of the vanadium(II) compounds are similar to those of the molybdenum binuclear complexes. In the former compounds, however, the superexchange via the bridging ligands forms a greater contribution to the total exchange. This is attributed to the shorter metal-ligand bonds in the AVX_3 compounds.

To the best of my knowledge and belief, this thesis contains no material which has been accepted for the award of any other degree or diploma in any University and contains no copy or paraphrase of material previously published or written by another person, except where due reference is made in the text.

Acknowledgements

It is a pleasure to acknowledge the guidance and supervision of Dr. P.W. Smith who at all times has been very helpful and encouraging.

Thanks are due to Dr. A.F. Reid and Dr. D.E. Scaife of CSIRO, for permission to use the far infrared spectrophotometer. I wish to acknowledge the value of discussion with fellow research students of the Chemistry Department.

I am indebted to Mr. A. Valentine for help with thesis diagrams. Thanks are also due to the technical staff of the Chemistry Department, and especially Mr. Bill Dixon.

Finally, I acknowledge receipt of a Commonwealth Postgraduate Scholarship.

CONTENTS

CHAPTER I

MAGNETIC INTERACTIONS IN POLYNUCLEAR TRANSITION ELEMENT COMPLEXES

A. Introduction:

The magnetic behaviour of magnetically dilute transition element compounds is now well understood (1-4). The theory for these systems in which interaction between the metal ions is negligible has been developed to a high degree of sophistication and generally, experimental results can be fitted very accurately by theory. In the case of magnetically concentrated systems the situation is not so clearly defined. Although the interaction between magnetic ions has been the subject of many theoretical treatments, the basic mechanisms of ferro- and antiferromagnetism are poorly understood. These problems have been examined mainly by physicists who have concerned themselves almost exclusively with studies of ionic lattice compounds and metals where the exchange interaction is propagated throughout the crystal. Two distinct theoretical treatments have been developed in which the magnetic electrons are considered either to be localized on the parent atoms as in the Heitler-London-Heisenberg approach (1,5-7) or collective as in the Molecular Orbital approach (8-10). The basis of the former model is the concept of a spin Hamiltonian. The

Hamiltonian operator for a crystal is given by:

$$\mathcal{H} = -2 \sum_{k=1}^{N} J_k \sum_{k\ pairs} S_i . S_j \qquad \text{I-1.}$$

where S_i and S_j are spin operators and J_k is the exchange integral between a pair of k^{th} nearest neighbours.

The enormous mathematical complexity of such a many-body problem prohibits the solution of this general equation and in the studies of the properties of ionic lattice compounds some drastic approximations have to be made. The usual initial approximation is the restriction to nearest neighbours only (k=1). As exchange interactions generally fall off rapidly with increasing atomic separation, this approximation is often justifiable and the model has been used with some success in interpreting the properties of such ionic compounds as perovskites and spinels. However, it is entirely unsatisfactory for explaining the magnetic properties of metals and semiconductors. Although the Molecular Orbital or Band Model is better suited to a description of these substances, there is no clear-cut solution to the problem and a more accurate model probably involves mixing the characteristics of both (11). Yet a third approach currently in favour considers the d electrons in metals to be localized on the parent atoms with the s electrons as itinerant or conduction electrons providing the interaction between localized moments (12).

The complexities associated with the interaction of a large number of magnetic ions as in the above systems are greatly reduced if the magnetic compound under study is diluted with an isomorphous diamagnetic substance (13). In this way the co-operative phenomena are restricted to isolated clusters. If the magnetic ions are randomly distributed throughout the host-lattice the number of pairs, triads, etc., can be calculated (14). Hence for such dilute systems the theory is fairly straightforward as only a small number of interactions have to be considered.

Isolated clusters also occur naturally in some pure compounds which are grouped under the general heading of polynuclear complexes. Generally the crystal structures of polynuclear compounds are complex and thus the extension of theories for these systems to magnetically concentrated systems is not straightforward. However, they form an important intermediate class for which the magnetic properties can be interpreted fairly precisely using the localized electron model.

The simplest form of naturally occurring "isolated cluster" is the binuclear complex of which copper acetate monohydrate is the classical prototype in magnetic studies. Copper ions occur in isolated pairs, bridged by four acetate ligands (15). The copper atoms are only 2.64 Å

apart (c.f. 2.56 Å in the metal) and the complex exhibits antiferromagnetic behaviour with an exchange integral $J = -205^{o}K$ (16). The occurrence of this structural type has also been established for the acetates of chromium (II) (17), molybdenum (II) (18) and rhodium (II) (19). X-ray studies have since revealed binuclear entities in many other transition element complexes (20-28), in which the metals are bridged by n ligands (n = 0 - 4). Recent structural studies have also shown the presence of trimeric and tetrameric "isolated clusters" in transition element compounds (29-32).

As mentioned above, the magnetic properties of these polynuclear complexes may be interpreted accurately using the Heisenberg localized electron model. The development of the spin Hamiltonian, as originally proposed by Van Vleck, leads to formulae for the magnetic susceptibilities which have been used with great success in fitting experimental data for numerous "isolated clusters".

Starting from a simplified form of the spin Hamiltonian

$$\mathcal{H} = -2J\sum_{i} S_i . S_j \qquad \text{I-2}$$

Earnshaw et al have calculated the magnetic moment as a function of temperature for chains of magnetic centres of spin S, each coupled to adjacent members only, by an exchange integral J (33). Results have been tabulated

for chains of up to ten members and for atoms with spins of 1/2, 1, 3/2, 2, and 5/2. (N = 10 members approximates very closely to an infinite chain). Using these formulae it has been possible to account for the antiferromagnetism of many binuclear and trinuclear complexes of copper (II), chromium (III) and iron (III) (34-39).

Using a similar approach, Wojciechowski (40) has derived expressions for the magnetic susceptibility of $d^n.d^m$ binuclear transition element systems (n,m = 1,2,3, 4,5) for both positive (ferromagnetic) and negative exchange integrals.

Very recently, Kakos and Winter have presented susceptibility expressions for a number of tetranuclear cluster models (41). They have had some success in applying these formulae to account for the observed magnetism of some iron (III) halo alkoxides (41).

However, although the spin Hamiltonian forms the basis for a well-developed mathematical procedure, this approach gives no insight at all into the nature of the exchange between the magnetic ions. In this context we will follow the convention used by Goodenough (42) in referring to all interactions which do not involve an anion intermediary as direct cation-cation interactions and those that do as cation-anion-cation interactions. In the case of copper acetate monohydrate the antiferromagnetic interaction has been variously attributed to

direct cation-cation interaction via both σ (43) and δ (44-46) bonds, and to cation-anion-cation interactions via the acetate anions (47). Numerous papers have been published in which these different approaches are examined critically but the problem is not yet resolved.

In a comprehensive review, Kato et al discuss the various mechanisms for exchange in a large number of copper (II) binuclear complexes (48). As with copper acetate monohydrate, it was not possible to assign specific mechanisms to many of these compounds. Some progress has been made in the determination of exchange mechanisms for copper (II) binuclear complexes by studying the variation of the exchange integral as the electron donating ability of the bridging atoms are altered. This may be achieved for suitable organic bridging ligands by changing the electronegativity of appropriate substituents. Hatfield and Paschal have reported magnetic data for a series of 4-substituted pyridine N-oxide complexes of copper (II) halides containing oxy-bridged binuclear species (47). The exchange integral was found to be very sensitive to the substituent on the pyridine ring. The observed trends indicated a dominant superexchange mechanism via π-overlap with the oxygen orbitals. Similarly Ginsberg et al have interpreted the antiferromagnetism of a series of 5-substituted N(2-hydroxyphenyl) salicylideneimine binuclear copper (II) complexes in terms of a superexchange mechanism (39).

In the corresponding vanadyl complexes, the exchange integral shows a quite different dependence on the substituents and the results have been interpreted in terms of direct metal-metal interaction between pairs of vanadium atoms (49).

Lewis and coworkers have made a detailed study of spin-spin interactions in polynuclear transition-metal complexes of iron (III) and chromium (III). The observed magnetic behaviour has been successfully interpreted on the basis of the dipolar coupling model (33-38). However, the determination of the actual mechanisms for coupling have been unsatisfactory. Such determinations have been attempted on the basis of simple molecular orbital theory. Most of the compounds studied however have very complex structures with low symmetry at the metal atoms, (e.g. five coordinated iron (III)) making detailed assignments of the ordering of molecular orbitals very difficult. For some of the compounds the structure of the binuclear unit is such that both superexchange and direct exchange mechanisms are possible (35,36). Again, the complexity of the systems and the lack of data on related systems prevents estimates being made of the relative contributions of each.

From this brief survey it is apparent that present interpretations of mechanisms for spin-spin coupling in polynuclear transition element complexes are poorly

developed. That the progress in this field has been so slow may well be due to the fact that the compounds studied have been too diversified, and of complex structure. Obvious developments involve the study of the variation of magnetic interactions in series of simple polynuclear complexes of closely related structures as the cation-cation separation is varied uniformly and as the polarizability of the anion is changed. Using this approach it should be possible to isolate the relative contributions of the different exchange mechanisms.

CHAPTER II

MECHANISMS FOR EXCHANGE INTERACTIONS BETWEEN d^3 TRANSITION ELEMENT IONS

A. Introduction:

In the following chapters the results of a detailed study of the magnetic interactions in polynuclear compounds of type $A_3M_2X_9$ (M = Mo (III), Cr (III)) and AMX_3 (M = V(II)) are reported. Both series of compounds contain face-shared $[MX_6]^{n-}$ octahedra. To form a basis for understanding the magnetic properties of these compounds, the mechanisms by which the spins on adjacent magnetic ions couple will be reviewed in this chapter. From symmetry considerations a qualitative estimate is made of the various mechanisms for exchange between two octahedrally coordinated d^3 transition metal ions when adjacent octahedra share edges. Extension to the more complex case of face-sharing octahedra is discussed and the literature on "right-angle" exchange mechanisms in d^3 metal complexes is reviewed.

B. General Magnetic Exchange Mechanisms in Isolated Clusters:

The simple Hamiltonian of equation I-2 forms the basis for calculations in isolated clusters. However, a

study of the Hamiltonian gives no insight into the actual mechanisms by which the spins couple to give rise to the typical ferro- and antiferromagnetic behaviour. As mentioned in Chapter I, the simplest classification of exchange mechanisms is into those which involve an anion intermediary and those that do not. According to Anderson (50) however, there is no distinction in principle between direct overlap and overlap via non-magnetic groups. He considers coupling from a molecular orbital approach in which the d orbitals of the magnetic ion are expanded by mixing with suitable orbitals on the diamagnetic anion. Thus even the traditional "superexchange" process can be considered as a direct cation-cation transfer via expanded molecular orbitals or alternatively, direct metal-metal overlap is a special case of this general superexchange mechanism.

The magnitude and sign of the general superexchange for a given transition element isolated cluster depends on the d electron configuration of the metal (orbital occupancy), the symmetries of both the metal and anion orbitals, the electronegativity of the anion, the radial extension of the metal d orbitals (e.g. Cr→ Mo → W) as well as other minor factors (51). Concerning the sign of the interaction, three main cases may be distinguished:

(a) Overlap of half-filled orbitals:

As an illustration, consider two Cr^{3+} ions separated linearly by a diamagnetic ligand such as occurs when two $[CrX_6]^{3-}$ octahedra share a corner. In Cr^{3+} each of the three t_{2g} orbitals are half filled; the e_g orbitals are empty. There is π overlap of the d_{yz} with the anion p_y orbitals as shown in Figure II-1.

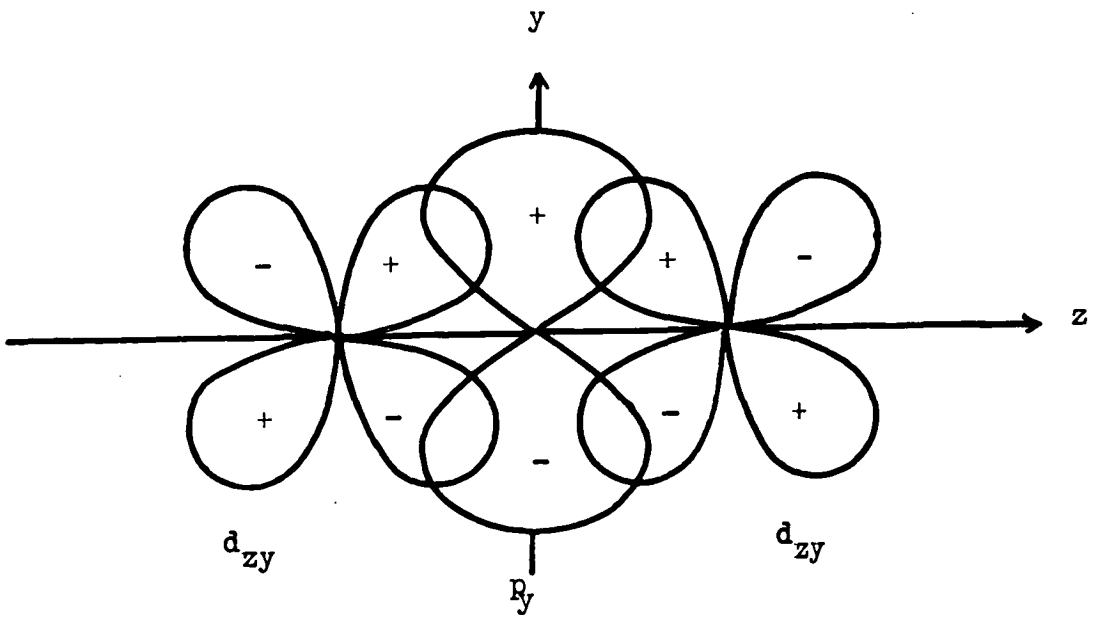

Fig. II-1.

Transfer of an electron from p_y to d_{yz} on Cr_1 can occur, resulting in antiferromagnetic pairing (Pauli principle). The remaining electron residing on X can then couple antiferromagnetically with the unpaired d_{yz} electron on Cr_2. Since the transfer integrals carry an electron without change of spin this mechanism can only occur if the interacting electrons on the two metals are anti-parallel. The resulting sign is thus negative. The

magnitude of the exchange integral has been estimated as (42):

$$J_{ij}\ (\text{half-filled, half-filled}) = \frac{-2\ b_{ij}^2}{4S^2U} \qquad \text{II-1}$$

where S is the total cation spin,

U is the energy of the excited state of M_1 resulting from the transfer of one electron to it and b_{ij} is the transfer integral, approximately proportional to the orbital overlap.

(b) Overlap of a half filled and an empty orbital:

Consider that orbital n on M_1 is empty and orbital n' on M_2 is half filled. Electron transfer is spin independent in this case unless there is an orthogonal, partially occupied orbital, n", on M_1. Transfer of an electron to n on M_1 is then favoured if the transferred electron is parallel to the spin of n". i.e., The system is stabilized by ferromagnetic intraionic exchange within M_1. The sign of the mechanism is thus positive. Its magnitude is proportional to the intraionic exchange constant J_{intra}:

$$J_{ij} = + \frac{2b_{ij}^2}{4S^2U} \times \frac{J_{intra}}{U} \qquad \text{II-2}$$

This ferromagnetic coupling is weaker than case (a) by the factor J_{intra}/U which may be a factor of 5 to 10.

(c) Overlap of a half filled and a full orbital:

This is also ferromagnetic and depends on intraionic coupling. As this case does not apply to d^3 transition metal ions it will not be discussed further.

The systems $A_3M_2X_9$ and AMX_3 contain face shared octahedra with approximately right angle metal-ligand-metal angles. In order to discern the various mechanisms of exchange it is of value to intially consider the simpler right angle superexchange case of two $[MX_6]^{3-}$ octahedra sharing an edge.

C. Exchange Mechanisms in Edge Sharing Octahedra:

The symmetry relations between the d^3 metal orbitals and the 90^o anion orbitals which apply for two octahedra sharing a common edge are illustrated in Figure II-2. The following relations exist:

p_x: orthogonal to d_{xy} on M_1 and $d_{x^2-y^2}$ on M_2

nonorthogonal to $d_{x^2-y^2}$ on M_1 and d_{xy} on M_2

p_y: orthogonal to $d_{x^2-y^2}$ on M_1 and d_{xy} on M_2

nonorthogonal to d_{xy} on M_1 and $d_{x^2-y^2}$ on M_2

p_z: orthogonal to d_{yz} on M_1 and d_{xz} on M_2

nonorthogonal to d_{xz} on M_1 and d_{yz} on M_2

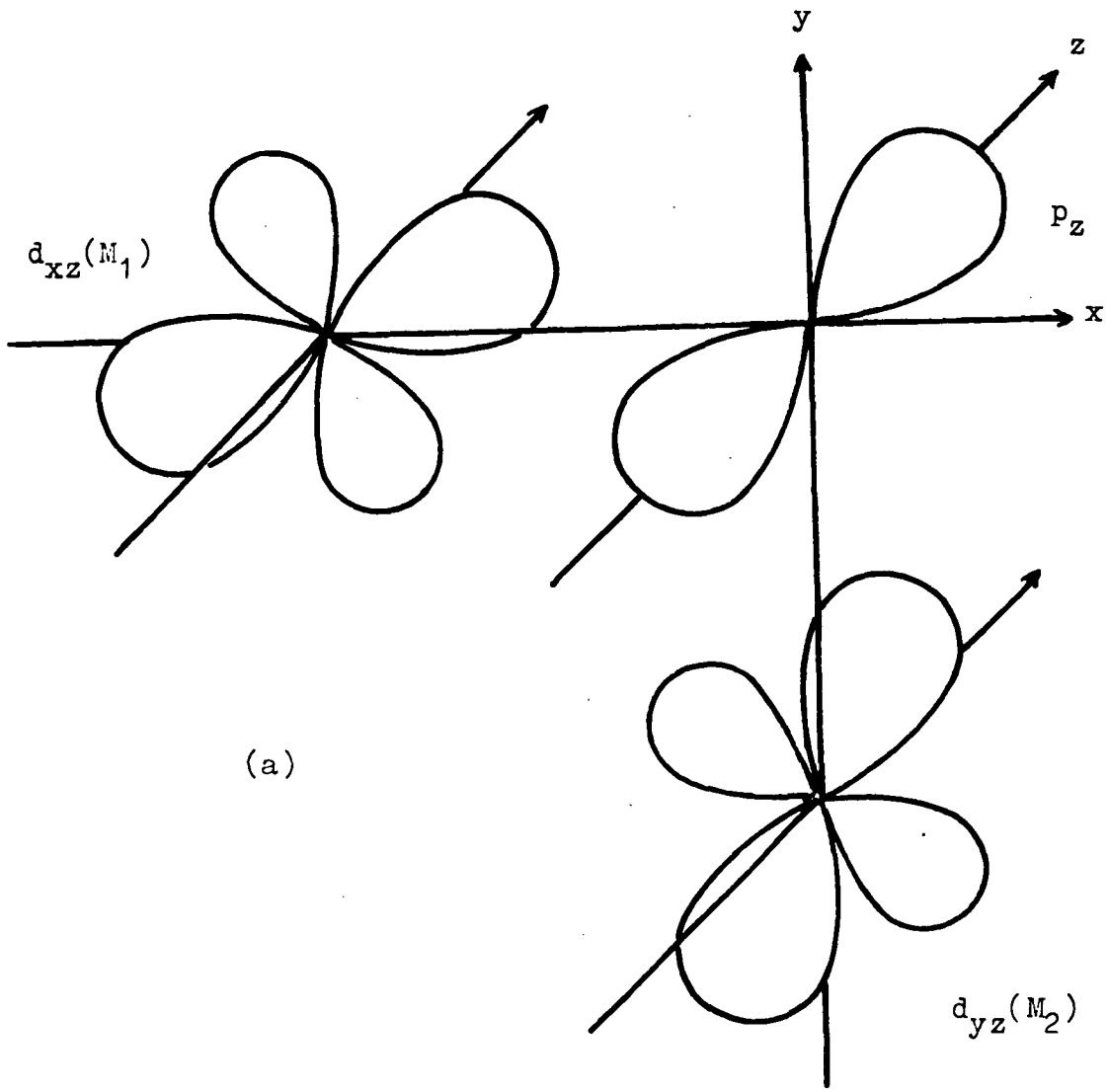

Fig.II-2. Symmetry relations applying in edge sharing octahedra.

(a) $d_{xz}(M_1)$ - p_z(ligand) - $d_{yz}(M_2)$

(b) $d_{xy}(M_1)$ - p_y(ligand) - $d_{xy}(M_2)$

(c) $d_{x^2-y^2}(M_1)$ - p_y(ligand) - $d_{x^2-y^2}(M_2)$.

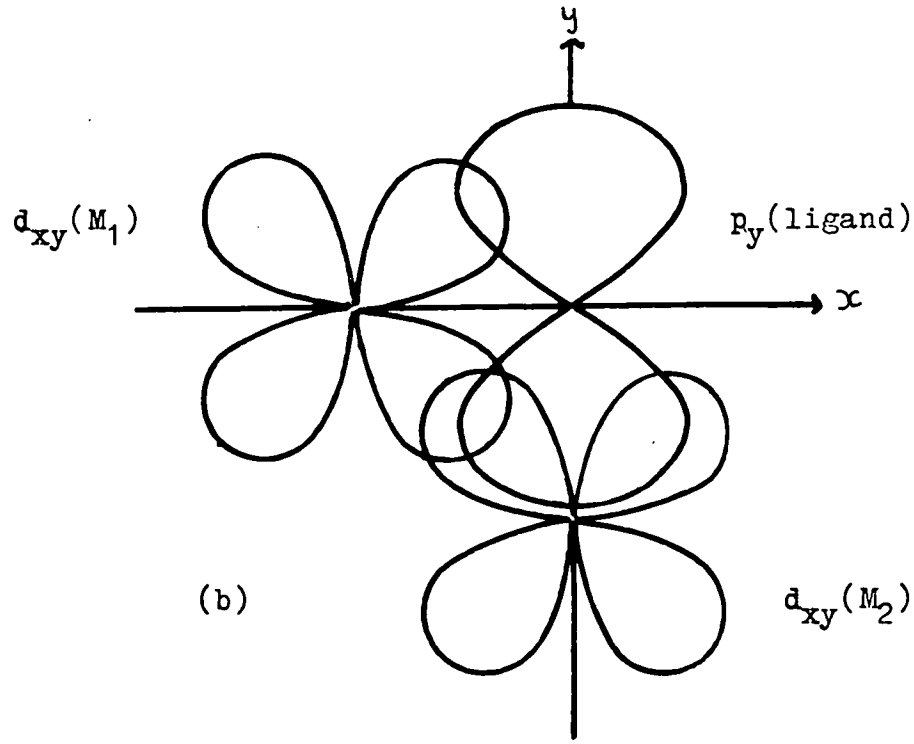

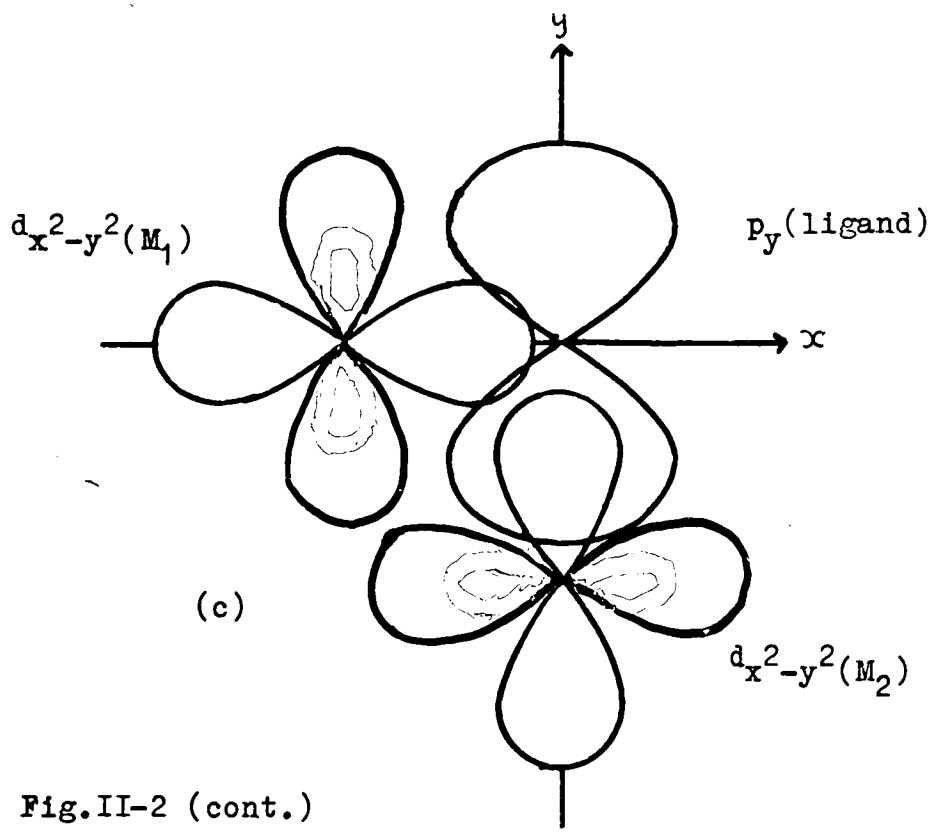

Fig.II-2 (cont.)

From an examination of Figure II-2 and the above relations the following mechanisms for spin-spin coupling may be formulated:

1. Direct overlap of d_{xy} orbitals (direct metal-metal bonding). This gives an antiferromagnetic interaction.

2. Half-filled, empty orbital superexchange - p_y is nonorthogonal to the empty e_g orbital, $d_{x^2-y^2}$, on M_2 and nonorthogonal to the half filled t_{2g} orbital, d_{xy}, on M_1. This represents the type (b) mechanism discussed in II-B and the resulting interaction is ferromagnetic. Similarly p_x overlaps $d_{x^2-y^2}$ on M_1 and d_{xy} on M_2, again giving a ferromagnetic interaction.

3. Half-filled, half-filled orbital superexchange - p_z overlaps the half filled t_{2g} orbitals - d_{xz} on M_1 and d_{yz} on M_2 through π bonding. Antiferromagnetic superexchange of the type described in case (a) above results.

4. Ferromagnetic exchange between d_{xy} on M_1 and M_2 - The ligand orbital p_x overlaps d_{xy} on M_2 and is orthogonal to d_{xy} on M_1. Similarly, p_y overlaps d_{xy} on M_1 and is orthogonal to d_{xy} on M_2. Ferromagnetic exchange results.

All these mechanisms require finite overlap of orbitals for their propagation. The original direct exchange of Heisenberg results from the interaction of

orthogonal orbitals and is always positive. However, its magnitude is extremely small compared to the mechanisms considered above and is ignored in this discussion. Similarly, spin polarization or indirect exchange, as formulated by Anderson, and other weaker effects are neglected.

The mechanisms discussed which involve an anion intermediary have been described above in terms of a delocalization exchange mechanism, i.e., drift of an electron from the anion to one of the cations. A second superexchange mechanism is considered by some workers to be as important as delocalization exchange (52-55). It is the correlation exchange in which a pair of electrons in an anion orbital interact and are excited simultaneously to form partial covalent bonds on opposite sides of the anion. Nesbet (53) has calculated that it is a more important contribution than even delocalization exchange in the interactions in binary oxides (MnO, FeO, CoO, and NiO). Anderson claims that the correlation effect, although correct in principle is very weak. However, the main correlation mechanism for the d^3/d^3 right angle system-namely two electrons from the same anion p orbital coupling simultaneously to a t_{2g} orbital on one metal and an e_g orbital on the other - has the same sign as the delocalization mechanism (2) discussed above and so does not affect this qualitative discussion.

D. Right Angle Exchange Interactions in Face-Sharing Octahedra:

Many polynuclear transition element complexes containing face-sharing octahedra are now well characterized. The detailed x-ray structures of a number of complexes $A_3M_2Cl_9$ have revealed the presence of binuclear complex anions, $[M_2X_9]^{3-}$ in which two octahedra share a face (20,21,56). Recently, the complex bis (acetylacetonato) nickel (II), $[Ni_3(acac)_6]$ has been found to contain linear trinuclear clusters, resulting from the sharing of faces of three adjacent octahedra (29). The structures of many compounds of formula AMX_3 containing infinite chains of face sharing octahedra have also been reported (57-61). The justification for including these in the category of polynuclear complexes is that the magnetic behaviour may be accounted for using the dipolar coupling approach.

For these systems of face sharing octahedra, close approach of the two metals is possible. In addition, the trigonal field stabilizes a d orbital on each metal directed along the metal-metal axis. Direct cation-cation interaction is hence expected to be important.

A detailed description of the various mechanisms for exchange via the bridging anions is not as simple as in the case of edge-sharing octahedra. When two undistorted octahedra share a face, the bridging angle is not 90°

but closer to 70^{o}. It is then an approximation to consider the ligand p orbitals to be directed along the metal-ligand bonds. The simple orthogonal relationships given in section II-C no longer hold. Ferromagnetic exchange mechanisms of type II-C (4) above are then formally forbidden. Calculations (62) show that this type of interaction is dominant in the case of $V^{2+}(d^3)$ pairs interacting via 90^{o} oxygen intermediaries (as in MgO). Huang and Orbach (63) stress that the orthogonality of the spin polarized ligand orbital to the occupied cation orbitals is essential for ferromagnetic exchange. For d^3 metals, this implies the cation-cation bond must lie along a (110) axis (as in edge-sharing octahedra). This applies in $CrBr_3$ which is ferromagnetic (64). Huang and Orbach point out that in ruby, where chromium pairs share a face, i.e., they are in a [111] configuration with respect to one another and ferromagnetic coupling would not be expected.

In order to interpret trends in the magnetic interactions observed experimentally a simplified model is however, obviously necessary. Ginsberg et al (65) were able to give a qualitative understanding of the magnetic interactions present in $[Ni_3(acac)_6]$ by making the approximation that the bridging Ni-O-Ni angles are all 90^{o} (experimentally the Ni-O-Ni angles vary between 76.5 and 89.3^{o}). Estimates of the various competing mechanisms were then made using

analogous symmetry relations to those given in section II-C for edge-sharing octahedra.

In the d^3 transition element complexes $A_3M_2X_9$ and AVX_3 the metals are subject to a trigonal field which splits the degenerate d orbitals into a singly degenerate a_{1g} orbital and two doubly degenerate e_g orbitals. The a_{1g} orbital is directed along the metal-metal axis, one pair of e_g orbitals (d_{yz}, d_{zx}) are directed more or less along the metal-ligand bonds and the second pair of e_g orbitals (d_{xy}, $d_{x^2-y^2}$) is directed approximately perpendicular to the trigonal axis. Fig.II-3 illustrates two face sharing $[MX_6]^{n-}$ octahedra with suitable cartesian coordinate systems centred on the metals and ligands. Exchange between the metals can then occur via the following mechanisms:

1. Direct exchange resulting from σ overlap of the d_{z^2} (a_{1g}) orbitals on each metal atom. Strong antiferromagnetism results if the metal-metal separation is small.

2. Antiferromagnetic superexchange between the half-filled d_{xy} and $d_{x^2-y^2}$ orbitals on each metal via π overlap with p_z on the ligand.

3. Ferromagnetic exchange from half-filled to empty orbitals via overlap with p_x and p_y.

4. If a p_σ overlaps a half-filled orbital on one metal and at the same time is orthogonal to a half-filled

orbital on the other metal, ferromagnetic exchange results. As mentioned above, this mechanism is formally forbidden in the case of face-shared octahedra but may occur if the overlap between p_σ and a half-filled d orbital is so small that the orbitals are effectively orthogonal.

In any particular complex, all these mechanisms are competing and depend critically on so many factors that the resultant sign and magnitude of the exchange is difficult to estimate. From symmetry considerations only, Kanamori has determined that the resultant sign of the various right angle superexchange mechanisms for octahedrally coordinated d^3 ions is positive (66). Goodenough (42) has estimated that the sum of the contributions (2) and (3) above, together with correlation superexchange is ferromagnetic and of magnitude $\sim 50^\circ C$ for right angle exchange through chlorides. Indeed, in the layer compounds $CrCl_3$ and $CrBr_3$ the large Cr-Cr separation (3.44 Å in $CrCl_3$)(67) precludes direct overlap as a major mechanism and the 90° intralayer interactions are observed to be ferromagnetic (64).

Huang (62) has investigated the exchange interaction between $V^{2+}(d^3)$ ion pairs in M_gO, where they are at right angles to bridging oxygens. Quantitative estimates were made of the following mechanisms: (refer Fig.II-2)

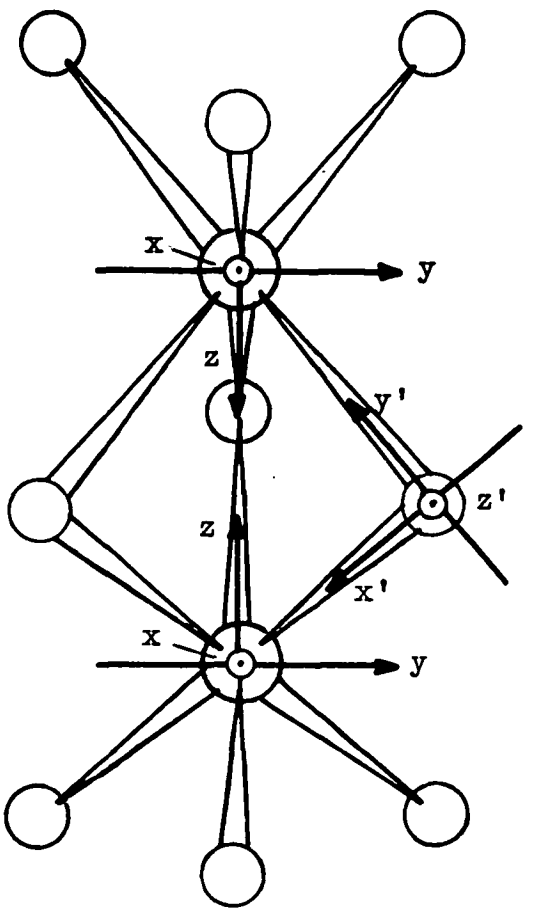

Fig.II-3. Coordinate systems on M (x,y,z) and X (x',y',z') for face sharing $[MX_6]^{n-}$ octahedra.

(i) direct overlap of d_{xy} on V_1 and V_2 - antiferromagnetic. (mechanism (1) above).

(ii) exchange between d_{xy} on V_1 and V_2 via the spin polarized ligand. This is ferromagnetic as p_y is non-orthogonal to d_{xy} (V_1) and orthogonal to d_{xy} (V_2). (mechanism D-(4) above). This contribution has not been considered by other workers, but Huang calculates it to be the dominant term.

(iii) Antiferromagnetic exchange between d_{xz} on V_1 and d_{yz} on V_2 via π overlap with p_z on the oxygen. (mechanism D(2) above). Again actual calculations revealed the very unexpected result, not obvious from symmetry considerations alone, that due to the non-orthogonality of the d_{yz} and d_{xz} orbitals, a ferromagnetic term arose which acted to cancel the nominally antiferromagnetic interaction. Ferromagnetic interaction between half filled and empty orbitals was not considered in the calculations as it was expected to be smaller than the interactions between half-filled orbitals by a factor of $\sim$ (10) (see section II-B). The resultant interaction was calculated to be ferromagnetic ($J = +8^{\circ}$ K). Huang and Orbach have applied these mechanisms (i)-(iii) to account for observed ferromagnetism in a series of chromium (III) chalcogenide spinels (63).

CHAPTER III

MAGNETIC STUDIES OF SOME BINUCLEAR COMPLEX HALIDES OF MOLYBDENUM (III) AND CHROMIUM (III).

The need for a detailed study on the relationship between magnetism and structure in a simple system of related polynuclear complexes has been emphasised in Chapter I.

A suitable system for study is that comprising complex halides of type $A_3M_2X_9$ with M = Cr(III), Mo(III), W(III); X = halogen; A = univalent cation, containing binuclear $\left[M_2X_9\right]^{3-}$ complex anions. As will be shown in later chapters, it has been possible to study the variation of magnetic exchange with change of metal-metal distance in this system by correlating detailed x-ray structural data with magnetic susceptibility measurements. The effect of polarizability of the ligand on superexchange has been ascertained from a study of both bromide and chloride complexes.

In this chapter, the results of magnetic studies will be reported for a number of chromium (III) binuclear compounds, for which the magnetic interactions are weak, and a range of molybdenum (III) complexes in which strong spin-spin coupling occurs.

Few studies of the magnetic properties of compounds

of formula, $A_3M_2X_9$ have previously been reported. Ijdo (68) has presented results of temperature dependence studies on $Cs_3Cr_2Cl_9$, $Cs_3V_2Cl_9$ and $K_3Ti_2Cl_9$. The two former compounds exhibit Curie-Weiss behaviour ($\chi'_A = C/T + \Theta$) with Θ values of 33° and 100° respectively. The titanium compound shows typical antiferromagnetic behaviour with a maximum in the susceptibility curve at 550°K. No attempt was made to determine the magnitude of the exchange integral in these compounds. The complex $K_3W_2Cl_9$ has been reported to be diamagnetic (69). Wentworth and Saillant (70) have recently published susceptibility data in the range 80-300°K for a number of enneahalodimetalates $A_3M_2X_9$ (A = K,Rb,Cs; M = Cr,V,Ti, W; X = Cl,Br,I). The results are not interpreted in any detail.

The only reported determinations of exchange integrals are for the compounds $(Et_4N)_3Cr_2Cl_9$ with J = -5°K (35) and $(Et_4N)_3V_2Cl_9$ with J = -57°K. (71)

A. Chromium (III) Binuclear Complexes:

The magnetic susceptibility of powdered samples of compounds $A_3Cr_2X_9$ (A = K,Rb,Cs; X = Cl and A = Cs, Et_4N; X = Br) has been measured by the Gouy method in the range 90-300°K. The results are summarized in Figs.III-1,2 and

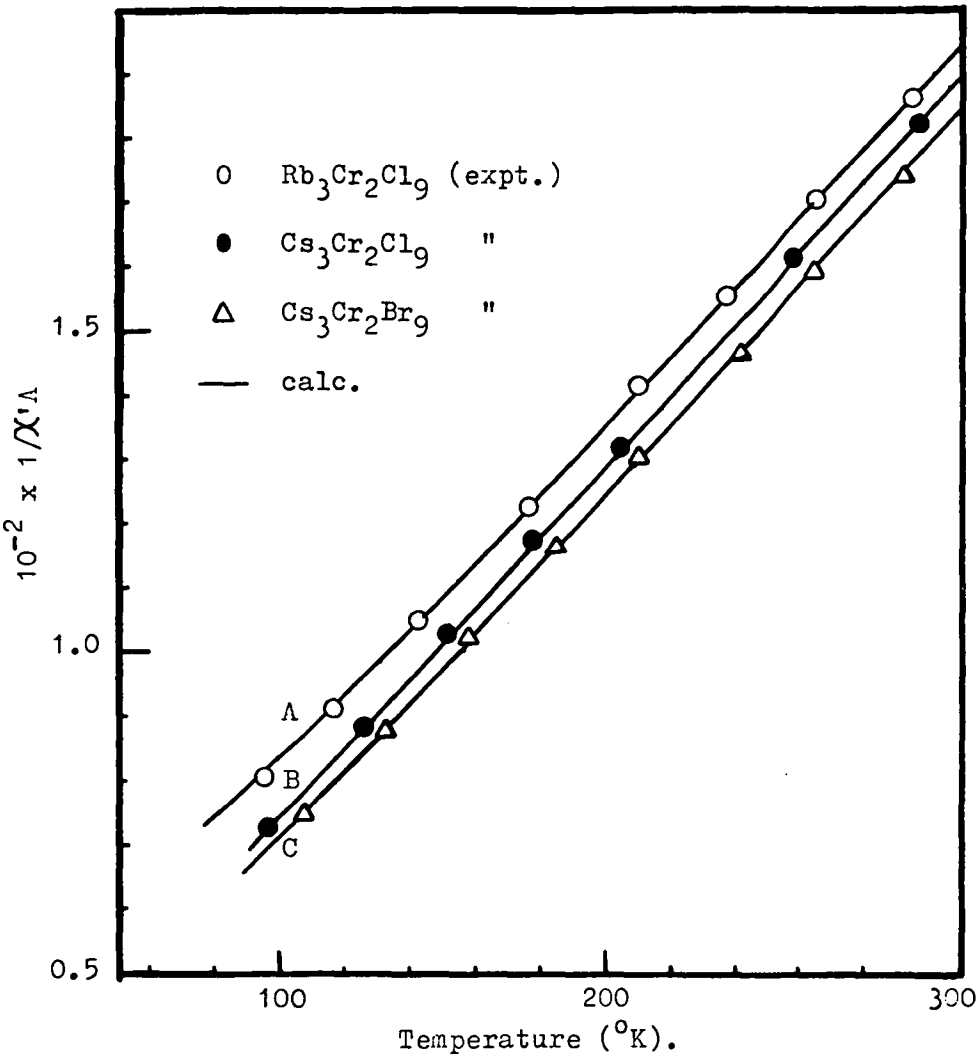

Fig.III-1: Reciprocal magnetic susceptibility versus temperature for

A. $Rb_3Cr_2Cl_9$, calculated curve for J = -13.3°K, g = 1.95, N(α) = 0.

B. $Cs_3Cr_2Cl_9$, calculated curve for J = -9.3°K, g = 1.94, N(α) = 0.

C. $Cs_3Cr_2Br_9$, calculated curve for J = -8.8°K, g = 1.965, N(α) = 0.

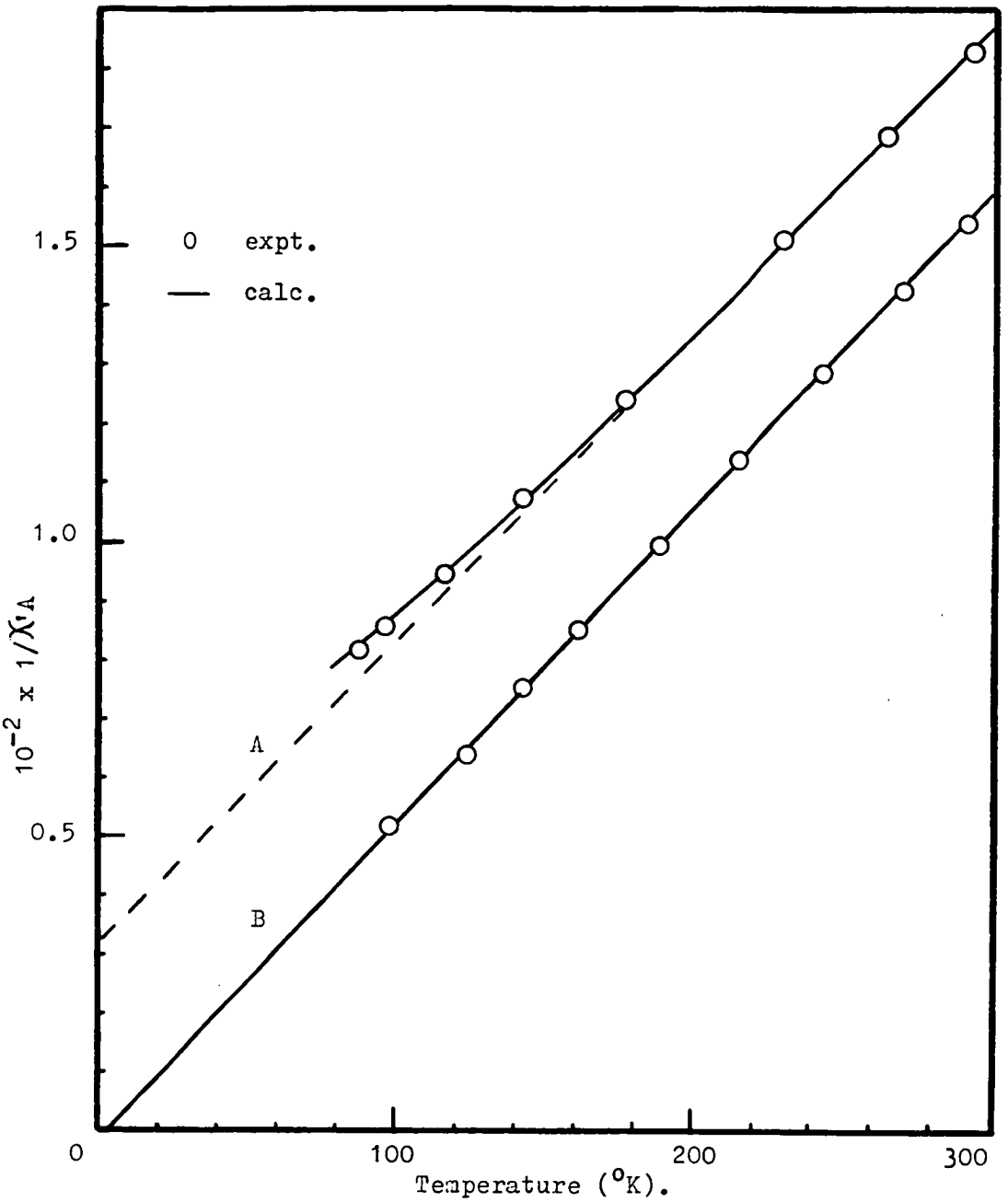

Fig.III-2. A. $K_3Cr_2Cl_9$, calculated curve for $J = -16.0^oK$, $g = 1.99$, $N(\alpha) = 0$;

B. $(Et_4N)_3Cr_2Br_9$, solid line is curve of best fit to the experimental results.

the calculated magnetic parameters are given in Table III -1. Actual susceptibility data are listed in Table III-3 in the Experimental section.

The susceptibility curves in Figs.III-1,2 are linear over most of the temperature range studied but show a distinct curvature at the lowest temperatures measured. The amount of curvature is negligible for the Et_4N^+ and Cs^+ salts but increases quite markedly as the cation size is decreased to K^+. The curves are typical of a complex with very weak antiferromagnetic interaction, i.e., very small J values. In Fig.III-3 theoretical curves are plotted for a binuclear d^3 complex ($g = 2.00$, $N(\alpha) = 0$) for different values of the exchange integral, J. When J is very small (-5^oK), Curie-Weiss law is obeyed over the range 90-300°C with a small θ value of $\sim 10^o$. As the interaction between the two ions is increased, deviations from the Curie Weiss law occur as shown by the increasing curvature of the lines below $T \simeq 100^oK$. Even at the small J value of -15^oK, the Curie Weiss constant has increased to 60^o. The presence of the interaction is also indicated in the reduction of the magnetic moment from the spin-free value of 3.87 B.M. to 3.64 B.M. ($J = -15^oK$).

Earnshaw and Lewis observed these slightly curved susceptibility curves for a number of binuclear chromium complexes with hydroxyl bridges (35). The results were fitted to the binuclear susceptibility equation for d^3 ions:

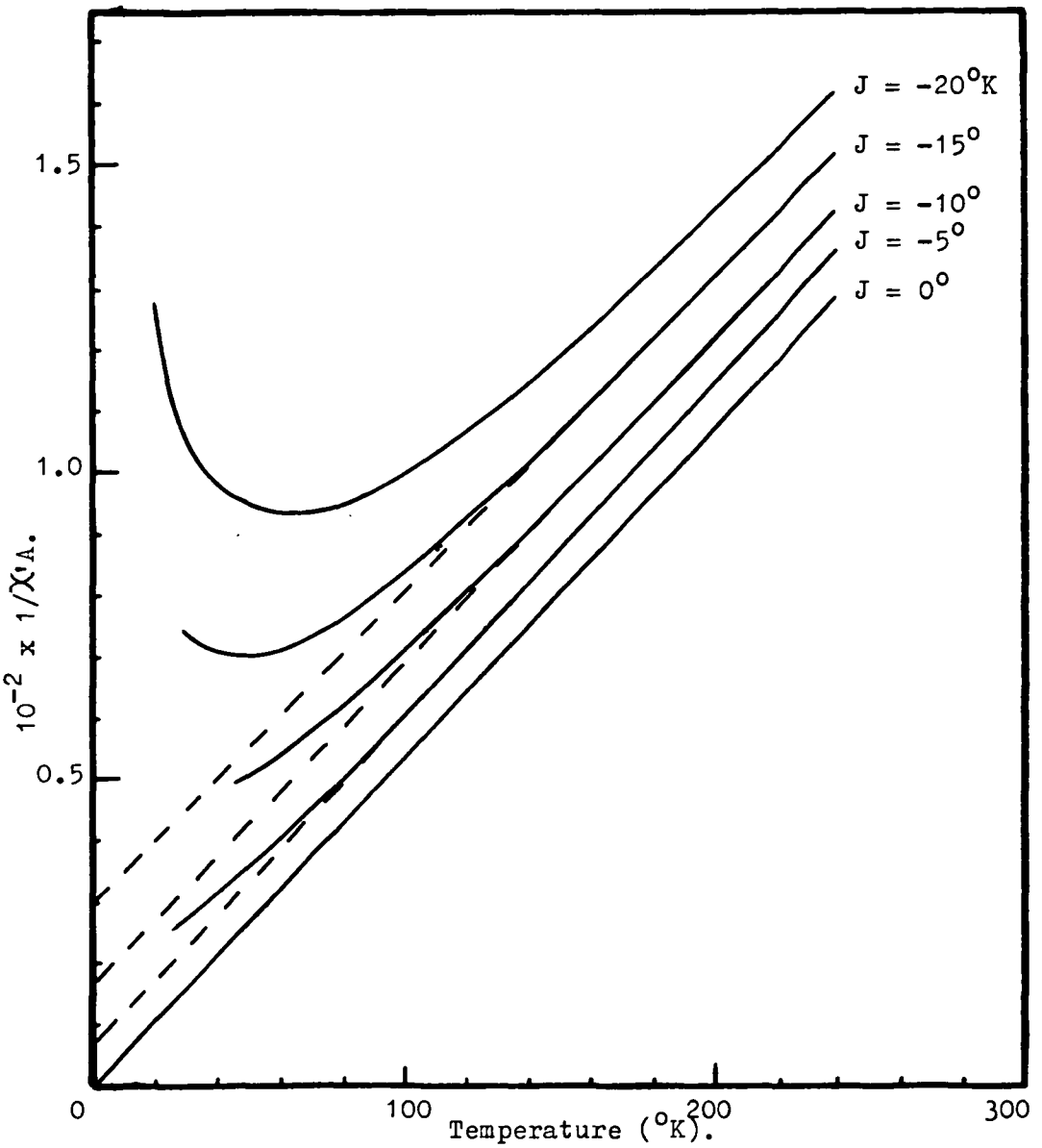

Fig.III-3. Theoretical reciprocal magnetic susceptibility versus temperature curves for a binuclear d^3 transition element complex. g = 2.00, N(α) = 0.

$$\chi'_A = \frac{K}{T}\left[\frac{42 + 15\exp(6x) + 3\exp(10x)}{7 + 5\exp(6x) + 3\exp(10x) + \exp(12x)}\right] + N(\alpha) \quad \text{III-1}$$

where $K = \frac{g^2 N\beta^2}{3k}$ and $x = \frac{-J}{kT}$

The exchange interaction between the two metal ions is represented by the exchange integral $-J$, $2J$ being the energy separation between the singlet and triplet states. Earnshaw and Lewis obtained J values of -5 to $-20^{\circ}K$ with values of g typically 1.9 to 2.0 and $N(\alpha) \simeq 50 \times 10^{-6}$. They remarked on the extreme sensitivity of the theoretical curve to the value of g used.

In Table III-1 are listed values of g, J and $N(\alpha)$ for the theoretical curves of best fit to susceptibility data for the chromium binuclear halide complexes $A_3Cr_2X_9$.

In adjusting the parameters to fit the theoretical curves it was observed that the value of $N(\alpha)$ had very little influence. In fact, the best agreement between theory and experiment was obtained with $N(\alpha) = 0$. In one case altering $N(\alpha)$ from 0 to 50×10^{-6} and recalculating J to give the best fit resulted in a change in J of less than 1%. However, in agreement with Earnshaw and Lewis, it was found the theoretical curve was extremely sensitive to the value of g used, especially for the compounds with very small interactions, e.g., for $Cs_3Cr_2Cl_9$, a change of g from 1.93 to 1.94 resulted in a

change of J for the curves of best fit from -8.5° to -9.3°, i.e., a 10% change. It was hence necessary to make a careful appraisal of the accuracy of resulting J values.

Results were obtained for duplicate determinations on two separately prepared samples of each of the complexes. It was noted that the absolute values of the susceptibility on separately packed specimens of the same sample agreed to 1%, whereas the values of the susceptibilities obtained on different samples (separate preparations) were in agreement to 1-2%. Calculations of J on the different sets of results yielded values which generally agreed to within $0.3 \rightarrow 1.0^{\circ}K$. Thus even though quite reproducible susceptibility results could be obtained, the values of J quoted in Table III-1 are considered to have an associated error of about $0.5 - 0.8^{\circ}K$.

The only reported parameters in the literature for comparison are J for $(Et_4N)_3Cr_2Cl_9$ ($-5^{\circ}K$) (35) and Tc for $Cs_3Cr_2Cl_9$ ($\sim 25^{\circ}K$) (72). This latter value is in quite reasonable agreement with our value of $28.7 \pm 2^{\circ}K$.

Since the completion of this work, Wentworth and Saillant (70) have published susceptibility data over the range $80-300^{\circ}K$ for the complexes $A_3\emptyset r_2Cl_9$ (A=K, Rb,Cs). The susceptibility curves differ consid-

TABLE III-1

MAGNETIC PARAMETERS FOR $A_3Cr_2X_9$

COMPLEX	g	-J (^oK)	T_{max} (^oK)	θ (^oK)[a]	μ_{eff} (300^oK)[b]
$K_3Cr_2Cl_9$	1.99	16.0	49.3	68	4.00
$Rb_3Cr_2Cl_9$	1.95	13.3	41.0	53	3.88
$Cs_3Cr_2Cl_9$	1.94	9.3	28.7	35	3.83
$(Et_4N)_3Cr_2Cl_9$[c]	2.08	5	15.4	12	3.91
$Cs_3Cr_2Br_9$	1.965	8.8	27.2	31	3.87
$(Et_4N)_3Cr_2Br_9$	-	0	-	-3	3.89

a. Constant from the Curie-Weiss equation:

$$\chi'_A = C/(T + \theta)^{-1}$$

b. $\mu_{eff} = 2.84\left[\chi'_A\,(T + \theta)\right]^{\frac{1}{2}}$ B.M.

c. Reference 35.

erably from those reported here. However, they report that in the preparation of the complexes, $CrCl_3$ obtained from Alfa Inorganics Inc., was used without further purification. It has been observed in this laboratory that samples of $CrCl_3$ from Alfa Inorganics contain considerable ferromagnetic impurity. Using such a sample for the preparation of the complexes, it was possible to duplicate Wentworth and Saillant's results. The resulting complexes showed field dependence and in fitting the susceptibility equation III-1, required unreasonable values of g (e.g., $K_3Cr_2Cl_9$ - g = 2.15).

B. Molybdenum (III) Binuclear Complexes:

The magnetic susceptibility of powdered samples of compounds $A_3Mo_2X_9$ (A = K, Cs, Me_4N, Et_3NH, Et_4N, H_3O; X = Cl and A = Cs, Et_4N; X = Br) has been measured in the temperature range 90-400°K. The results are listed in Table III-4 (Experimental). The susceptibilities for the two caesium salts were corrected for the presence of small traces of paramagnetic impurity. Both the measured χ'_A (uncorr.) and the corrected, χ'_A (corr.) susceptibilities are listed in Table III-4. The method of correcting for the impurity has been described in detail (Appendix). The susceptibilities (per Mo atom) are plotted as a function of temperature in Figs. III 4-7. The curves show the typical behaviour of a strongly

antiferromagnetic complex.

The application of the theoretical susceptibility expression III-1 to the fitting of these curves was simplified by substituting g values available from powder e.s.r. measurements on the complexes (73). The problem reduced to a least-squares fit including two variables, J and N (α). Approximate values of N(α) were obtained from extrapolation of the experimental curves to T = 0^{o}K. These initial values were then adjusted in steps of 5×10^{-6}, recalculating J until the best fit of equation III-1 to the experimental results was achieved.

In Table III-2, final values of g, -J (actually -J/k in ^{o}K), N(α) and T_{max} (= -J/0.324) are listed. It is difficult to estimate the magnitude of the error associated with the exchange integral -J. On a basis of a precision of weight change of $\pm$ 0.01 mgms. (an average change being 2 mgms.), the limits of error are calculated to be $\pm$ 10 - 20^{o} for the range of temperatures studied. However, J is fixed by the position of the maximum in the susceptibility curve. For the potassium salt, T_{max} = 2470^{o}K and so the experimental results extend over only $1/6^{th}$ of the susceptibility curve to T_{max}. i.e., small errors in fitting the data over the

temperatures measured will result in appreciable errors in $T_{max.}$ and hence J. For the salts with small cations an error in J of $\sim 50^{\circ}$ is probably not pessimistic. For the salts with larger cations (smaller values of J) the error in J will be correspondingly smaller.

From a study of the magnetic data summarized in Tables III-1,2, the expected variation of magnetic exchange in the compounds $A_3M_2X_9$ with both change of metal, M, and ligand, X, is apparent. However, it is also apparent that the magnetic interactions in these compounds are markedly dependent on the cation, A. For both the chromium and molybdenum series, increase in the size of the cation is accompanied by a decrease in the magnitude of the exchange integral.

To obtain useful information on the different exchange mechanisms from these trends, it is necessary to be able to correlate the magnetic results with structural data on the complexes $A_3M_2X_9$. In the following chapter, the results of detailed x-ray structural studies on these complexes will be presented, to form a basis for the interpretation of the magnetic data presented in this chapter.

TABLE III-2

MAGNETIC PARAMETERS FOR $A_3Mo_2X_9$

COMPLEX	$-J(^oK)$	g	$10^6.N(\alpha)$ (c.g.s.)	T_{max} (^oK)
$K_3Mo_2Cl_9$	800	1.95	75	2469
$Cs_3Mo_2Cl_9$	605	1.95	45	1867
$(Me_4N)_3Mo_2Cl_9$	400	1.95	210	1235
$(Et_4N)_3Mo_2Cl_9$	345	1.955	40	1065
$Cs_3Mo_2Br_9$	555	1.995	150	1713
$(Et_4N)_3Mo_2Br_9$	310	2.01	230	957
$(Et_3NH)_3Mo_2Cl_9$	415	2.01	35	1281
$(H_3O)_3Mo_2Cl_9.3H_2O$	485	2.00	100	1497
$(Ph_4As)_2.H_3O.Mo_2Cl_9.xH_2O$	458	2.00	45	1414

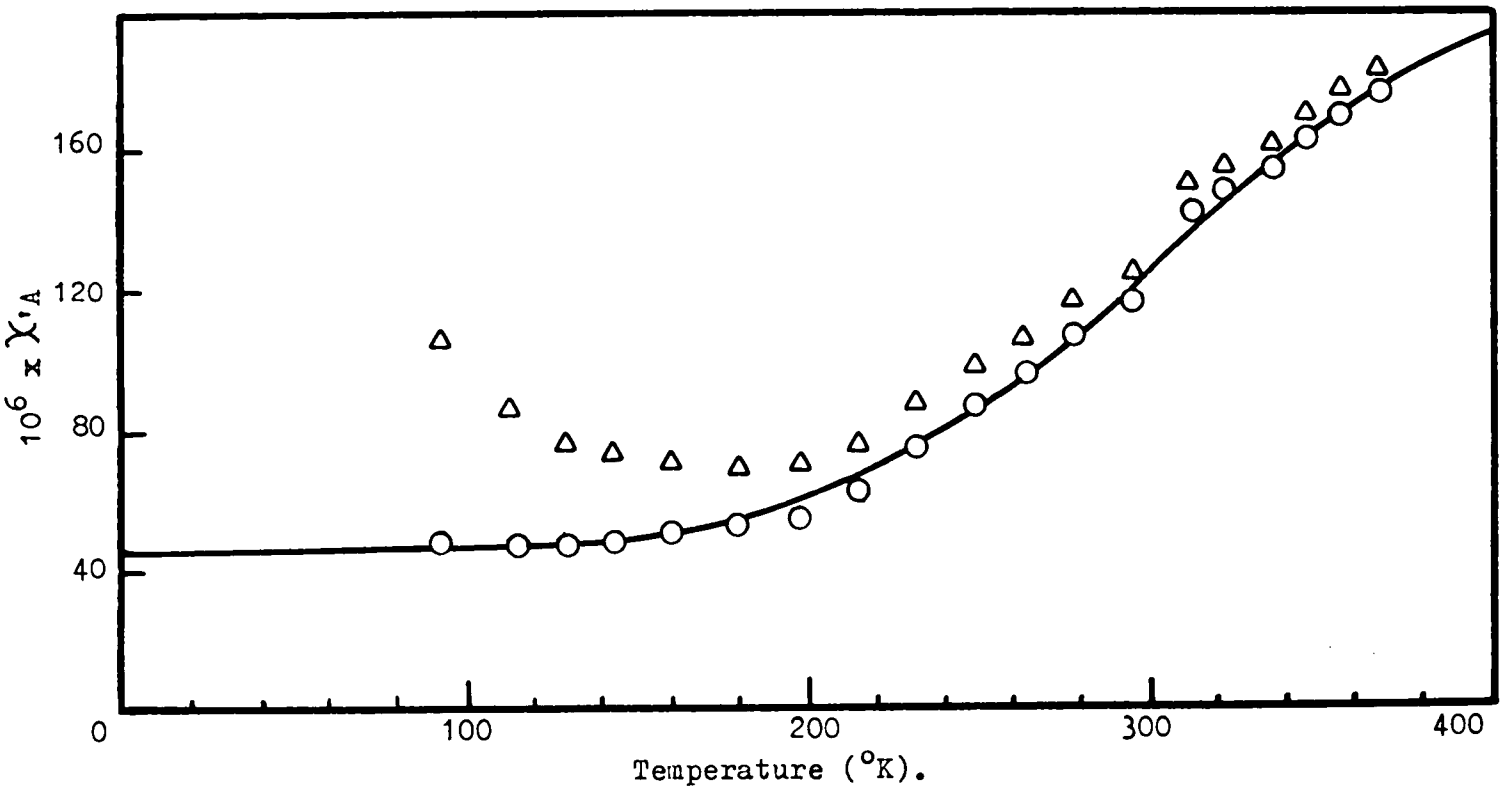

Fig.III-4. Temperature dependence of susceptibility for $Cs_3Mo_2Cl_9$

Δ - χ'_A (uncorr.); O - χ'_A (corr.); calculated curve for J = -605°K, g = 1.95, $N(\alpha) = 45 \times 10^{-6}$.

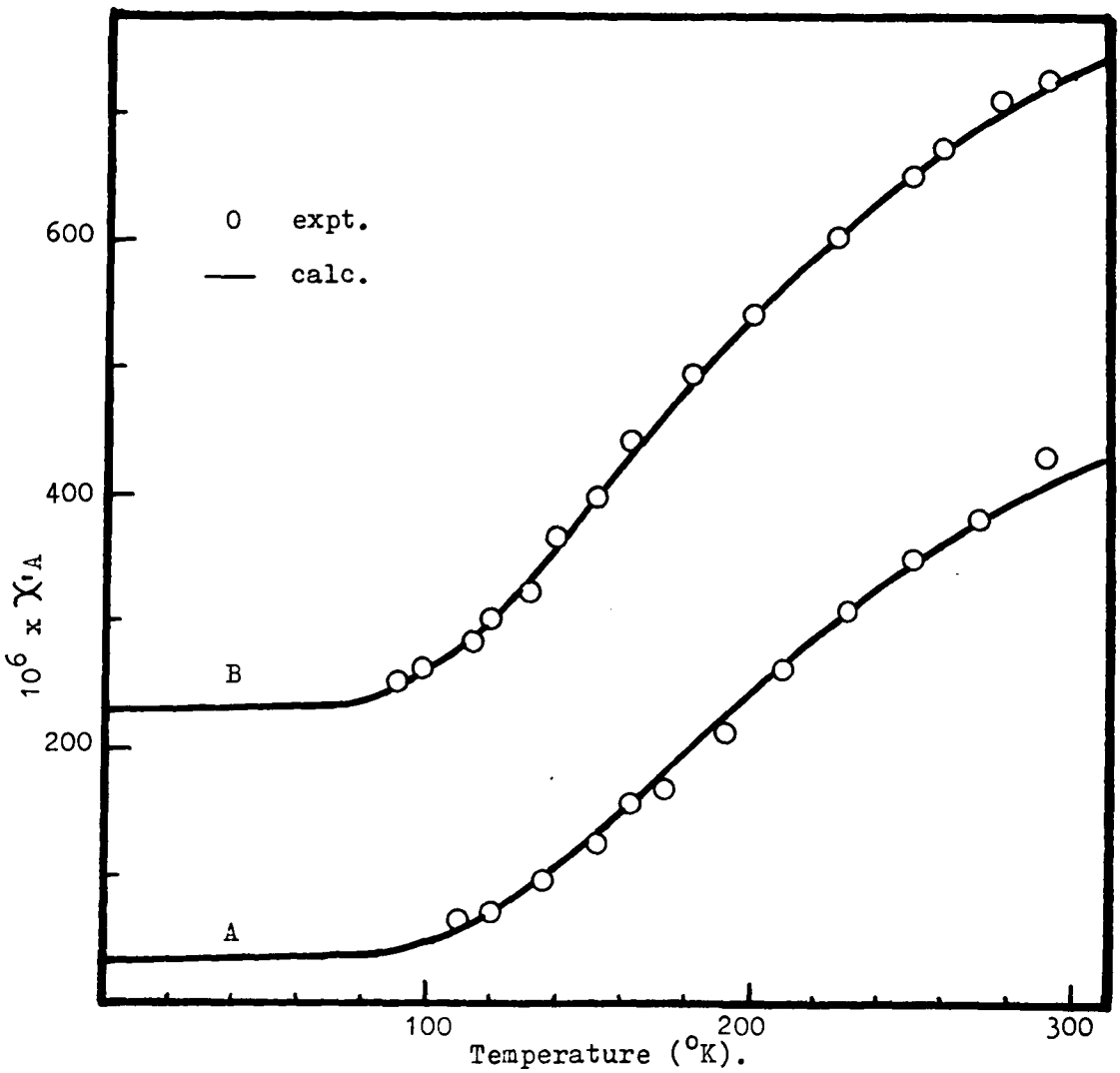

Fig.III-5. Temperature dependence of susceptibility.

A. $(Et_4N)_3Mo_2Cl_9$, calculated curve for

$J = -345^oK$, $g = 1.955$, $N(\alpha) = 40 \times 10^{-6}$;

B. $(Et_4N)_3Mo_2Br_9$, calculated curve for

$J = -310^oK$, $g = 2.01$, $N(\alpha) = 230 \times 10^{-6}$.

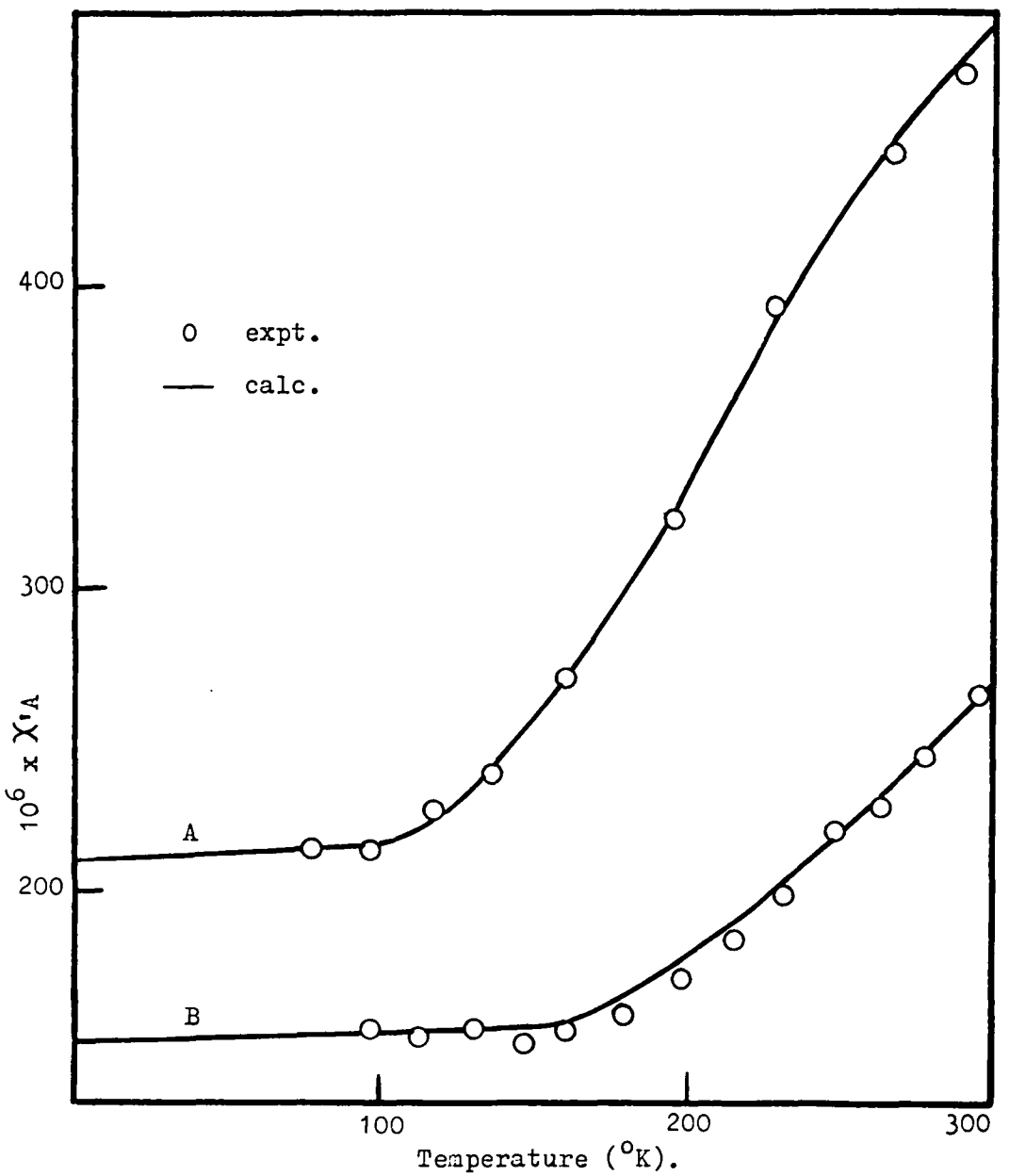

Fig.III-6. Temperature dependence of susceptibility.

A. $(Me_4N)_3Mo_2Cl_9$, calculated curve for $J = -400^oK$, $g = 1.95$, $N(\alpha) = 210 \times 10^{-6}$.

B. $Cs_3Mo_2Br_9$, calculated curve for $J = -555^oK$, $g = 1.995$, $N(\alpha) = 150 \times 10^{-6}$.

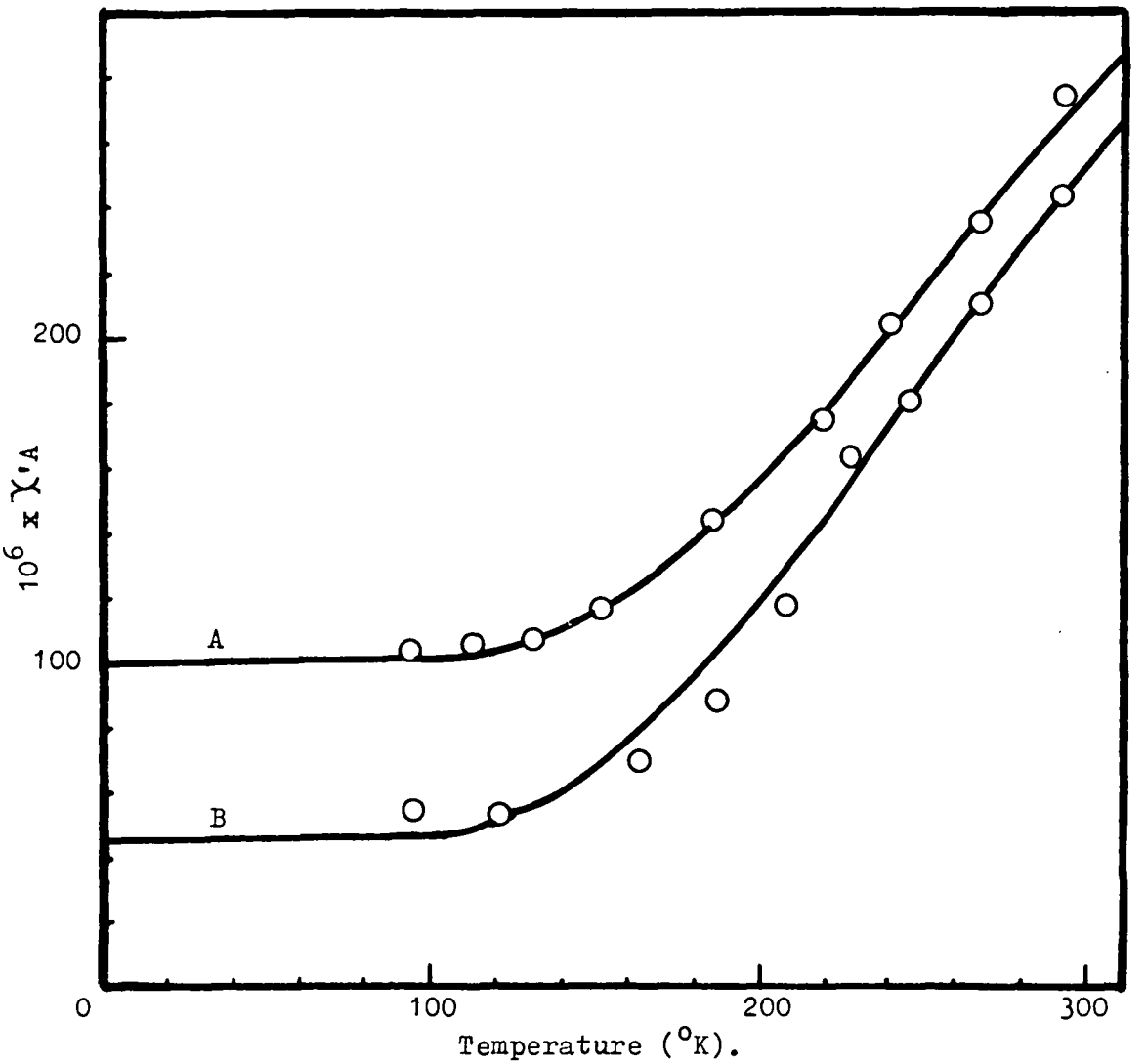

Fig.III-7. Temperature dependence of susceptibility.

A. $(H_3O)_3Mo_2Cl_9.3H_2O$, calculated curve for $J = -485^oK$, $g = 2.00$, $N(\alpha) = 100 \times 10^{-6}$;

B. $(Ph_4As)_2.H_3O.Mo_2Cl_9.xH_2O$, calculated curve for $J = -458^oK$, $g = 2.00$, $N(\alpha) = 45 \times 10^{-6}$.

C. Experimental:

The compounds $Cs_3Mo_2X_9$ (X = Cl,Br) were kindly supplied by Dr. A. G. Wedd.

The preparative procedure and results of analyses have been described elsewhere and are given in Appendix II for the compounds $(Et_3NH)_3Mo_2Cl_9$ and $(Et_4N)_3Mo_2X_9$ (X = Cl,Br).

1. Tripotassium tri-μ-chloro-hexachlorodimolybdate (III).

It has been noted that the complexes $A_3Mo_2Cl_9$, where A is a small alkali metal cation, when prepared from solution are contaminated by the corresponding mononuclear complex A_3MoCl_6. Small amounts (< 1%) of the mononuclear species have a marked effect on the magnetic properties of the binuclear species. The following solid-state method of preparation is suitable for preparing compounds $A_3Mo_2Cl_9$ free from the mononuclear complex.

Molybdenum (III) acid chloride solution (30mls) was evaporated to dryness. The resulting solid was transferred to a nitrogen filled glovebox. About half the stoichiometric amount of KCl was finely powdered and the molybdenum acid dimer added to the KCl in three portions. After the addition of each portion, the mixture was intimately ground. The extremely hygroscopic acid dimer slowly absorbed traces of moisture in the glovebox and

the mixture gradually turned to a paste. It was then vacuum dried and 50 mls. of "superdry" ethanol added. This dissolved out the excess acid dimer. The insoluble $K_3Mo_2Cl_9$ was filtered off, washed with ethanol and dried under vacuum to a light orange-brown coloured powder. A Debye-Scherrer powder x-ray photograph of the compound showed no lines attributable to KCl. All lines could be indexed on hexagonal cell closely resembling that for $Cs_3Mo_2Cl_9$ (68).

Found: Mo, 30.2, 30.3; Cl, 50.7%.

$K_3Mo_2Cl_9$ requires Mo, 30,54; Cl, 50.78%.

2. Reaction between molybdenum (III) chloride and tetraphenyl arsonium chloride:-

Acid molybdenum (III) chloride solution (25 mls) was evaporated to dryness. Three grams of tetraphenylarsonium chloride (one third stoichiometric quantity) in 50 mls. of dry ethanol was added dropwise to the solid acid dimer. A pink crystalline precipitate formed immediately which was filtered, washed with dry ethanol and vacuum dried. Yield = 3.2 grammes. An infrared spectrum run on the compound immediately after preparation showed the absence of water. On exposure to air however the compound rapidly took up ~four moles of water (as indicated by the molybdenum and chlorine analyses below). A sample which was sealed immediately and sent for micro-analyses gave

C, H, and As analyses very close to those predicted for the anhydrous $(Ph_4As)_2\ H_3O.Mo_2Cl_9$. Presumably there are holes in the structure, due to the poor packing of the $[Mo_2Cl_9]^{3-}$ anions and the bulky $(Ph_4As)^+$ cations, which can easily be filled with water molecules, leading to a stabilization of the structure:

	C	H	As	Mo	Cl
Found	44.69	3.38	11.45	13.97	23.1
$(Ph_4As)_2H_3O.Mo_2Cl_9$:	44.46	3.34	11.56	14.80	24.61
$(Ph_4As)_2H_3O.Mo_2Cl_9.4H_2O$:	42.12	3.76	10.95	14.02	23.31
$(Ph_4As)_3.Mo_2Cl_9$:	52.06	3.64	13.53	11.55	19.21

3. Tri(tetramethylammonium) tri-μ-chloro-hexachloro-dimolybdate (III).

The compound was prepared by the same method as for the tetraethylammonium salt. The complex is light orange in colour.

Found: C, 19.60; H, 5.01; Cl, 43.1; Mo, 26.2; N, 5.60%.

$(Me_4N)_3Mo_2Cl_9$ requires: C, 19.68; H, 4.95; Cl, 43.51; Mo, 26.16; N, 5.73%.

4. Tri(oxonium)tri-μ-chloro-hexachlorodimolybdate.

Acid molybdenum (III) chloride solution (30 mls.) was evaporated to dryness at room temperature. A high vacuum

was maintained for 24 hours. The dry solid was a deep red colour.

Found: Cl, 31.3; Mo, 51.0%. $(H_3O)_3Mo_2Cl_9.3H_2O$ requires: Cl, 30.9; Mo, 51.2%. Mo:Cl - 1:4.42.

5. Chromium trichloride:

Chromium trichloride was used in the preparation of the chromium complexes A_3CrCl_6 and $A_3Cr_2Cl_9$. As detailed magnetic measurements were carried out on the binuclear chromium complexes, it was essential that the materials for the preparation of these compounds be completely free from paramagnetic impurity. The most satisfactory preparative method found was a modification of the method given in Inorganic Syntheses (74). Hydrated chromium (III) chloride is reacted with carbon tetrachloride at 625°C. The reaction vessel is designed so that ferromagnetic impurities such as iron compounds distil away from the $CrCl_3$ and can be removed easily.

The product, in the form of small violet flakes, was completely field independent over the range 300-90°K. It obeyed a Curie-Weiss law - $\chi'_A = \frac{C}{(T + \theta)}$, $\theta = -32°$. μ eff = 3.89 B.M. at 300°K (μ eff = $2.84\sqrt{\chi'_A (T + \theta)}$). Found: Cr,32.72. 32.84%. $CrCl_3$ requires Cr,32.83%.

6. Chromium tribromide:

This was prepared by passing a bromine-nitrogen mixture over powdered chromium metal (99.99%) at 800°C. The compound was formed as large metallic flakes - olive green by transmitted light, and dark brown by reflected light. No field dependence of the susceptibility was noted in the range 300-90°K. $CrBr_3$ obeyed a Curie-Weiss law at high temperatures with $\Theta = -52^{\circ}$. Slight curvature was noted at temperatures $< 100^{\circ}K$. $\mu_{eff} = 3.97$ B.M. at 300°K. These results are in excellent agreement with the results of Hansen and Griffel (75).

7. Tricaesium tri-μ-chloro-hexachlorodichromate (III):

Strong precautions were taken in this preparation to remove all traces of water. Caesium chloride (Koch-Light-99.99%) was maintained under high vacuum at 200°C for four hours prior to using. Stoichiometric quantities of $CrCl_3$ and CsCl (2:3) were accurately weighed (total weight $\simeq$ 2g.) and intimately mixed in a nitrogen filled glovebox. The mixture was transferred to a small silica tube (3 cm. x 1 cm.) which had been outgassed at 700° under vacuum. The tube was sealed off at a vacuum of 10^{-6} mm. and placed in a constant temperature furnace. The temperature was increased to about ten degrees above the melting point of $Cs_3Cr_2Cl_9$ and the tube was maintained at this temperature

for three days, then slowly cooled. The tube was carefully opened in the glovebox and found to contain a glassy melt, which when broken open, was found to consist of aggregates of violet hexagonal prisms.

All lines of the powder photograph for the complex could be indexed on the hexagonal cell given by Ijdo and Wessel (20).

Found: Cl, 38.6%. $Cs_3Cr_2Cl_9$ requires: Cl, 38.83%.

The compounds $K_3Cr_2Cl_9$ and $Rb_3Cr_2Cl_9$ were prepared in exactly the same way.

8. Tricaesium tri-μ-bromo-hexabromodichromate (III):

This complex was prepared by a transpiration method. A mixture of bromine and pure dry nitrogen was passed over a mixture of CsBr : $CrBr_3$ (3:2) at 800°C. A temperature gradient was maintained along the length of the tube and the large hexagonal green crystals of the complex deposited at the cool end.

Found: Br, 58.5%. $Cs_3Cr_2Br_9$ requires: Br, 58.85%.

From powder photographs, the compound appeared to be isos-tructural with $Cs_3Cr_2Cl_9$. All observed lines could be indexed on the basis of a bimolecular hexagonal unit cell analogous to that for $Cs_3Cr_2Cl_9$.

9. Tri(tetraethylammonium) tri-μ-bromo-hexabromo-dichromate (III):

A 3:2 mixture of tetraethyl ammonium bromide and "active" chromium tribromide were refluxed in acetyl bromide for an hour and the solution then cooled in ice. The green complex precipitated as small hexagonal prisms, which were filtered, washed with acetyl bromide and vacuum dried.

Found: C, 23.6; H, 5.0; Br, 58.6; Cr, 8.45; N, 3.6%.

$C_{24}H_{60}N_3Cr_2Br_9$ requires: C, 23.75; H, 5.0; Br, 59.2; Cr, 8.55; N, 3.5%.

Analyses:

Molybdenum and chromium were determined gravimetrically as the oxinate and as barium chromate respectively (76). For those compounds with organic cations, molybdenum was also determined as MoO_3. Chlorine and bromine were analysed gravimetrically as the silver salt (77). Carbon, nitrogen and hydrogen were estimated by the Alfred Bernhardt Mikoroanalytisches Laboratorium, Mulheim, Germany.

Magnetic Measurements:

Magnetic susceptibilities were measured between 90°

and 400°K by the Gouy method. The general design of the apparatus employed closely follows that of Figgis and Nyholm(78). A 4 in. Newport Type A magnet was employed in conjunction with a Stanton centre-zero Type SM12 balance sensitive to 0.02 mgms. The field was calibrated with $CoHg(SCN)_4$ and temperatures were measured with a calibrated copper-constantan thermocouple. The dependence of susceptibility on magnetic field strength was checked at 3300 and 5770 oersteds; all measurements reported were made at 5770 oersteds. Diamagnetic corrections were made in accordance with standard values (79).

TABLE III-3

MAGNETIC DATA FOR CHROMIUM (III) BINUCLEAR COMPLEXES
(χ in C.G.S. units)

T (^{o}K)	$1/\chi'_A$	T (^{o}K)	$1/\chi'_A$
$K_3Cr_2Cl_9$		$Cs_3Cr_2Cl_9$	
293.8	182.8	297.4	182.3
265.8	168.6	259.0	161.3
230.8	151.0	231.2	146.3
176.8	123.9	204.8	131.7
142.5	107.4	178.0	117.3
116.7	94.8	152.0	102.9
96.4	85.5	126.7	88.6
88.0	81.8	97.0	72.8
$Rb_3Cr_2Cl_9$		$Cs_3Cr_2Br_9$	
295.6	186.2	293.0	174.0
266.0	170.4	265.6	159.4
238.0	155.7	242.0	146.9
210.8	141.2	211.5	130.6
176.7	122.8	185.0	116.3
143.3	105.0	158.0	102.3
117.0	91.1	133.0	88.1
96.0	80.8	108.0	75.02
91.0	78.7		

TABLE III-3
(continued)

T (^{o}K)	$1/\chi'_A$
$(Et_4N)_3Cr_2Br_9$	
291.5	153.7
271.0	142.5
244.2	128.5
215.5	114.0
188.8	99.6
161.8	85.3
143.5	75.1
124.0	63.9
98.0	51.8

TABLE III-4

MAGNETIC DATA FOR
MOLYBDENUM (III) BINUCLEAR COMPLEXES
(χ in C.G.S. units)

T (^{o}K)	$10^{6}\chi'_{A}$ (uncorr.)	$10^{6}\chi'_{A}$ (corr.)	μ_{eff} B.M.
	$Cs_3Mo_2Br_9$		
295.8	285.7	264.5	0.52
277.8	267.2	244.2	0.46
263.5	252.5	227.9	0.42
249.1	246.9	220.4	0.375
232.5	226.7	197.6	0.30
215.3	215.6	183.3	0.24
198.0	206.3	169.8	0.18
179.4	200.8	158.5	0.11
159.8	204.6	153.7	0.07
147.0	208.2	149.6	0.00
129.8	226.7	153.2	0.06
113.4	248.8	151.5	0.04
97.0	294.9	155.0	0.03

TABLE III (continued)

T (^{o}K)	$10^{6}\chi'_{A}$ (uncorr.)	$10^{6}\chi'_{A}$ (corr.)	μ_{eff} B.M.
	$Cs_3Mo_2Cl_9$		
368.3	183.9	176.9	0.62
357.2	178.0	170.7	0.60
347.5	172.0	164.5	0.58
337.0	162.6	154.8	0.545
323.1	156.8	148.6	0.52
312.8	151.5	143.0	0.50
295.5	126.3	117.0	0.415
293.3	130.9	121.7	0.43
277.8	117.5	101.6	0.375
263.6	107.0	96.5	0.33
249.0	98.2	86.9	0.29
232.5	87.7	75.3	0.24
215.3	76.0	62.3	0.17
198.0	70.2	54.8	0.125
179.6	70.2	52.5	0.10
161.5	71.9	51.2	0.09
143.0	73.7	48.6	0.06
129.8	77.2	47.6	0.05
113.4	86.0	48.0	0.05
93.3	107.0	48.7	0.05

TABLE III (continued)

T (°K)	$10^6\chi'_A$	μ_{eff} B.M.
	$K_3Mo_2Cl_9$	
449.0	172.4	0.59
428.0	156.2	0.53
406.4	143.0	0.47
386.0	132.6	0.42
376.5	129.0	0.405
364.3	123.7	0.38
349.0	116.2	0.34
320.7	99.6	0.25
293.5	87.2	0.17
260.0	83.1	0.13
226.0	87.2	0.15
192.3	83.1	0.11
152.8	87.2	0.12
128.3	83.1	0.09
98.0	75.0	0.00
	$(Me_4N)_3Mo_2Cl_9$	
291.0	468.7	0.78
266.0	442.8	0.705
229.3	393.5	0.58
195.5	323.0	0.42
160.5	271.3	0.28

T (°K)	$10^6\chi'_A$	μ_{eff} B.M.
(cont.)	$(Me_4N)_3Mo_2Cl_9$	
136.3	238.5	0.18
116.6	226.6	0.125
97.0	212.7	0.045
	$(Et_4N)_3Mo_2Cl_9$	
291.7	430.5	0.96
271.3	383.5	0.865
251.0	349.5	0.79
230.5	306.2	0.70
210.2	263.0	0.615
193.0	212.9	0.52
173.0	167.5	0.42
162.5	158.2	0.39
152.8	126.5	0.325
136.5	99.0	0.255
120.3	71.5	0.175
110.4	67.0	0.155
98.0	67.0	0.15

TABLE III (continued)

T (°K)	$10^6\chi'_A$	μ_{eff} B.M.
	$(Et_4N)_3Mo_2Br_9$	
293.3	728.4	1.09
277.8	711.4	1.04
260.2	674.6	0.965
249.9	653.4	0.92
226.0	604.4	0.83
200.5	541.9	0.71
182.3	496.1	0.625
163.3	442.1	0.53
153.7	396.6	0.455
146.7	388.4	0.43
131.8	322.0	0.31
119.5	305.5	0.27
114.5	284.7	0.225
98.0	264.0	0.16
90.5	255.8	0.14
	$(Et_3NH)_3Mo_2Cl_9$	
296.3	304.2	0.80
271.3	276.5	0.73
264.2	253.7	0.68
249.8	230.9	0.63
232.8	200.4	0.56
(cont.)	$(Et_3NH)_3Mo_2Cl_9$	
215.4	167.2	0.48
198.3	138.8	0.41
179.6	110.0	0.33
163.5	88.3	0.265
147.0	70.6	0.205
129.6	56.2	0.15
115.2	51.2	0.12
100.0	44.1	0.085
	$(H_3O)_3Mo_2Cl_9.3H_2O$	
293.0	275.3	0.64
291.7	270.5	0.63
267.0	236.3	0.54
240.0	205.0	0.45
219.0	175.9	0.37
185.5	144.4	0.26
151.5	117.7	0.15
131.7	108.2	0.095
112.5	106.7	0.08
94.0	105.0	0.06

TABLE III (continued)

T (^{o}K)	$10^{6}\chi_{A}$	μ_{eff} B.M.
$(Ph_4As)_2H_3O.Mo_2Cl_9.xH_2O$		
291.7	244.6	0.69
268.0	211.2	0.61
247.4	181.4	0.52
228.0	163.8	0.47
208.1	118.3	0.35
187.3	88.2	0.255
163.8	70.5	0.18
147.8	53.2	0.10
120.6	53.5	0.09
115.0	51.7	0.08
95.0	55.4	0.09

CHAPTER IV

X-RAY STRUCTURAL STUDIES ON $A_3M_2X_9$ COMPLEXES OF CHROMIUM (III) AND MOLYBDENUM (III).

A. Review:

The structure of a binuclear transition element complex of type $A_3M_2X_9$ was first reported by Wessel and Ijdo (20) for $Cs_3Cr_2Cl_9$. The complex has a bimolecular hexagonal cell with a = 7.22, c = 17.93 A, and space group $P6_3/mmc$.

The structure is best described as hexagonal close packing of caesium and chloride ions, which are approximately the same size, to form layers $CsCl_3$. The chromium ions occupy two thirds of the octahedral sites between layers, with chlorines as nearest neighbours. The ordering of the layers is as shown in Fig.IV-1, resulting in pairs of chromium atoms. In the binuclear anions, the chromium atoms are displaced away from the centres of the octahedra to give a relatively large Cr-Cr separation of 3.12 A (c.f. 2.5 A in the metal). The direct metal-metal bond is expected to be negligible and in fact, the compound exhibits normal paramagnetic behaviour, the room temperature moment being reduced only slightly below the spin-only value of 3.87 B.M. The electronic spectrum (80) also closely resembles that for mononuclear $[CrCl_6]^{3-}$.

(a)

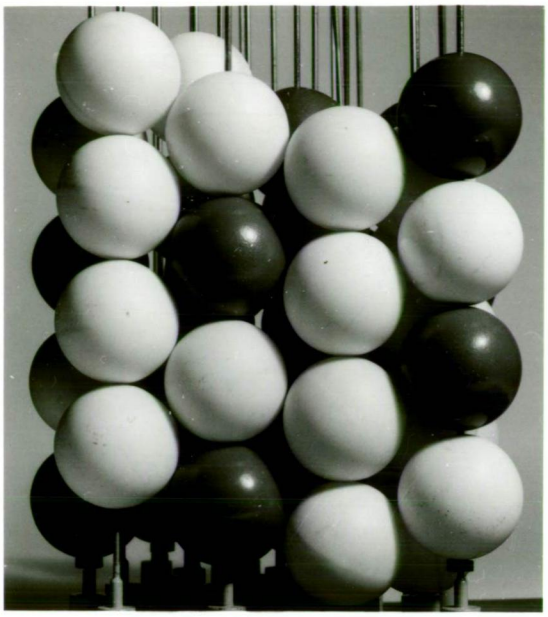

B A B C A C

(b)

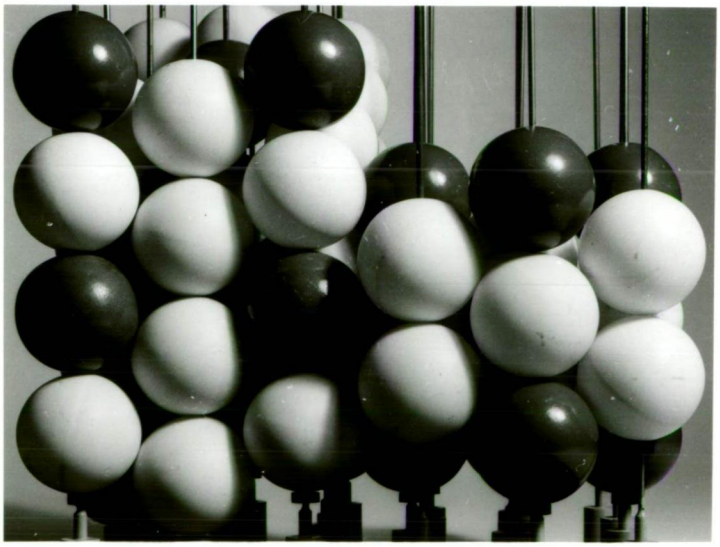

Fig.IV-1. (a) Packing of cations A and ligands X to form layers AX_3.

(b) Ordering of layers in a unit cell for $A_3M_2X_9$.

A detailed structural determination for $K_3W_2Cl_9$ revealed that in the binuclear anion the tungsten atoms are displaced towards each other to give a very short W-W distance of 2.409 Å (c.f. 2.74 Å in the metal) (21). The reported diamagnetism (69) is consistent with the presence of a strong W-W bond.

In this laboratory, P.W. Smith has recently determined the structure of $Cs_3Mo_2Cl_9$ (56). Although this compound has the same space group as $Cs_3Cr_2Cl_9$, the binuclear unit is more closely analogous to that in $K_3W_2Cl_9$ in that the two molybdenum atoms are displaced towards each other, giving a Mo-Mo separation of 2.68 Å (c.f. 2.73 Å in the metal). The electronic spectra of the tungsten and molybdenum binuclear complexes, although generally similar to the spectra for the $[MCl_6]^{3-}$ compounds, show additional peaks which apparently are due to essentially metal-metal transitions (80).

The stability incurred by the formation of a metal-metal bond is indicated by the existence of binuclear $[W_2Cl_9]^{3-}$ and $[Mo_2Cl_9]^{3-}$ ions in solution, whereas the corresponding chromium complex anion $[Cr_2Cl_9]^{3-}$ is not known in aqueous solution.

The investigations reviewed here serve to illustrate the particular interest of the binuclear complexes $A_3M_2X_9$ in the study of metal-metal interactions. The influence

of the metal on the strength of the metal-metal bond and on the structure of the binuclear anion has been discussed in several reviews (70,81,82)

The results of the magnetic studies of Chapter III and of spectral studies (83) on this system indicate that the binuclear anion is also very sensitive to change in the size of the cation, A. In fact, increasing the cation size results eventually in a change of the stoichiometry from $A_3M_2X_9$ to $A_2BM_2X_9$ ($B = H_3O^+$, $M = Mo$).

In this investigation the influence of the cation on the structure of the binuclear anion has been examined quantitatively by determining the three-dimensional structure of $K_3Mo_2Cl_9$ from a single crystal x-ray analysis and comparing it with the structure of $Cs_3Mo_2Cl_9$ (56). Detailed correlations with powder data have enabled important structural parameters for the other compounds $A_3M_2X_9$ (M = Cr(III), Mo(III)) studied, to be determined.

In the following sections the results of these x-ray studies are discussed in detail to form a basis for the understanding of the mechanisms for magnetic interactions in $A_3M_2X_9$ binuclear complexes to be discussed in Chapter V.

TABLE IV-1

INTERATOMIC DISTANCES AND ANGLES FOR $A_3M_2Cl_9$

	$Cs_3Cr_2Cl_9$	$Cs_3Mo_2Cl_9$	$K_3Mo_2Cl_9$	$K_3W_2Cl_9$
Cl_t-Cl_t (Å)	3.40	3.42	3.46	3.44
Cl_{br}-Cl_{br}	3.43	3.70	3.715	3.76
Cl_t-Cl_{br}	-	3.395	3.355	3.29
M-M	3.12	2.680	2.532	2.409
M-Cl_t	2.34	2.40	2.41	2.40
M-Cl_{br}	2.52	2.52	2.50	2.48
Cl_t-M-Cl_t (°)	93.2	91.0	91.5	91.4
Cl_{br}-M-Cl_{br}	85.8	95.3	96.5	98.4
Cl_t-M-Cl_{br}	-	87.3	86.4	84.8
M-Cl_{br}-M	76.5	64.3	61.0	58.1

B. The effect of the cation in $A_3M_2X_9$ compounds:

The details of the single crystal x-ray structural investigation on $K_3Mo_2Cl_9$ are given in the Experimental Section. Relevant structural parameters associated with the complex anion $[Mo_2Cl_9]^{3-}$, for both $K_3Mo_2Cl_9$ and $Cs_3Mo_2Cl_9$ are compared in Table IV-1. Also listed are the corresponding parameters for $Cs_3Cr_2Cl_9$ and $K_3W_2Cl_9$.

From Table IV-1 it is apparent that the change of cation has negligible effect on the molybdenum-chlorine bond lengths. However, on decreasing the size of the cation from caesium to potassium, the molybdenum-molybdenum bond length decreases from 2.68 to 2.53 A. Also, although there is negligible change in the angles associated with the terminal halogens, the metal-bridging chlorine-metal angle is decreased from 64.3° to 61.0°.

The overall effect of the change of cation is thus to "concertina" the $[Mo_2Cl_9]^{3-}$ anion. Decreasing the size of the cation, then has the same qualitative effect as increasing the metal-metal bonding power of the central metal, i.e. a compression of the M-X_3-M bridging structure. This is illustrated by comparing with the tabulated parameters for $Cs_3Cr_2Cl_9$ and $K_3W_2Cl_9$.

The effect of the cation on the structure of the $[M_2X_9]^{3-}$ anion is easily seen from a study of the actual three dimensional packing, illustrated in Figure IV-2. The structure contains two distinct cation sites, designated as (A) and (B) in the diagram. Cation type (A), of which there are two per molecular formula, is shared by four $[M_2X_9]^{3-}$ anions. It has twelve nearest halogen neighbours - two terminal halogens and one bridging halogen from each of three lateral $[M_2X_9]^{3-}$ units, and three terminal halogens from the fourth $[M_2X_9]^{3-}$ anion. As the cation size is increased, the interstice can expand to incorporate it both laterally (in the aa' plane) by the moving apart of the three lateral $[M_2X_9]^{3-}$ units, and longitudinally, by the fourth $[M_2X_9]^{3-}$ anion moving apart from the three lateral units.

Cation type (B), one per molecular formula, is shared by only three lateral type $[M_2X_9]^{3-}$ anions. It packs in the plane of the bridging halogen atoms and thus is shared by two bridging and two terminal (one above and one below) halogens from each of the three anions. Cation site (B) is restricted with respect to change in cation size. As the cation size is increased, again there is lateral expansion of the three anionic units. However to incorporate the longitudinal increase in cation size, the separate $[M_2X_9]^{3-}$ units must expand. Thus the concertina effect observed is the result of the restricted

(B) cation site. This restriction is manifested in the changeover in stoichiometry from $A_3M_2X_9$ to $A_2B\ M_2X_9$ when one reaches a limiting cation size. For molybdenum complexes, it has been observed that the cation Et_4N^+ forms complexes of the former type while Ph_4As^+ gives rise to a complex of formula $(Ph_4As)_2.(H_3O).Mo_2Cl_9$.

To summarize, the effect of change of cation is to give rise to a trigonal distortion of the bridge structure of the complex anion. Increase in cation size results in an expansion of the binuclear unit. The increased metal-metal separation should result in a weaker direct magnetic interaction.

In the complexes $A_3M_2X_9$, as typified by $K_3Mo_2Cl_9$ and $Cs_3Cr_2Cl_9$, the metal atoms occupy special positions

2M in(1/3, 2/3, z); (1/3, 2/3, 1/2 - z)

in the bimolecular hexagonal unit cells. The separation between pairs of metals in the binuclear anions is then simply (2z - 0.5) x c, where c is the length of the c axis. In an isostructural series of such complexes, the metal-metal separations would hence be in direct ratio to the lengths of the c axes.

However, a basic assumption underlying

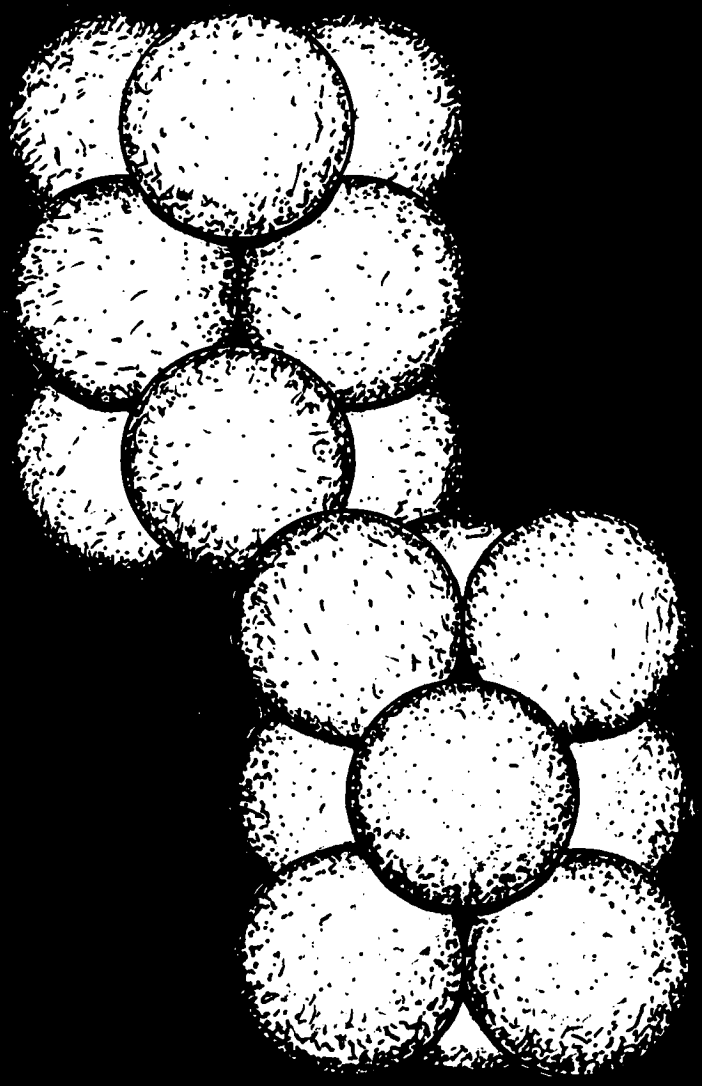

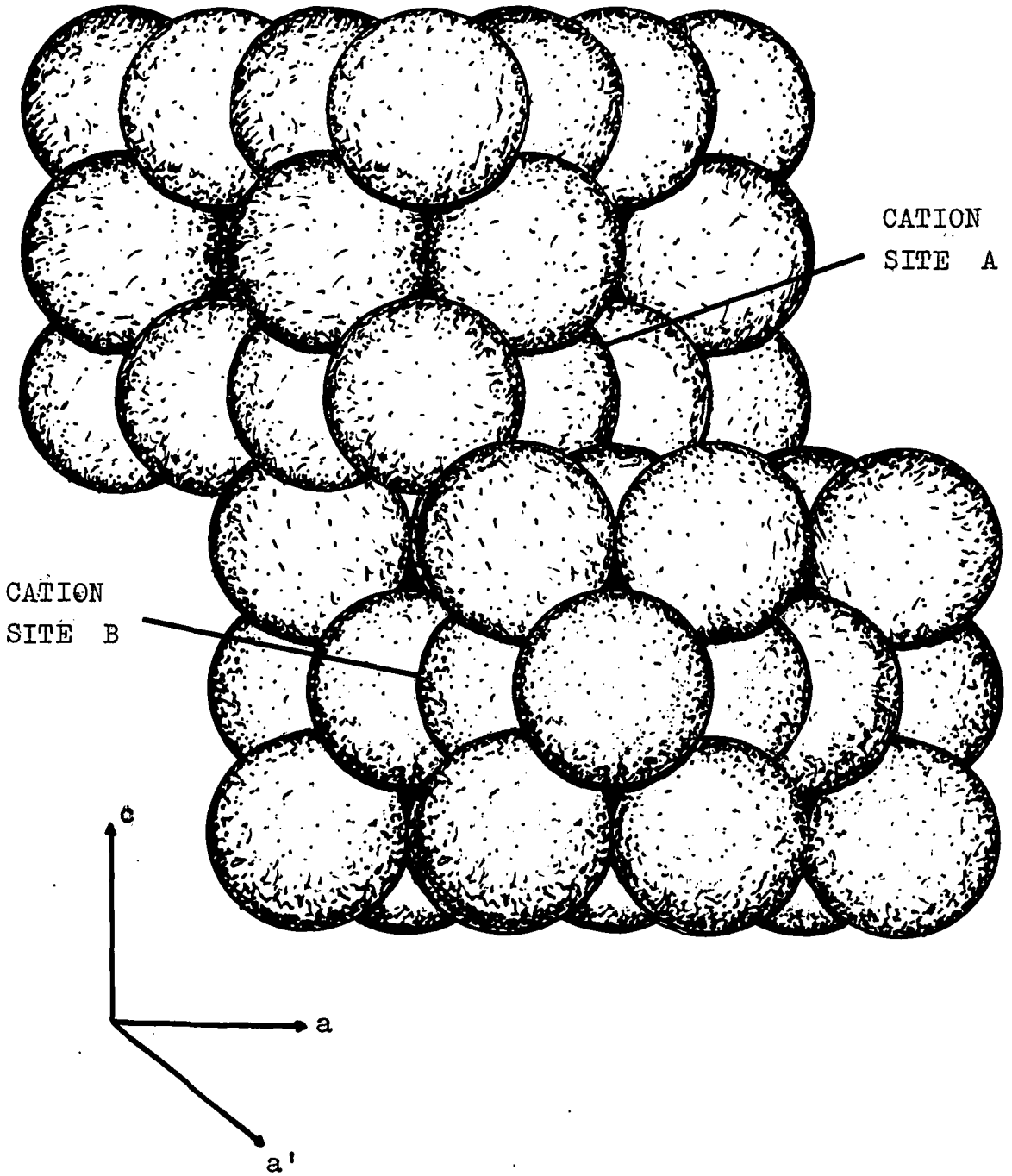

Fig.IV-2. Cation sites in $A_3M_2X_9$.

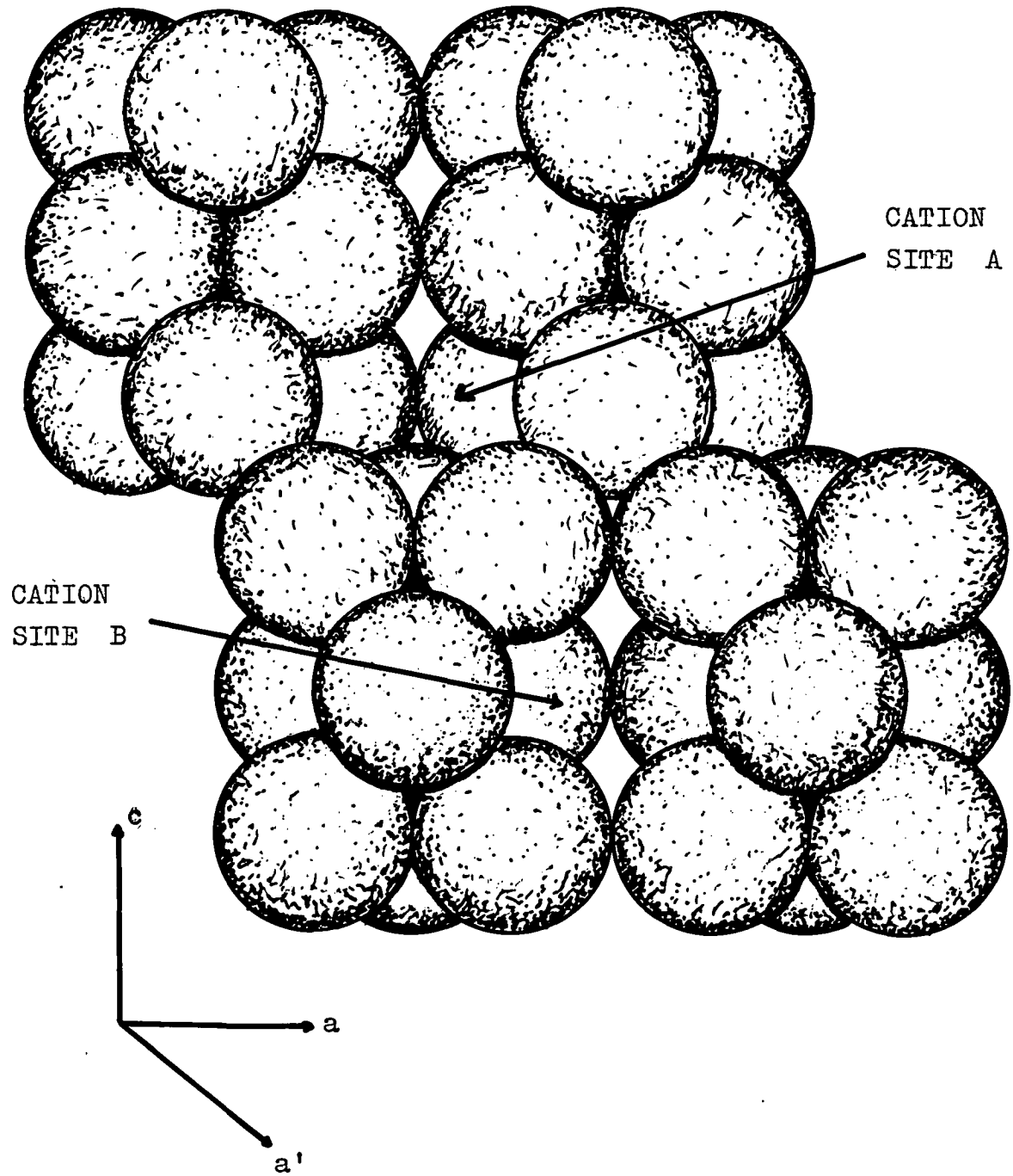

Fig.IV-2. Cation sites in $A_3M_2X_9$.

the definition of isostructuality is the absence of perturbing forces on the packing of the atoms, i.e., geometrical packing alone must influence the variation of cell dimensions in an isostructural series. The presence of metal-metal bonding is such a perturbing force and its variation in the series of complexes studied implies they cannot be classed as members of a strictly isostructural series. This is illustrated by the variation of the metal "z" cordinate from $K_3W_2Cl_9$ to $Cs_3Cr_2Cl_9$ in Table IV-2. The metal z coordinates show a definite relationship to the metal-metal bonding, as represented by the magnetic exchange integral, J. i.e., the larger the magnetic exchange integral, the smaller is the metal z coordinate.

TABLE IV-2

COMPLEX	$K_3W_2Cl_9$	$K_3Mo_2Cl_9$	$Cs_3Mo_2Cl_9$	$Cs_3Cr_2Cl_9$
z (Metal)	0.3241	0.3261	0.3265	0.3370
$-J$ (^oK)	$>1000^o$	800	605	9

It was important therefore, to determine the extent to which the strict isostructuality is violated as the metal-metal bonding is changed in a series with the same metal and different cations. From Table IV-2 almost identical values of z(Mo) are obtained for $K_3Mo_2Cl_9$ and $Cs_3Mo_2Cl_9$ even though there is an appreciable change in Mo-Mo bonding (magnetic exchange parameter, J, varies from -800^o to -605^o). Thus from $K_3Mo_2Cl_9$ to $Cs_3Mo_2Cl_9$, the metal-metal separation is simply (2 x 0.326 - 0.5) x c, = 0.152 c, i.e., a function only of the c axial length.

To enable a quantitative interpretation of the magnetic data in terms of metal-metal separation, this relationship was carried over to estimate the Mo-Mo distance for the series of molybdenum complexes studied, directly from the length of the c axis as obtained from powder photographs. This is a reasonable interpolation for those complexes whose powder x-ray photos indicate isostructuality with the caesium salt. The interpolation is likely to be in error only for complexes with very large cations such as $(Et_4N)^+$, ($J \simeq -300^oK$). In this case, Table II-2 indicates a larger z(Mo) may be necessary.

Similarly using the fractional coordinate,

$z = 0.3370$ for $Cs_3Cr_2Cl_9$ gives the relation:

$$Cr - Cr = 0.174\ c$$

from which the chromium- chromium separations in the other chromium complexes studied were calculated. Unit cell c parameters were determined from powder photographs on the compounds.

Finally, in the discussion of possible superexchange mechanisms in $A_3M_2X_9$ it would be of value to have estimates of the bridging angles, $\angle$M-X-M for the compounds. The results listed in Table IV-1 indicate that there is negligible change in the metal-bridging ligand bond lengths, M-X_{br}, with change in the bridging angle. This is supported by the far infrared results in Appendix-1. Using the values of M-Cl_{br} from Table IV-1 and M-M from Table IV-3 the bridging angle $\angle$M-X-M was then calculated directly using trigonometry. For the bromide complexes an estimate of M-Br_{br} was obtained from the values of Ti-Br_{br} in $Rb_3Ti_2Br_9$ and $Cs_3Ti_2Br_9$ which are isostructural with $Cs_3Cr_2Cl_9$ (85).

In Table IV-3 unit cell parameters are tabulated for the complexes studied in both the chromium and molybdenum series, together with calculated metal-metal separations and metal-halogen-metal bridge angles.

TABLE IV-3

UNIT CELL PARAMETERS, METAL-METAL SEPARATIONS AND BRIDGING ANGLES - $A_3M_2X_9$.

COMPOUND	a(Å)	c(Å)	M-M(Å)	Angle M-X-M(°)
$K_3Mo_2Cl_9$	7.11	16.63	2.53	61
$Rb_3Mo_2Cl_9$	7.18	16.98	2.59	62
$Cs_3Mo_2Cl_9$	7.35	17.51	2.68	64
$(Me_4N)_3Mo_2Cl_9$	9.27	20.50	3.13	77
$(Et_4N)_3Mo_2Cl_9$	10.08	22.45	3.43	86
$Cs_3Mo_2Br_9$	7.64	18.35	2.80	62.5
$(Et_4N)_3Mo_2Br_9$	10.30	23.13	3.53	82
$K_3Cr_2Cl_9$	6.88	17.52	3.048	74.5
$Rb_3Cr_2Cl_9$	6.99	17.65	3.07	75
$Cs_3Cr_2Cl_9$	7.22	17.93	3.12	76.5
$(Et_4N)_3Cr_2Cl_9$	9.96	22.35	3.89	100
$Cs_3Cr_2Br_9$	7.51	18.72	3.26	74
$(Et_4N)_3Cr_2Br_9$	10.18	23.03	4.00	95

C. Experimental:

Determination of the structure of $K_3Mo_2Cl_9$:

The preparation of $K_3Mo_2Cl_9$ is described in Section III-C. Lattice parameters for the compound were obtained from powder photographs taken on a Guinier-Hägg focusing camera, with potassium chloride as an internal calibrant. The parameters are in close agreement with those obtained by Ijdo (68) and confirm the bimolecular hexagonal cell with

$$a = 7.115 \pm 0.005,\ c = 16.632 \pm 0.01\ A.$$

Single crystals were obtained by fusing the powdered compound in a sealed evacuated quartz tube placed in a temperature gradient. Small hexagonal plates developed in the cool end of the tube.

Intensity data were obtained with Cu Kα radiation from a small crystal measuring 0.15mm x 0.15mm x 0.05mm. The intensities of 300 unique observable reflections from the 0kl→ 2kl zones were collected by means of a Weissenberg camera using the multiple film technique and estimated visually by comparison with a calibrated intensity scale. Lorentz-polarization corrections were applied.

The systematic extinctions found (00l only when $l \neq 2n$) are compatible with the space group C_{6h}^2 - $P6_3/m$.

This is the space group established for the related $K_3W_2Cl_9$ by Watson and Waser (21). Using the refined atom fractional coordinates for this compound, reasonable agreement with the intensity data was obtained, as indicated by an initial R factor of 0.18. ($R = \sum(|Fc| - |Fo|)/\sum|Fo|$). These parameters were refined by six cycles of least squares refinement incorporating isotropic temperature factors to a final R-factor of 0.135. The refinements were run on an Elliot 503 Computer using a least squares refinement programme written in machine code by Dr. P.J. Wheatley and made available by the late Dr. A.D. Wadsley. As this programme is not suitable for refining in hexagonal symmetry the refinements were carried out in triclinic symmetry. Suitable corrections to atom shifts were made after each refinement to satisfy the higher symmetry requirements of the hexagonal space group.

Table IV-4 lists the final fractional coordinates together with standard deviations, from the least squares treatment. Also listed are the isotropic thermal parameters, $U = B/8\pi^2$, where B is employed in the usual expression $\exp(-B\sin^2\theta/\lambda^2)$ in the calculation of the structure factors. The observed and calculated structure factors are given in Table IV-6. Important bond lengths and angles associated with the binuclear $[Mo_2Cl_9]^{3-}$ anion

are listed in Table IV-5, together with standard deviations.

From Table IV-4 it is seen that the standard deviations for the chlorine "x" coordinates are quite large. This is mainly due to the limited reflection data used, from the zero and first two levels about the a axis only. Also the linear absorption coefficient for this compound when subjected to CuKα radiation is quite large, although no correction was applied for absorption. An accurate refinement of the structure, using reflections from the levels okl→8kl and hko→hk4, obtained with Mo radiation is being carried out.

However the main object of the structure determination was to determine accurately the molybdenum-molybdenum separation, which reflects the distortion of the binuclear anion. From Table IV-5 it is seen that this has been achieved, the standard deviation for Mo-Mo being only 0.005 Å.

The structure of the complex bears a strong resemblance to that for $K_3W_2Cl_9$. The pairs of octahedra forming the binuclear anion, $[Mo_2Cl_9]^{3-}$, are drawn together resulting in a "bulging out" of the shared face (Clbr-Clbr = 3.72 Å c.f. Clt-Clt = 3.46 Å). The two molybdenum atoms are displaced from the centres of the chlorine octahedra towards one another to give a short Mo-Mo separation of 2.532 Å (c.f. 2.73 Å in the metal).

Thus in this compound, as with the tungsten analogue, strong metal-metal bonding is present.

Powder Photographs:

The unit cell parameters for the complexes studied, listed in Table IV-3 were obtained using a Hägg-Guinier focusing powder camera with potassium chloride or silicon as an internal calibrant. Many of the complexes were extremely moisture sensitive and a special sampling technique, developed in the course of this work and described elsewhere, was employed. (Appendix 2) In some cases the cell parameters were obtained from data collected on a Debye-Scherrer camera.

TABLE IV-4

REFINED FRACTIONAL COORDINATES AND TEMPERATURE FACTORS

Atom	Space Group Position	Parameters	Standard Deviation	Isotropic Thermal Parameter U
2K	2a	-		0.030
4K	4f	z = 0.5694	0.0011	0.033
4Mo	4f	z = 0.3261	0.0004	0.008
$6Cl_{br}$	6h	x = 0.4623	0.0084	0.016
		y = 0.4508	0.0028	
$12Cl_{t}$	12i	x = 0.1292	0.0084	0.021
		y = 0.3460	0.0028	
		z = 0.4075	0.0012	

TABLE IV-5

INTERATOMIC DISTANCES AND ANGLES FOR $K_3Mo_2Cl_9$

Atoms	Separation (Å)	Standard Deviation (Å)
Mo-Mo	2.532	0.005
Mo-Cl_t	2.41	0.038
Mo-Cl_{br}	2.50	0.035
Cl_t-Cl_t	3.46	0.054
Cl_{br}-Cl_{br}	3.71	0.050
	Angles (Degrees)	
Cl_t-M-Cl_t	91.5	1°
Cl_{br}-M-Cl_{br}	96.5	1°
Cl_t-M-Cl_{br}	86.4	1°
M-Cl_{br}-M	61.0	0.5°

TABLE IV-6

STRUCTURE FACTORS FOR $K_3Mo_2Cl_9$

h	k	l	Fo	Fc	h	k	l	Fo	Fc
0	0	2	796	-995	0	1	19	304	312
0	0	4	752	-605	0	1	21	471	-482
0	0	6	1757	-1573	0	2	0	648	-689
0	0	8	670	-582	0	2	1	236	-165
0	0	10	97	-9	0	2	2	1020	-1082
0	0	12	2650	2212	0	2	3	1662	1807
0	0	14	1382	-1273	0	2	4	1516	1634
0	0	16	123	115	0	2	5	1382	1407
0	0	18	110	-148	0	2	6	663	-685
0	1	0	828	-851	0	2	7	1515	-1695
0	1	1	1072	1185	0	2	8	1200	1338
0	1	2	294	265	0	2	9	579	-520
0	1	3	164	-137	0	2	10	926	-859
0	1	4	201	206	0	2	11	319	275
0	1	5	990	-1196	0	2	12	235	-217
0	1	6	565	-593	0	2	13	403	-333
0	1	7	711	754	0	2	14	124	-74
0	1	8	746	684	0	2	15	983	784
0	1	9	549	-450	0	2	16	650	493
0	1	10	244	176	0	2	17	111	103
0	1	11	106	-142	0	2	18	583	-443
0	1	12	518	-404	0	2	19	899	-779
0	1	13	1448	1098	0	2	20	522	503
0	1	14	299	264	0	3	0	1631	1754
0	1	15	410	-341	0	3	1	188	-179
0	1	16	299	-218	0	3	2	715	638
0	1	17	524	-385	0	3	3	87	-84
0	1	18	265	-253	0	3	4	181	-239

TABLE IV-6
(continued)

h	k	l	Fo	Fc	h	k	l	Fo	Fc
0	3	5	133	-105	0	5	1	522	-603
0	3	6	790	759	0	5	2	120	-24
0	3	7	145	171	0	5	3	450	600
0	3	8	894	-1005	0	5	4	321	378
0	3	10	308	-345	0	5	5	600	759
0	3	12	988	862	0	5	6	536	-565
0	3	14	723	-570	0	5	7	791	-812
0	3	16	497	363	0	5	10	120	-77
0	3	18	521	443	0	5	11	257	262
0	4	0	564	-595	0	5	12	110	-197
0	4	1	400	402	0	5	13	685	-615
0	4	2	441	-472	0	5	15	521	493
0	4	3	708	-907	0	6	0	1444	1477
0	4	4	933	950	0	6	1	85	-125
0	4	5	988	-1038	0	6	2	570	-495
0	4	6	480	-508	0	6	3	84	-56
0	4	7	1039	1188	0	6	4	253	-229
0	4	8	752	926	0	6	5	84	-80
0	4	9	121	161	0	6	6	201	269
0	4	10	426	-526	0	6	7	80	133
0	4	11	174	-221	0	6	8	515	-589
0	4	12	244	-250	0	6	9	75	34
0	4	13	461	447	0	6	10	70	-150
0	4	15	648	-571	0	6	11	64	35
0	4	16	390	303	0	6	12	1019	886
0	4	17	115	-161	0	7	0	283	-414
0	4	18	275	-349	0	7	1	345	360
0	5	0	239	-373	0	7	4	422	523

TABLE IV-6
(continued)

h	k	l	Fo	Fc	h	k	l	Fo	Fc
0	7	5	536	-658	1	2	5	1220	-1215
0	7	6	272	-336	1	2	6	969	-1036
0	7	7	570	776	1	2	7	966	1005
0	7	8	434	559	1	2	8	536	622
1	1	0	1565	1452	1	2	9	318	-316
1	1	2	702	-670	1	2	10	408	438
1	1	3	801	-849	1	2	11	86	-94
1	1	4	181	-183	1	2	12	89	-102
1	1	5	177	134	1	2	13	1080	788
1	1	6	1261	1231	1	2	15	398	-351
1	1	7	90	126	1	2	16	575	-403
1	1	8	1257	-1237	1	2	17	442	-359
1	1	9	515	497	1	2	18	490	-364
1	1	10	547	-476	1	2	19	484	456
1	1	11	232	-193	1	2	20	391	461
1	1	12	769	702	1	3	1	567	-358
1	1	13	127	-107	1	3	2	507	539
1	1	14	532	-471	1	3	3	72	78
1	1	15	289	-268	1	3	4	300	-296
1	1	16	665	456	1	3	5	1217	1310
1	1	17	252	189	1	3	6	794	-927
1	1	18	768	584	1	3	7	1071	-1169
1	1	19	60	70	1	3	8	417	443
1	1	20	936	-799	1	3	9	429	451
1	2	1	790	700	1	3	10	474	574
1	2	2	467	397	1	3	11	129	-62
1	2	3	329	-319	1	3	12	224	-114
1	2	4	167	-113	1	3	13	676	-553

TABLE IV-6
(continued)

h	k	l	Fo	Fc	h	k	l	Fo	Fc
1	3	14	77	199	1	5	5	339	-300
1	3	15	233	218	1	5	8	248	352
1	3	16	677	-501	1	5	9	120	-162
1	3	17	536	443	1	5	10	81	-83
1	3	18	260	-315	1	5	11	324	-422
1	4	0	957	1155	1	5	12	529	-563
1	4	1	119	146	1	5	13	1134	1148
1	4	2	561	-637	1	5	14	366	350
1	4	3	662	788	1	5	15	429	-421
1	4	4	86	-65	1	6	0	626	-670
1	4	5	87	-48	1	6	1	899	-928
1	4	6	827	861	1	6	2	82	-35
1	4	7	221	-254	1	6	3	81	-55
1	4	8	742	-815	1	6	4	278	420
1	4	9	501	-569	1	6	5	369	386
1	4	10	406	-424	1	6	6	151	-148
1	4	11	127	188	1	6	8	388	445
1	4	12	623	646	1	6	9	371	354
1	4	13	232	238	1	6	11	266	260
1	4	14	588	-498	1	7	0	505	675
1	4	15	362	327	1	7	1	56	104
1	4	16	455	425	1	7	2	269	-297
1	4	17	181	-228	1	7	3	291	-466
1	5	0	867	-951	1	7	4	174	-241
1	5	1	1213	1183	1	7	5	158	175
1	5	2	224	128	1	7	6	456	695
1	5	3	224	-237	2	1	0	1081	-1027
1	5	4	204	302	2	1	1	1395	-1357

TABLE IV-6
(continued)

h	k	l	Fo	Fc	h	k	l	Fo	Fc
2	1	2	220	123	2	3	3	239	-327
2	1	3	521	459	2	3	4	282	286
2	1	4	358	371	2	3	5	876	-1069
2	1	5	856	745	2	3	6	393	-479
2	1	6	418	-311	2	3	7	842	1045
2	1	7	457	-449	2	3	8	495	557
2	1	8	586	602	2	3	9	273	-226
2	1	9	169	188	2	3	10	79	25
2	1	11	282	350	2	3	11	78	-67
2	1	12	439	-494	2	3	12	375	-307
2	1	13	1497	-1189	2	3	13	622	530
2	1	14	432	297	2	3	14	168	200
2	1	15	643	478	2	3	15	332	-333
2	1	16	73	-89	2	3	16	55	-95
2	1	17	332	224	2	3	17	283	-316
2	1	18	268	-186	2	4	0	456	-491
2	1	19	212	-193	2	4	1	553	-566
2	1	20	261	288	2	4	2	248	-192
2	2	2	703	-727	2	4	3	658	635
2	2	4	379	-383	2	4	4	641	592
2	2	6	425	-466	2	4	5	707	726
2	2	8	541	-612	2	4	6	460	-437
2	2	10	77	-94	2	4	7	824	-814
2	2	12	1696	1577	2	4	8	649	677
2	2	14	1068	-975	2	4	9	75	-77
2	3	0	542	-550	2	4	10	330	-292
2	3	1	494	421	2	4	11	314	275
2	3	2	70	95	2	4	12	208	-243

TABLE IV-6
(continued)

h	k	l	Fo	Fc
2	4	13	540	-573
2	4	14	132	94
2	4	15	557	509
2	5	0	1363	1532
2	5	2	455	-387
2	5	4	333	-357
2	5	6	236	176
2	5	8	494	-609
2	5	10	58	-11
2	5	12	743	915
2	6	0	306	-362
2	6	1	327	384
2	6	2	58	60
2	6	3	58	-114
2	6	4	233	233
2	6	5	522	-671
2	6	6	268	-352
2	6	7	597	684
2	6	8	328	399

CHAPTER V

MECHANISMS FOR MAGNETIC EXCHANGE IN BINUCLEAR HALIDE COMPLEXES OF CHROMIUM(III) AND MOLYBDENUM(III).

The results of the magnetic studies on the $A_3M_2X_9$ compounds reported in Chapter III indicate a marked dependence of the magnetic exchange on the metal M. Within series of complexes of a particular metal the exchange integral also shows significant trends as both the cation A and the ligand X are varied. In the preceding chapter the structural variations within these series of compounds have been discussed.

The aim of this chapter is to obtain information on the mechanisms for magnetic exchange in the $A_3M_2X_9$ compounds, from a correlation of the magnetic results with the structural data.

A. Molybdenum(III) Binuclear Complexes:

The molybdenum compounds will be considered first as the structural and magnetic data for these compounds are considered to be more reliable than the data for the chromium complexes. The discussion of the magnetic interactions in this system is restricted to those compounds for which powder x-ray photographs indicate they are isostructural with $K_3Mo_2Cl_9$. For these compounds

Mo-Mo bond lengths have been estimated and are listed in Chapter IV (Table IV-3).

A discussion of the mechanisms for exchange interactions in these complexes is best made by reference to Fig.V-1. Here, the value of the exchange integral, -J, for each complex is plotted against the Mo-Mo separation. A smooth curve has been drawn through the points for the chloro-complexes. Now J is a measure of the resultant exchange energy of the competing exchange mechanisms which are both direct and via the intervening ligand (superexchange). For the chloro-complexes however, the direct exchange is expected to be dominant because;

a) The short Mo-Mo separations and the extensive nature of the d wave functions for molybdenum(III) both support strong antiferromagnetic exchange via direct overlap of the d orbitals which are stabilized by the trigonal field and directed along the Mo-Mo axis.

b) chlorine is a poor intermediary for super-exchange processes (due to high electronegativity and large diameter).

c) right angle superexchange between d^3 metal ions is small because the e_g orbitals are empty.

d) the ferro- and antiferromagnetic superexchange mechanisms tend to cancel one another.

As a result the large antiferromagnetic J values for the chloro-complexes may be considered to result mainly from direct exchange. The curve joining the points for the chloro-complexes in Fig.V-1 thus should closely represent the direct exchange between two molybdenum atoms as a function of their separation. It is interesting to note that this is an exponential curve as expected. The curve may be closely fitted by the empirical function

$$J = -\left[4.79\ e^{-3.2r} + 0.001\right] \qquad \text{V-1.}$$

where r = Mo-Mo separation and J is in atomic units (1 a.u. = 3.15×10^5 °K).

Herring and Flicker (86) have calculated the exchange coupling constant, J, for a pair of hydrogen atoms as:

$$J = -0.818\ r^{5/2}\ e^{-2r} + (\text{terms in } r^2.e^{-2r}.$$

There is thus quite a close resemblance between the two formulae.

Although equation V-1 probably has little quantitative significance, the exponential shape of the curve should be a close approximation to the dependence of the direct exchange integral on the metal-metal separation. The largest experimental errors are associated with the values of J for complexes with small cations

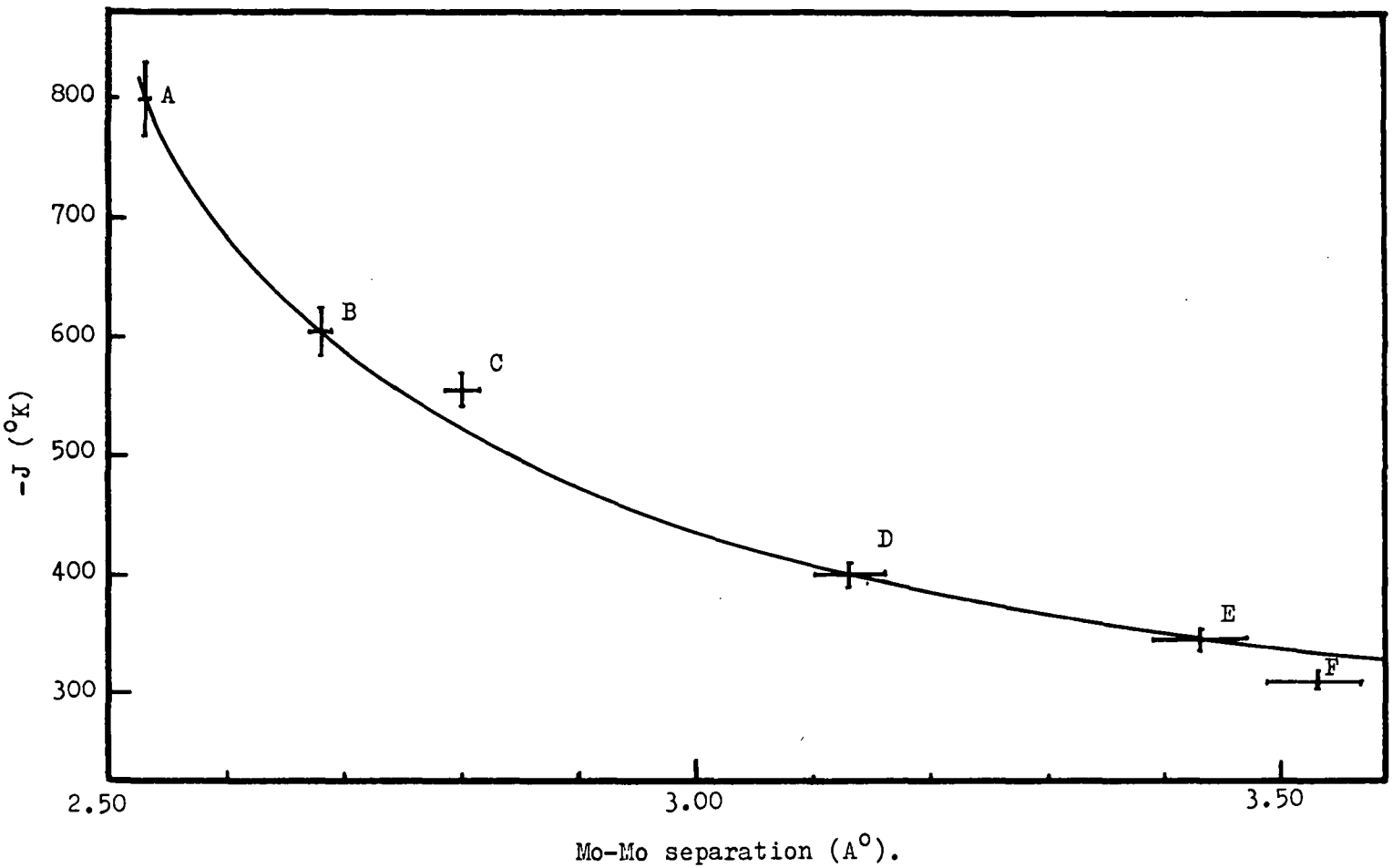

Fig.V-1. Magnetic exchange integral, -J, versus molybdenum-molybdenum separation.

A. $K_3Mo_2Cl_9$; B. $Cs_3Mo_2Cl_9$; C. $Cs_3Mo_2Br_9$; D. $(Me_4N)_3Mo_2Cl_9$;
E. $(Et_4N)_3Mo_2Cl_9$; F. $(Et_4N)_3Mo_2Br_9$.

(Section III-B) and with r for complexes with large cations (Section IV-B). These errors can be incorporated by replacing the points on the graph by horizontal and vertical lines of length corresponding to the experimental errors in r and J respectively. It can be seen from Fig.V-1 that the shape of the curve is affected very little by allowing even large errors of this type.

One puzzling feature which cannot be easily explained at this stage is the fact that the exponential curve appears to flatten off at quite a large value of J ($-300^{o}K$). This implies that at infinite separation of the metal ions an appreciable exchange still exists. Compounds with larger Mo-Mo separations cannot be investigated to check this anomaly as cations, A, larger than Et_4N^+ form only complexes of type $A_2BM_2X_9$ where B is a small cation.

The most important aspect of Fig.V-1 is that the points for the bromo-complexes do not lie on the curve through the points for the chloro-complexes. It is well known that exchange coupling (both antiferromagnetic as in CuX_2 (87) and ferromagnetic as in CrX_3 (75) between metal atoms bridged by bromide ion is greater than that in the corresponding chloride. This is mainly a consequence of the increase in magnitude of the transfer integral with decrease of electronegativity of the anion.

The differing shapes of the curves for the bromo- and chloro- binuclear complexes is thus an accurate measure of the difference in magnitudes of the superexchange mechanisms via chloride and bromide ions.

For the pairs of complexes with the same cation ($Cs_3Mo_2Cl_9$ and $Cs_3Mo_2Br_9$, $(Et_4N)_3Mo_2Cl_9$ and $(Et_4N)_3Mo_2Cl_9$) the chloro-complex in each case has a larger value of -J. This may be explained in terms of a dominant direct exchange mechanism. The greater Mo-Mo separation brought about by the substitution of the bulkier Br^- ions for Cl^- ions results in a decrease in the antiferromagnetic direct exchange which exceeds the increase in exchange via the various superexchange paths.

Consider a vertical line drawn from the poiht for $Cs_3Mo_2Br_9$ (C) to intersect the curve for the chloro-complexes at C'. The valye of J at C' is a measure of the direct exchange interaction d plus the exchange via the chlorines s'. At C, J=d+s where s is the exchange via the bromine ions. The separation $CC' = \Delta J = s - s'$ thus represents the difference in superexchange coupling when chlorine is replaced by bromine in a hypothetical $[Mo_2X_9]^{3-}$ ion with Mo-Mo = 2.8 Å. That CC' is so small (40°K) relative to the absolute magnitude of J validates the hypothesis that the curve through the chloro-complexes is a good representation of the direct exchange

between two molybdenum atoms. The sign of ΔJ shows that there is an increase in antiferromagnetic superexchange when chlorine is replaced by bromine. This may be rationalized in the following way. Table IV-3 shows that in $Cs_3Mo_2Br_9$, the bridging angle $\angle$M-X-M is only about 62°.

a) Ferromagnetic exchange cannot occur by mechanism (4) discussed in Section II-D because the orthogonality of the p_σ orbitals with the t_{2g} orbitals is destroyed. The calculations of Huang indicate that this is the strongest superexchange for right angle exchange between V^{2+} ions via oxygens (62).

b) The ferromagnetic exchange mechanism (3) (Section II-D) which occurs between half-filled to empty orbitals is diminished by a factor of approximately 0.1 relative to the transfer between half filled/half filled orbitals and so is a minor contributing factor.

c) The antiferromagnetic superexchange between half filled t_{2g} orbitals on both metals via π overlap with p_z on the halogen is thus expected to be the major mechanism for superexchange. The replacement of chlorine for bromine then results in an increase in the antiferromagnetic exchange via the bridging ligands.

If now we consider a large cation complex, it is seen that replacement of bromide for chloride in $(Et_4N)_3Mo_2X_9$ results in an increase in the ferromagnetic

character of the superexchange, i.e., just the opposite trend observed for $Cs_3Mo_2X_9$. This may be rationalized in the following way. From Table IV-3 it is seen that for $(Et_4N)_3Mo_2Br_9$, the bridging angle is quite close to 90°. The ferromagnetic exchange mechanism (4) may now occur. At the same time the Mo-Mo separation has increased to 3.5 Å. As π overlap of orbitals decreases quite rapidly with increasing separation, the antiferromagnetic exchange by mechanism (2) will be diminished considerably. The overall superexchange via the ligands may then be expected to be ferromagnetic in character. Replacement of bromide for chloride in $(Et_4N)_3Mo_2X_9$ results in an increase in the exchange integral, J, of approximately +20°K. Although there are only two experimental points for bromides in Fig.V-1, if a smooth curve is drawn through them then it is clear that there is a steady increase in the ferromagnetic character of the superexchange, relative to the antiferromagnetic superexchange, as the Mo-Mo separation is increased.

The discussion may be summarized:

a) The observed antiferromagnetism in the $A_3Mo_2X_9$ complexes is due predominantly to exchange via direct overlap of the metal d orbitals. The various superexchange effects via the bridging halogens contribute no

more than 10% of the total exchange.

b) At small Mo-Mo separations (Mo-Mo $\simeq$ 2.8 Å) the resultant exchange via the superexchange paths is antiferromagnetic. The increase in the coupling on replacing bromide for chloride is approximately $-40^{\circ}K$.

c) As the Mo-Mo separation is increased in the isostructural series, there is an increase in exchange via the ferromagnetic superexchange mechanisms relative to the antiferromagnetic mechanisms. At a Mo-Mo separation of 3.5 Å the increase in the ferromagnetic coupling on replacement of bromide for chloride is $+20^{\circ}K$.

B. Chromium (III) Binuclear Complexes:

As with the molybdenum complexes, the exchange integrals, $-J$, for the chromium compounds have been plotted against the chromium-chromium separations (from Table IV-3) in Fig.V-2. Although this curve must be considered with caution because of the error associated with the J values, it is interesting that it shows exactly the same trends as observed in the results for the molybdenum complexes. However, the absolute values of the exchange integral are diminished by a factor of 50 from $A_3Mo_2X_9$ to $A_3Cr_2X_9$. This is to be expected as

a) The Cr-Cr separations are greater than the Mo-Mo separations in the corresponding binuclear complex by ~0.5 Å.

b) There is a decrease in the radial extension of the d orbitals from molybdenum to chromium.

Following the procedure for the molybdenum complexes, a smooth curve was drawn through the points for the chloride complexes. An exponential curve was obtained. No attempt was made to fit it with an exponential expression because of the uncertainties in the J values. Again, the points for the bromides were displaced off this curve. The deviations are more marked than in the molybdenum complexes and are of the same order of magnitude as the absolute values of J for the chlorides, i.e., the super-exchange via the halogens is comparable to the direct exchange for these complexes.

For $Cs_3Cr_2Br_9$, the vertical separation from the curve for the chloride complexes, ΔJ, is positive. i.e. at a chromium-chromium separation of 3.25 Å, which corresponds to a bridging angle of 74°, the antiferromagnetic superexchange between half-filled d orbitals exceeds the ferromagnetic contributions. The increase of J on replacing bromide for chloride is $-2^{\circ}K$. However the increase in the antiferromagnetic super-exchange via halogens is cancelled by the decrease in

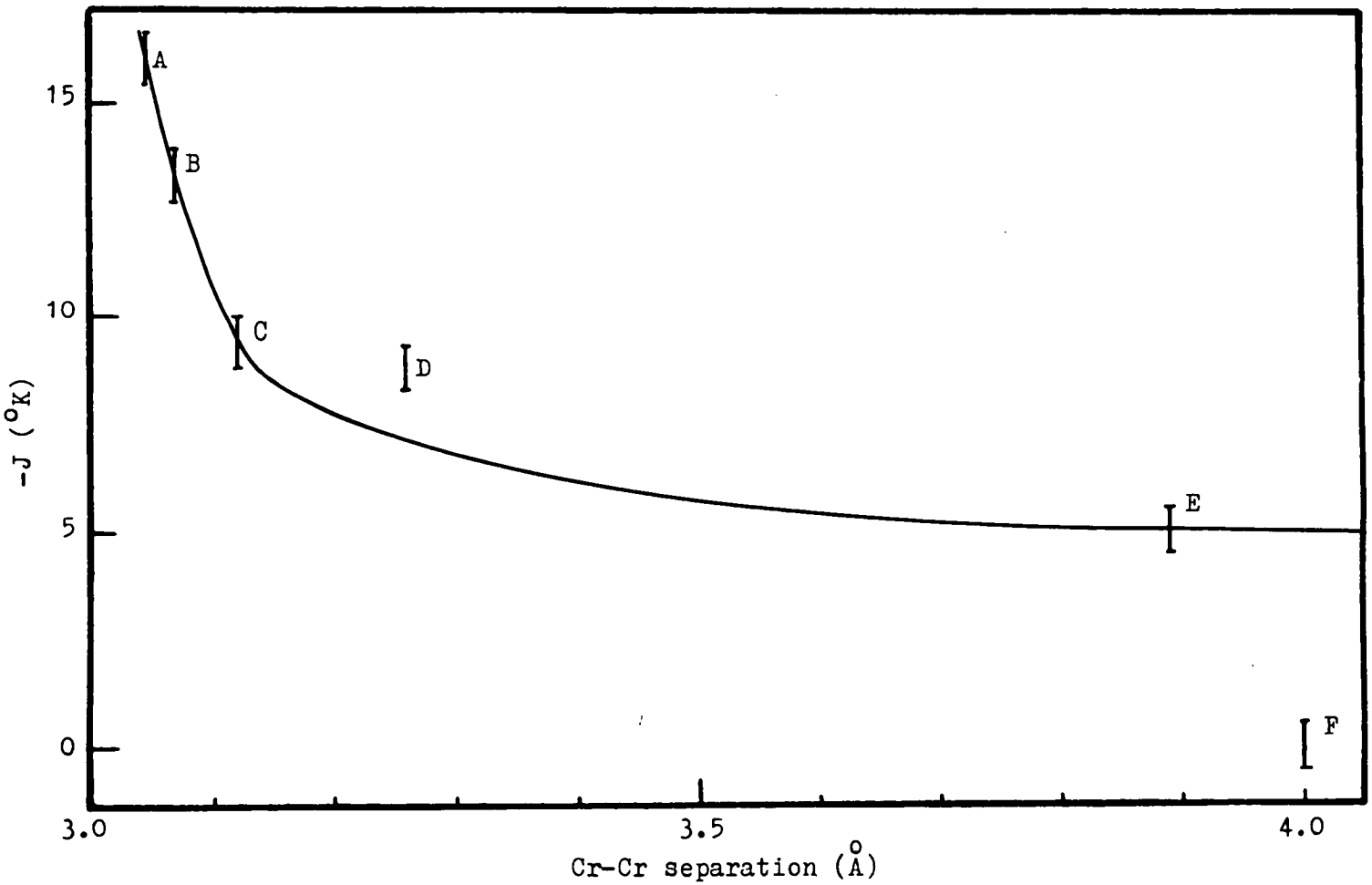

Fig.V-2. Magnetic exchange integral, -J, versus chromium-chromium separation.

A. $K_3Cr_2Cl_9$; B. $Rb_3Cr_2Cl_9$; C. $Cs_3Cr_2Cl_9$; D. $Cs_3Cr_2Br_9$
E. $(Et_4N)_3Cr_2Cl_9$; F. $(Et_4N)_3Cr_2Br_9$.

the antiferromagnetic direct exchange due to increase in Cr-Cr separation. As a result, $Cs_3Cr_2Br_9$, with Cr-Cr = 3.26, has a slightly lower value of the exchange integral J than $Cs_3Cr_2Cl_9$ where Cr-Cr = 3.12Å.

The tetraethyl ammonium complex $(Et_4N)_3Cr_2Br_9$ is very interesting in that it represents the critical point at which both antiferromagnetic direct and superexchange are exceeded by the ferromagnetic contributions. The compound obeys a Curie-Weiss law with a small negative Θ value. Now for $(Et_4N)_3Cr_2Br_9$, the Cr-Cr separation is estimated to be 4.0 Å. At this very large separation, direct exchange is expected to be almost zero. At the same time, the bridging angle is very close to 90° (95°). Orthogonality requirements for the main ferromagnetic superexchange mechanisms, are thus satisfied. The experimental results indicate that these mechanisms exceed both the direct and superexchange antiferromagnetic mechanisms. The increase in the ferromagnetic exchange, in replacing bromide for chloride in $(Et_4N)_3Cr_2X_9$ is + 5°K.

C. Complexes $(H_3O)_3.Mo_2Cl_9$ and $(Ph_4As)_2.H_3O.Mo_2Cl_9$:

Although not included in the preceeding discussion, these compounds warrant special comment as they provide

important confirmation of the ideas developed in Section IV-B, on the effect of the cation on the binuclear anion in $A_3M_2X_9$.

When a molybdenum (III) chloride solution is evaporated to dryness at room temperature, a deep red-brown solid remains which analyses fairly closely as $MoCl_{4.5}\cdot 3H_2O$. This was originally formulated as $(H_3O)_3Mo_2Cl_9\cdot xH_2O$ by P.W. Smith (84). Wedd has recently noted that its absorption spectrum is very similar to that for other complexes $A_3Mo_2Cl_9$ (80). The susceptibility results for this compound can be closely fitted by the equation for binuclear complexes - III-1, which is strong evidence for its formulation as an $A_3Mo_2Cl_9$ species.

The complex formed from molybdenum (III) chloride solution when tetraphenyl arsonium is used as a precipitating cation analyses as $(Ph_4As)_2H_3O.Mo_2Cl_9.xH_2O$, i.e., it is formulated as an $A_2.B.Mo_2Cl_9$ complex. Both these compounds have a common cation type B (H_3O^+) which packs in the plane of the bridging halogens.

As discussed in the preceeding chapter, it is this cation which has a very strong influence on the geometry of the binuclear anion, and in particular on the metal-metal separation. For these compounds then, those properties which depend critically on the metal-metal separation should be similar.

It is thus very rewarding to find that the susceptibility data for the tetraphenyl arsonium complex can be fitted very closely using a J value of $-458^{o}K$ which is very comparable with $J = -485^{o}K$ for $(H_3O)_3Mo_2Cl_9.xH_2O$.

CHAPTER VI

MAGNETIC AND STRUCTURAL INVESTIGATIONS OF SOME VANADIUM(II) HALIDE COMPLEXES.

A. Introduction:

As an extension of the investigations on magnetic interactions in systems containing face-sharing octahedra, a study on some complexes of type AVX_3 (X=Cl,Br) was undertaken. These compounds contain infinite linear chains $(-VX_3-)_n^{1-}$ of face-sharing octahedra (88). There is the possibility of magnetic exchange interactions occurring over many magnetic centres along the chain. These compounds form one of the simplest systems in which collective magnetic phenomena are observed (60). A comparison with the two-centre interactions present in the $A_3M_2X_9$ compounds studied in previous chapters would be expected to yield information helpful to the understanding of magnetically concentrated systems.

The magnetic properties of a compound of formula AVX_3 were first reported by Ijdo (68). He prepared $CsVCl_3$ by a high temperature method and measured the magnetic susceptibility in the temperature range 290-750°K. Although the susceptibility data was not tabulated, Ijdo presented graphs of both susceptibility and magnetic moment as a function of temperature. The susceptibility curve showed a

maximum at ~370°K. The magnetic moment showed a strong dependence on temperature and was reduced well below the spin only value, 3.87 B.M., for a d^3 ion.

It is interesting to compare the magnetic properties of this compound with those of related compounds of other transition elements, containing infinite linear chains. The results are tabulated in Table VI-1.

TABLE VI-1.

REPORTED MAGNETIC PROPERTIES OF COMPOUNDS $CsMCl_3$.

COMPOUND	Θ (°K)	μeff. (300°K)	μ (spin only)	REFERENCE
$CsVCl_3$	antiferro.	1.68 (273°K)	3.87	68
$CsCrCl_3$	328	3.40	4.90	68
$CsMnCl_3$	145	5.03	5.92	89
$CsCoCl_3$	14	4.66	3.87	68
$CsNiCl_3$	76	3.01	2.83	89
$CsCuCl_3$	1	1.97	1.73	58

For these compounds, the strength of magnetic interactions, measured by the Weiss constant Θ, is seen to be quite dependent on the d electron configuration of the metal. The very strong interaction present in the vanadium compound, relative to the other compounds listed, is expected as a

result of the larger radial extension of the d orbitals of this ion. Recently Seifert et al (90) have prepared $Me_4N.VCl_3$ and found it to be isostructural with $CsVCl_3$. They report the magnetic moment at temperatures 289, 196 and 82°K. as 2.13, 1.81 and 1.30 B.M. respectively. Thus in this compound the moment is reduced well below the spin only value, indicating strong interaction between the spins on the vanadium atoms. Seifert et al also reported results of dilution studies on $CsVCl_3$ in the isomorphous compound, $CsMgCl_3$. With increasing dilution the magnetic moment of $CsVCl_3$ was observed to steadily approach the spin only value. The results were interpreted as indicating dominant spin-spin coupling via the bridging halogens. There are no other reported magnetic studies on the system of compounds AVX_3.

In this chapter the results of temperature dependence magnetic studies on the compounds $RbVCl_3$ and $RbVBr_3$ will be reported. A possible structural model is proposed which is consistent with the results of powder x-ray diffraction studies, and with the recorded electronic and far infrared spectra for these compounds. This model is then used to explain the magnetic properties of the compounds $RbVX_3$. From a correlation of the magnetic and structural data, estimates for the different mechanisms for magnetic

exchange are made and the results compared with those for the binuclear complexes $A_3M_2X_9$ discussed in previous chapters.

B. Magnetic Studies on $RbVX_3$:

The magnetic susceptibilities of powdered samples of $RbVCl_3$ and $RbVBr_3$ have been measured in the temperature range 90-500°K by the Gouy method. The results are listed in Table VI-2. Below ~150°K, the susceptibilities for $RbVBr_3$ increased with decreasing temperature due to the presence of a small amount of the hydrated complex (see Experimental). The susceptibilities were corrected for the paramagnetic impurity (91) and Table VI-2 lists both measured (uncorr.) and corrected (corr.) susceptibilities.

The susceptibility curves for both complexes were typical of compounds with strong antiferromagnetic interactions. Maxima in the curves for $RbVCl_3$ and $RbVBr_3$ were observed at ~350°K and 280°K respectively. It would seem that these compounds constitute suitable examples to which the theory for linear chains may be applied. As mentioned in Chapter I, Earnshaw et al (33) have recently published tables of μeff as a function of kT/J for chains of up to ten members, each interacting with nearest neighbours only, for spins 1/2, 1, 3/2, 2, 5/2. Considering the number of members in a chain to be greater than ten had negligible

additional effect on the functions.

In this instance, S = 3/2 and Fig.VI-1 illustrates the relation of $\chi'A$ to T for n = 10 and Tmax = 330°K.

From a comparison with the experimental data for $RbVCl_3$, it is clear that the linear chain model cannot explain the magnetic behaviour. To bring the theoretical curve even approximately into line with experiment it is necessary to consider an unreasonable T.I.P. term of 1000×10^{-6} c.g.s. units.

A possible explanation to this behaviour is that a pairing of vanadium atoms occurs along the chains, as in $RuBr_3$ (92) and NbI_4 (93). This will be discussed fully in later sections of the chapter.

A second possibility however is that the expressions developed by Earnshaw et al (33) are not suitable for explaining the cooperative magnetic phenomena that occur in infinite chains. These expressions were derived from an application of the spin Hamiltonian,

$$H = -2J \sum_i Si.Sj$$

to determine the energy levels in the chain of magnetic centres, which were then substituted into the normal Van Vleck susceptibility equation (1).

Earnshaw et al stress that the resulting expression for the susceptibility is only valid if the condition:

$-JkT \gg n$ is satisfied. In the compounds AVX_3,

TABLE VI-2

MAGNETIC DATA FOR $RbVX_3$

T (°K)	$10^6 \chi'_A$ (uncorr.)	$10^6 \chi'_A$ (corr.)	μ_{eff}* (B.M.)
	$RbVBr_3$		
365.0	1629	1607	2.17
338.5	1656	1624	2.11
299.0	1661	1625	1.98
279.0	1664	1624	1.91
242.0	1668	1621	1.78
200.0	1654	1593	1.60
159.0	1654	1567	1.42
126.5	1656	1527	1.25
97.0	1714	1481	1.08
	$RbVCl_3$		
510.0	1360		2.36
410.0	1408		2.16
380.0	1420		2.09
350.0	1425		2.01
320.0	1426		1.92
292.3	1422		1.80
252.5	1404		1.69
212.3	1380		1.54
185.5	1362		1.43
158.2	1345		1.31
138.0	1331		1.22
99.0	1303		1.02

* $\mu_{eff} = 2.84\sqrt{\chi'_A . T}$

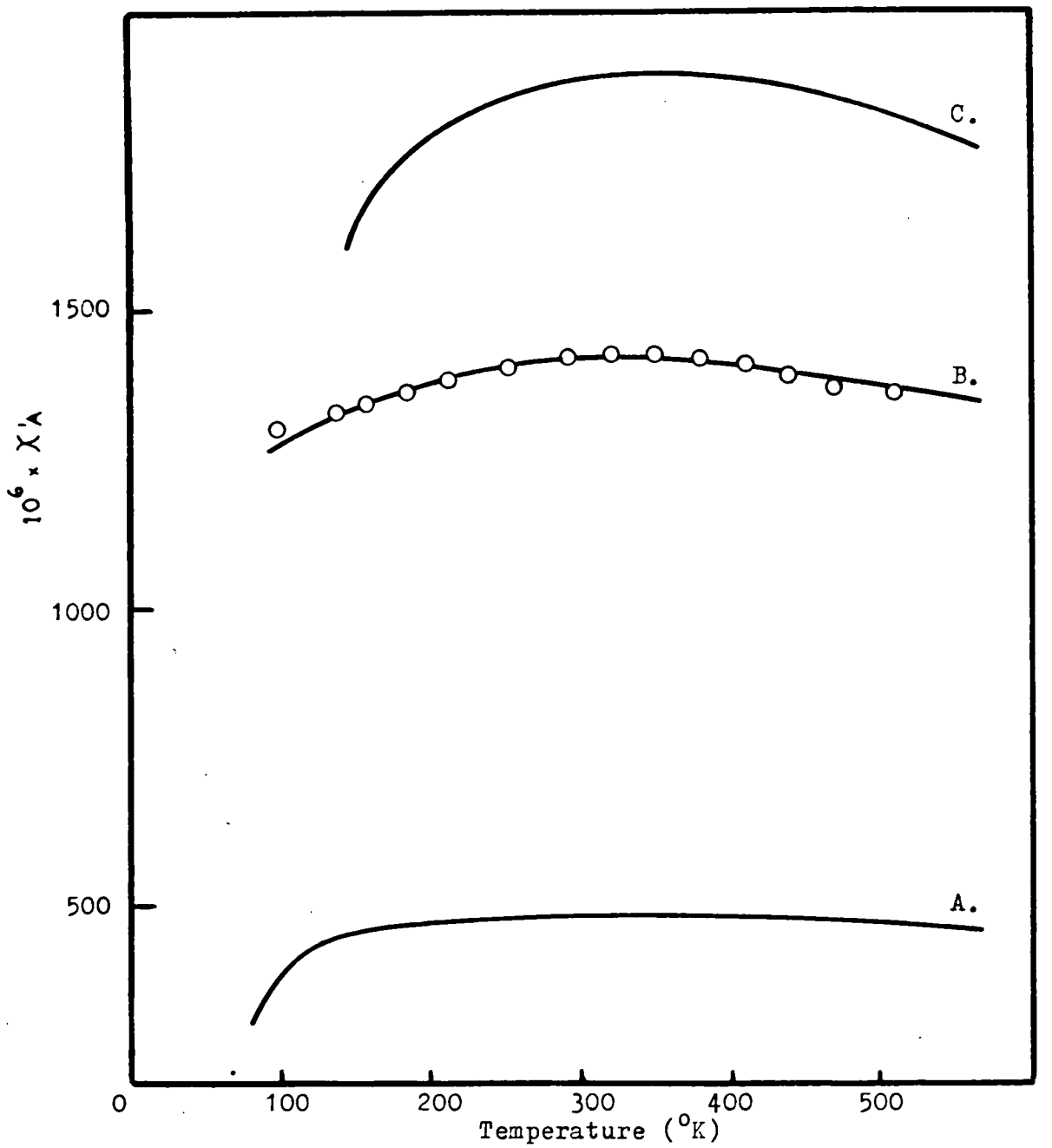

Fig. VI-1. Temperature dependence of magnetic susceptibility for $RbVCl_3$.

O Experimental points; — theoretical curves for
A. n=10, Θ =0°, Tn=330°; B. n=2, Θ =136°, Tn=350°;
C. n=2, Θ=0°, Tn=350°.

n theoretically is infinitely large and so this condition no longer holds.

The usefulness of the expression given by Earnshaw et al for the case of large numbers of interacting atoms was examined by application to the compound $CuCl_2$. This compound contains infinite planar chains $(-CuX_2-)_n$ (94) and recently Adams et al have obtained a good fit to the susceptibility results using formulae based on the one-dimensional Ising model for antiferromagnetic compounds (95). The application of the expression given by Earnshaw ($S = 1/2$, $N = 10$) to the fitting of the data for $CuCl_2$ was unsatisfactory however. As with $RbVCl_3$, the theoretical susceptibilities were smaller than the experimental values by greater than 1000×10^{-6} c.g.s. units.

In the following section, the results of spectral and x-ray studies on $RbVX_3$ will be presented and possible structures proposed to form a basis for the further discussion of the magnetic properties of these compounds.

C. Structural Studies on Compounds, AVX_3:

1. Electronic spectra. Diffuse reflectance spectra have been recorded for the compounds NH_4VCl_3, $RbVCl_3$, and $RbVBr_3$. The observed band positions (in cm^{-1}) together with proposed assignments are listed in Table VI-3. Included for comparative purposes is the spectrum of the

$[VCl_6]^{4-}$ ion both in a LiCl-KCl eutectic (96) and in VCl_2 (97).

The compounds exhibit broadly a three band spectrum. These bands correspond to the three spin allowed transitions $^4T_2g \leftarrow {}^4A_2g$, $^4T_1g(F) \leftarrow {}^4A_2g$, and $^4T_1g(P) \leftarrow {}^4A_2g$, for a d^3 ion in octahedral symmetry. The observed bands are broad and show splittings into a number of components. The most likely causes for these splittings are (i) slight oxidation, (ii) appearance of spin forbidden transitions, and (iii) symmetry lower than octahedral.

To check if any of the extra bands were due to superficial oxidation, the spectrum of a compound was recorded after successive stages of deliberate oxidation. The main effect of the oxidation was to produce a very broad band centred at approximately 22,000 cm^{-1}. The second possibility is that the additional bands are spin-forbidden transitions. For a d^3 ion in octahedral symmetry the spin forbidden transitions are $^2E_g \leftarrow {}^4A_{2g}$ and $^2T_{2g} \leftarrow {}^4A_{2g}$. These have transition energies 9B + 3C and 15B + 5C respectively where B and C are the Racah parameters (2). For a number of related hydrated complexes $AVX_3.xH_2O$, a well defined shoulder at ~ 11,000 cm^{-1} has been assigned to the transition $^2E_g \leftarrow {}^4A_{2g}$ (Appendix II). This is illustrated for the compounds $RbVCl_3.2H_2O$ and $RbVCl_3.6H_2O$ in Fig.VI-2. Using a value of B = 600 cm^{-1} (97)

TABLE VI-3

DIFFUSE REFLECTANCE SPECTRA ($cm^{-1} \times 10^{-3}$).

COMPOUND	Observed transitions: $^4A_{2g} \rightarrow$			
	$^4T_{2g}$	$^4T_{1g}(F)$	$^4T_{1g}(P)$	$^2T_{2g}$
NH_4VCl_3	9.1 (broad, unresolved)	14.3	21.2 24.2 25.8	
$RbVCl_3$ (at 70°K)	7.3 8.9 9.7	13.2 14.0 14.9	21.9 23.8 25.6	16.7
$RbVBr_3$	 7.8 8.6	12.4 13.1 13.6	20.4 21.5 24.6	16.8
VCl_2 [a.]	9.0	14.0	21.5	
$[VCl_6]^{4-}$ [b.] (LiCl-KCl melt)	7.2	12.0	19.0	

a. Reference 97
b. Reference 96

the value of C is calculated to be ~1800 cm^{-1}(2). The $^2T_{2g} \leftarrow {}^4A_{2g}$ transition is then calculated to be near 18,000 cm^{-1}. In agreement with this, a weak, sharp peak was observed at ~17,000 cm^{-1} in $RbVBr_3$ and a shoulder was observed in the spectrum of $RbVCl_3$ in this region. From the elimination of possible causes (i) and (ii) it is concluded then that the splittings of the three main bands in the compounds AVX_3 are the result of a lowering of the symmetry from octahedral.

For $RbVCl_3$, the spectrum was studied at low temperatures and it was observed that each of the three bands were clearly split into three components. The spectrum of this compound is illustrated in Fig.VI-2. The observed band splittings correspond, in the energy level scheme for a d^3 ion, to each of the triply degenerate ^4T levels breaking down to three orbital singlets (^4A or ^4B). For this to be achieved the symmetry at the vanadium ion has to be reduced to at least D_2h. Although energy level diagrams have been constructed for d^3 ions in both trigonally (D_{3h} and C_{3v}) and tetragonally (D_{4h} and C_{4v}) distorted octahedral fields (98) there has been no detailed treatment of the lower symmetry fields that appear to apply in the compounds AVX_3.

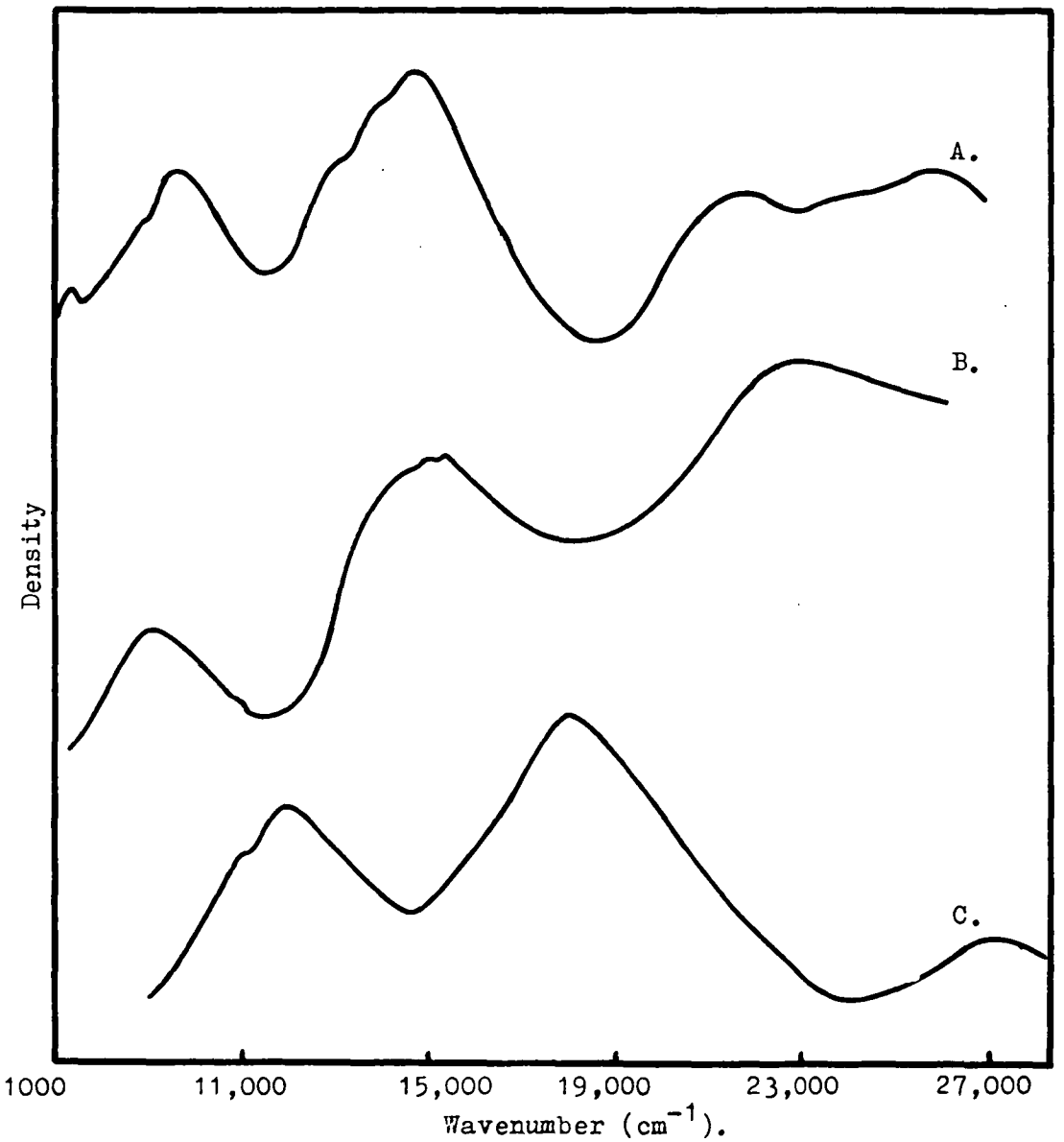

Fig.VI-2. Reflectance spectra for A, $RbVCl_3$; B, $RbVCl_3.2H_2O$; C, $RbVCl_3.6H_2O$.

Curves displaced vertically for clarity.

2. Far infrared spectra - The far infrared spectral bands observed in the range 200-400 cm^{-1} are given in Table VI-4 for NH_4VCl_3 and $RbVCl_3$. For both compounds the spectrum consists of two strong broad bands centred at ~310 and 260 cm^{-1}. The bands are assymetric and show definite signs of splitting into two components. These spectra may be compared with that for $CsCuCl_3$ (99) which has a split band at 290 cm^{-1} and a second band at 263 cm^{-1} (see Table VI-4). These are considered to be associated with terminal Cu-Cl bonds (2.28 A) and bridging Cu-Cl bonds (2.35 A) respectively. Also as discussed in Appendix 1 the binuclear complexes $A_3Mo_2Cl_9$ have two sets of bands - one band system centred at ~310 cm^{-1} associated with molybdenum-terminal chlorine bonds and the second system centred at ~260 cm^{-1} associated with the longer metal-bridging chlorine bonds.

3. Powder x-ray diffraction studies - In this investigation the basic structure of $RbVCl_3$ has been determined from a study of Debye-Scherrer x-ray powder photographs. The cell dimensions of the binuclear hexagonal cell are:

$$a = 7.04 \pm 0.01, \quad c = 6.00 \pm 0.01 \text{ Å}.$$

A comparison with the diffraction data for $CsNiCl_3$ (57) indicates that the two compounds are isostructural.

TABLE VI-4

FAR INFRARED SPECTRA OF AMX_3 (200-400 cm^{-1}).

COMPLEX	BAND POSITION	ASSIGNMENT
$RbVCl_3$	317 sh, 314 s. 268 s.	$\nu(V\text{-}Cl_t)$ $\nu(V\text{-}Cl_{br})$
NH_4VCl_3	309(s), 301 sh 275 sh, 263 vs	$\nu(V\text{-}Cl_t)$ $\nu(V\text{-}Cl_{br})$
$CsCuCl_3$ [a.]	293 s, 287 s 263 s	
$CsCuBr_3$ [a.]	256 s, 251 s 234 s	

a. Reference 99.

The atoms were hence placed in the special positions of space group $P6_3/mmc$

2 V in 0, 0, 1/4; 0, 0, 3/4

2 Rb in 1/3, 2/3, 0; 2/3, 1/3, 1/2

6 Cl in x, 2x, 1/2; $2\bar{x}$, $\bar{x}$, 1/2; x, $\bar{x}$, 1/2

$\bar{x}$, $2\bar{x}$, 0; 2x, x, 0; $\bar{x}$, x, 0.

and the parameter x was refined to give the best agreement between observed and calculated structure factors. A final value of x of 0.1555 was obtained for which the R factor

$$(\sum ||F_o| - |F_c|| / \sum |F_o|) \text{ was } 0.07.$$

The close agreement between the calculated and observed structure factors is illustrated in Table VI-5.

The basic structure of $RbVCl_3$ then can be considered to consist of linear chains of $(-VCl_3-)_n^-$ parallel to the 'c' axis with rubidium atoms packing between the chains. The vanadium atoms are symmetrically arranged 3.0 Å apart and all V-Cl bond lengths are equivalent.

That the corresponding bromide, $RbVBr_3$ has this "symmetric chain" structure also is indicated by the close correspondence between the powder photographs for this compound and $RbVCl_3$. The hexagonal cell dimensions were found to be

$$a = 7.43 \pm 0.01, \quad c = 6.30 \pm 0.01 \text{ Å}.$$

TABLE VI-5

STRUCTURE FACTORS - MODELS FOR $RbVCl_3$.

Index	F_{obs}	F_{calc}	
		Model 1*	Model 2
1 0 0	74.5	76.2	76.2
1 0 1	112.1	123.8	123.8
1 1 0	184.1	183.7	183.7
2 0 0	83.4	84.8	84.8
0 0 2	149.1	151.3	153.0
2 0 1	461.7	409.1	409.1
1 0 2	161.2	160.4	156.6
2 0 2	341.3	324.9	321.5
3 0 0	163.3	158.0	158.0
2 1 2	260.7	278.8	273.9
2 2 0	375.9	338.6	338.6
2 0 3	307.3	327.7	327.7
2 2 2	253.8	257.0	260.1
0 0 4	188.6	191.1	180.8
4 0 1 3 1 2	349.0	350.0	349.5
2 3 1 4 0 2	278.8	312.0	311.9
1 1 4	169.2	191.9	180.8
4 1 0	218.1	193.3	193.3
2 4 1	363.8	353.3	353.3
2 2 4	311.2	378.6	369.3

* Model 1 - Symmetric Chain Model

Vanadium positions $(0, 0, \frac{1}{4};\ 0, 0, \frac{3}{4}.)$

Model 2 - Paired Atom Model

Vanadium positions $(0, 0, z;\ 0, 0, \bar{z};)$

$z = 0.27.$

On the basis of this structural model, the local symmetry of the vanadium ion is very close to perfect octahedral, Oh and so the electronic spectra should be typical of an undistorted d^3 octahedral complex, consisting of three symmetrical bands. The small trigonal distortion introduced by x(Cl) not being exactly 1/6 has been observed to have no measurable effect on the spectrum of the related nickel compounds $Me_4N.NiCl_3$ (100) and $Me_4N.NiBr_3$ (60).

That the electronic spectral results of Section VI-C-1 are in conflict with these predictions indicates that there must be subtle changes in the basic "symmetric chain" model which cause a lowering of the symmetry at the vanadium atoms. These changes must be such as to have little effect on the x-ray diffraction data.

In attempting to explain this unusual situation, the observation was made that for a number of compounds, MX_n, which were originally assigned "symmetric chain" structures, more recent detailed x-ray studies have led to the reassignment to a structure in which the metal atoms pair together along the chain. (92, 101, 102). The most notable case applies to the compound $RuBr_3$, recently re-examined by Broderson et al (92). They originally assigned this compound to the TiI_3 type symmetric chain structure in

which metal atoms occupied 1/3 of the octahedral sites in hexagonal close packing of bromine atoms, giving a Ru-Ru bond length of 2.93 Å. On the basis of 80 reflections taken from single crystal data about the 'c' axis an R factor of 0.074 was achieved. However, when this compound was re-examined, very faint reflections were observed which could be accounted for by pairing together ruthenium atoms along the chain to give a $Ru_2Br_3(Br_{6/2})$ building unit. The Ru-Ru bond distances alternated 2.7 to 3.1 Å. At the same time the pairing together of the ruthenium atoms caused a distortion of the halogen close packing, resulting in a site symmetry of C_{2v} for the $Ru_2Br_3(Br_{6/2})$ unit.

From structure factor calculations it has been determined that a similar distortion of the vanadium atoms in $RbVCl_3$ would have negligible effect on the intensities of the 22 observed powder lines. In Table VI-5 are compared the symmetric chain model with the 'paired metal' model in which V-V bond lengths are alternately 2.75 and 3.25 Å. The changes in intensities are below the accuracy of measurement.

However, such a distortion would result in the appearance of extra, very weak lines consistent with the lowering of the space group symmetry. To examine this possibility single crystals of $RbVCl_3$ were carefully grown using high

temperature techniques. The crystals develop as long fibrous needles whose needle axis corresponds with the crystallographic 'c' axis. Single crystals studies were then limited by the shape of the crystal to taking Weissenberg photographs about the 'c' axis. In these photographs no extra weak spots were observed. However, the studies were hampered by the crystals decomposing before very long exposures could be completed. At this stage it may be noted only that the intensity measurements on the observed reflections are not in conflict with the proposed 'paired atom' model for $RbVCl_3$.

The 'paired atom' model could be reconciled with the electronic spectra of the compounds AVX_3. In $RuBr_3$, the highest symmetry at a ruthenium site is C_{2v}. Thus if an analogous model applied to the compounds AVX_3, it would be consistent with the observed splittings of the bands into three components. (In C_{2v} symmetry, a triply degenerate T state reduces to three singlet states).

In the paired atom model there would be both 'long' and 'short' metal ligand bonds. Again, taking $RuBr_3$ as an illustrative example, Ru-Br bonds of length 2.46 and 2.52 $\mathring{A}$ are found. The model is thus consistent with the observed two band far infrared spectra for the compounds NH_4VCl_3 and $RbVCl_3$.

In the following section the applicability of the

'paired-atom' structure of AVX_3 to the interpretation of the magnetic results is discussed and possible mechanisms for spin-spin coupling in these compounds are proposed.

D. Correlation of Magnetism and Structure for AVX_3:

With the assumption of the 'paired atom' model for AVX_3, it is possible to account for the temperature dependence magnetic behaviour. As noted in Section VI-B the linear chain model developed by Earnshaw et al (33) cannot be reconciled with the experimental results. If the theoretical curve assuming a binuclear complex is applied the agreement with experiment is improved considerably (Fig. VI-1). However, in this case the observed susceptibilities are smaller than the calculated values at all temperatures.

Exactly the same observation has been recently made for the complex $KCuBr_3$ (103), which contains planar binuclear complex ions $[Cu_2Br_6]^{2-}$. The discrepancy between theory and experiment was attributed to the binuclear ions not being completely isolated in the crystal, but subject to the orienting effect of the Weiss field exerted by neighbouring binuclear units. The Bleaney and Bowers (104) theoretical equation for the susceptibility of isolated dimeric clusters was modified to take into account the spin interaction between dimer ions by including the Weiss constant θ .

The modified Bleaney and Bowers equation then becomes:

$$\chi'_A = \frac{Ng^2\beta^2}{3K(T-\theta)} \cdot \left[1 + \tfrac{1}{3}\exp \frac{J}{kT} \right]^{-1} + N(\alpha)$$

With $\theta = -17^\circ$ very good agreement with experiment was achieved.

For the paired atom model for AVX_3 a similar argument would apply. i.e., there would be dominant spin interaction between the pairs of vanadiums with the shorter V-V separation, but these dimeric units would be subject to the influence of adjacent dimers along the chain. A similar treatment was thus applied to $RbVCl_3$ in which T was replaced by T' (= T- θ) in the theoretical susceptibility equation (III-1). It was found that for $\theta = -136^\circ$ an almost exact fit of the theoretical curve to the experimental data was achieved. (curve B of Fig.VI-1). This treatment must be considered with reservation, however. In particular, θ must be considered only as another parameter which may be varied to fit the experimental data. The parameter allows a relaxation of the rigid theory in a manner which has no obvious physical or theoretical basis. It was also possible to fit the corrected susceptibility data for $RbVBr_3$. The magnetic parameters for both $RbVBr_3$ and $RbVCl_3$ are listed as follows in Table VI-6.

TABLE VI-6

MAGNETIC PARAMETERS FOR AVX_3.

	$-J$ (^oK)	Θ (^oK)	$\mu_{eff}(300^o)$ B.M.
$RbVCl_3$	151	-136	1.85
$RbVBr_3$	132	-130	1.99
$Me_4N.VCl_3$	110	-150	2.13

Also included in this table are the corresponding parameters for $Me_4N.VCl_3$, calculated from the data of Seifert et al (90). The results for this compound are approximate, as susceptibility data for the complex were given at only three temperatures. In addition it was necessary to correct for a small amount (~2%) of paramagnetic impurity. Using the information in this table it should be possible to determine the relative magnitudes of the different mechanisms for exchange in the compounds AVX_3, by an application of the method used for the binuclear complexes in Chapter V, i.e., by a critical examination of the graph of the exchange integral versus the metal-metal separation.

Irrespective of the "fine structure" of the compounds AVX_3, the basic structure contains chains of vanadium atoms parallel to the c axis of the unit cell. The discussion of Chapter IV for the binuclear complexes $A_3M_2X_9$ may be applied

here, i.e., the metal-metal separation is proportional to the length of the c axis in an isostructural series. The close similarity of the powder patterns for the compounds AVX_3 indicate they are isostructural.

In Fig.VI-3 the exchange integral is plotted as a function of the length of the c axis for the compounds $RbVCl_3$, $RbVBr_3$, and $Me_4N.VCl_3$. An approximate exponential curve has been drawn through the points for the chloro-complexes.

As in the case of the binuclear $A_3M_2X_9$ complexes a perpendicular is drawn from the point for $RbVBr_3$ at C to intersect the line through the chloro-complexes at C'. CC' then represents the change in the superexchange via the ligands when bromide ion replaces chloride ion in a hypothetical AVX_3 compound in which the vanadium-vanadium separation is kept constant. From Fig.VI-3 it is seen that replacement of bromide for chloride results in an increase in the antiferromagnetic superexchange mechanisms. This may be explained as follows. The bridging angle, $V\text{-}Cl_{br}\text{-}V$ in $RbVCl_3$ is estimated to be $\sim 80^{\circ}$ on the basis of the symmetric chain model and will certainly be less than this between pairs of vanadium atoms in a "paired atom" structure. The compounds AVX_3 are thus very similar, in the geometry of the $M\text{-}X_3\text{-}M$ bridging unit, to the compounds $A_3Mo_2X_9$ where A is a small cation such as caesium. The

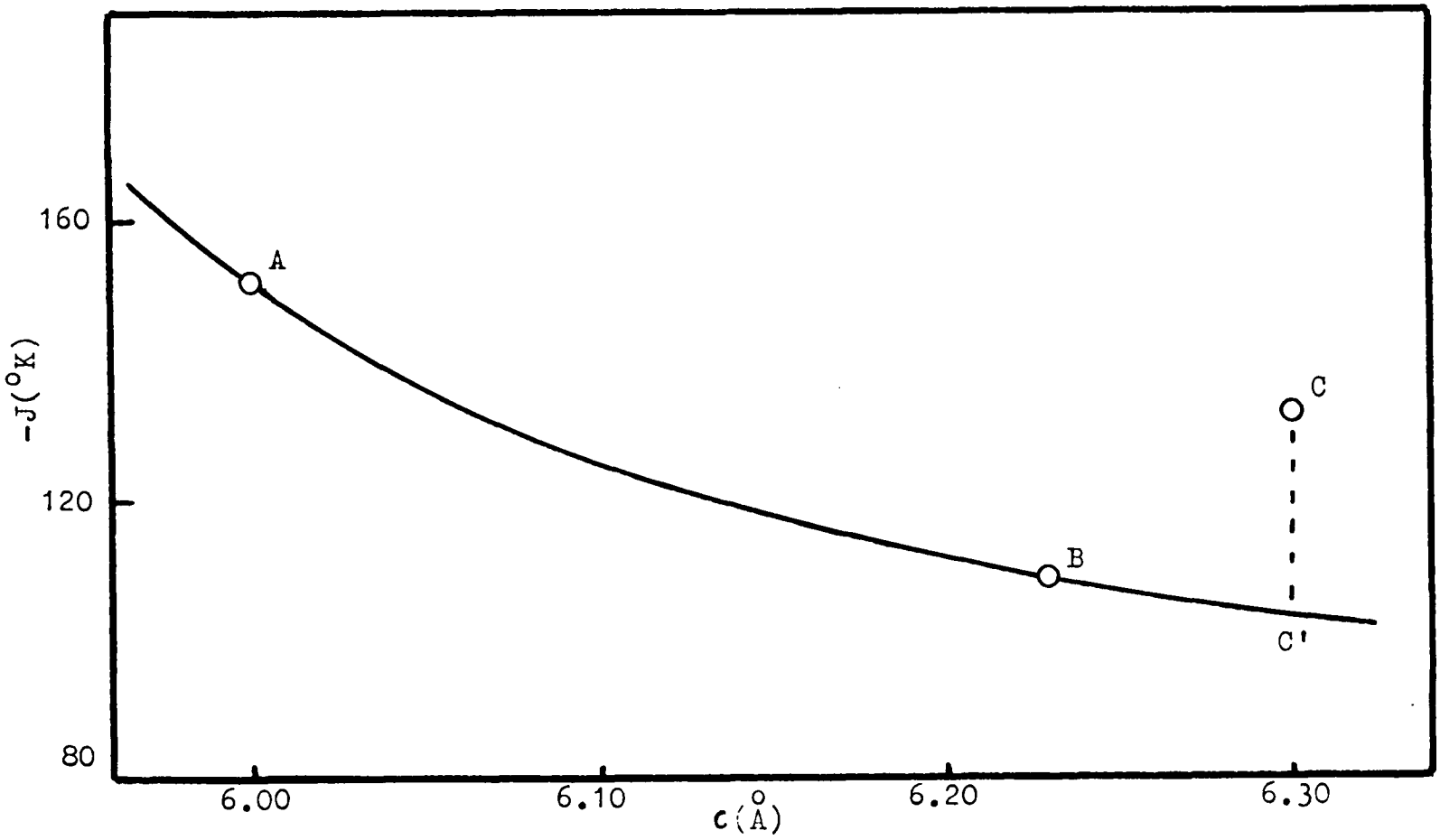

Fig.VI-3. Magnetic exchange integral, -J, versus unit cell parameter, c.
A. $RbVCl_3$; B. $Me_4N.VCl_3$; C. $RbVBr_3$.

increase of the antiferromagnetic superexchange on replacing bromide for chloride is then explained using the arguments given in Chapter V.

There is one major difference between the magnetic behaviour in AVX_3 and that in $A_3Mo_2X_9$. In the latter compounds, the superexchange mechanisms accounted for only a small amount of the total exchange (10%). For these binuclear complexes the major mechanism is via direct overlap of the metal orbitals. For $RbVX_3$, however, the increase in the antiferromagnetic superexchange on replacing bromide for chloride is $\sim -30^{\circ}$ which represents a quarter of the total exchange, i.e., in the compounds AVX_3 the exchange mechanisms which operate through the bridging ligands play a more important role than in the binuclear complexes.

This may be rationalized in terms of the shorter $M\text{-}X_{br}$ bond lengths in the compounds AVX_3, of divalent vanadium. As an illustration, consider a comparison of $Cs_3V_2Cl_9$ and $CsVCl_3$. In the former compound, which is isostructural with $Cs_3Cr_2Cl_9$ (20), the vanadium(III) - bridging chlorine bond length is estimated to be 2.53 A. For $CsVCl_3$, using the fractional coordinates for $RbVCl_3$ (symmetric chain model, see Section VI-C (3)) and the cell dimensions given by Seifert et al (88) and the vanadium(II)- bridging chlorine bond length is calculated to be only 2.44 A. Superexchange mechanisms are extremely

sensitive to the separation of the metal and the ligand (60). It is thus clear that in the compounds AMX_3 the superexchange will be greater relative to the direct exchange, than in the compounds $A_3M_2X_9$, assuming that the M-M separation is comparable.

The concept of atom pairing along a linear chain as proposed for the compounds AVX_3, implies that strong bonding between the vanadium atoms must occur. Thus if the true structure of these compounds is of the paired atom type then the direct exchange via direct overlap of the vanadium d orbitals should be appreciable. From Fig.VI-3 it is estimated that for the direct exchange mechanisms between adjacent vanadium atoms, the exchange integral, $-J$ is of the order of $100^{\circ}K$. This may be compared with the numerical calculation of Huang (62) who determined that the exchange integral associated with the direct exchange mechanisms between two vanadium atoms separated by 2.97 $\mathring{A}$ is $-J = 24^{\circ}K$.

To summarize: the results of magnetic interaction studies on the system of compounds AVX_3 are consistent with a structural model in which weak covalent bonding causes pairing of vanadium atoms along infinite linear chains $(-VX_3-)_n^-$. The magnetic interactions in this system show a close resemblance to the interactions in the compounds $A_3Mo_2X_9$ where A is a small cation. In the

compounds AVX_3, however, the superexchange via the bridging ligands forms a much greater contribution to the total exchange than in the compounds $A_3Mo_2X_9$. This is attributed to the shorter $M-X_{br}$ bonds in the former compounds.

E. Experimental:

Preparation of $RbVCl_3$.

Two grams of the hexahydrate complex (105) were ground to a fine powder in a nitrogen atmosphere. The compound was transferred to a glass tube fitted with a cold finger and a Gouy tube (Fig.VI-4). The apparatus was evacuated and sealed at A. The tube B was immersed in an oil bath at 120°C and the cold finger placed in a liquid nitrogen trap. When completely dehydrated (after 20 hours) the compound acquired a bright green colour. At this point the cold finger was sealed off. The finely powdered anhydrous complex was transferred to the Gouy tube G which was then sealed at D.

It was observed that even after prolonged dehydration some water remained, as evidenced by weak peaks in the infrared spectrum. Hence the magnetic susceptibilities given in Table VI-2 are probably slightly high.

On the completion of the magnetic studies on $RbVCl_3$ the glass Gouy tube was opened and the contents analysed.

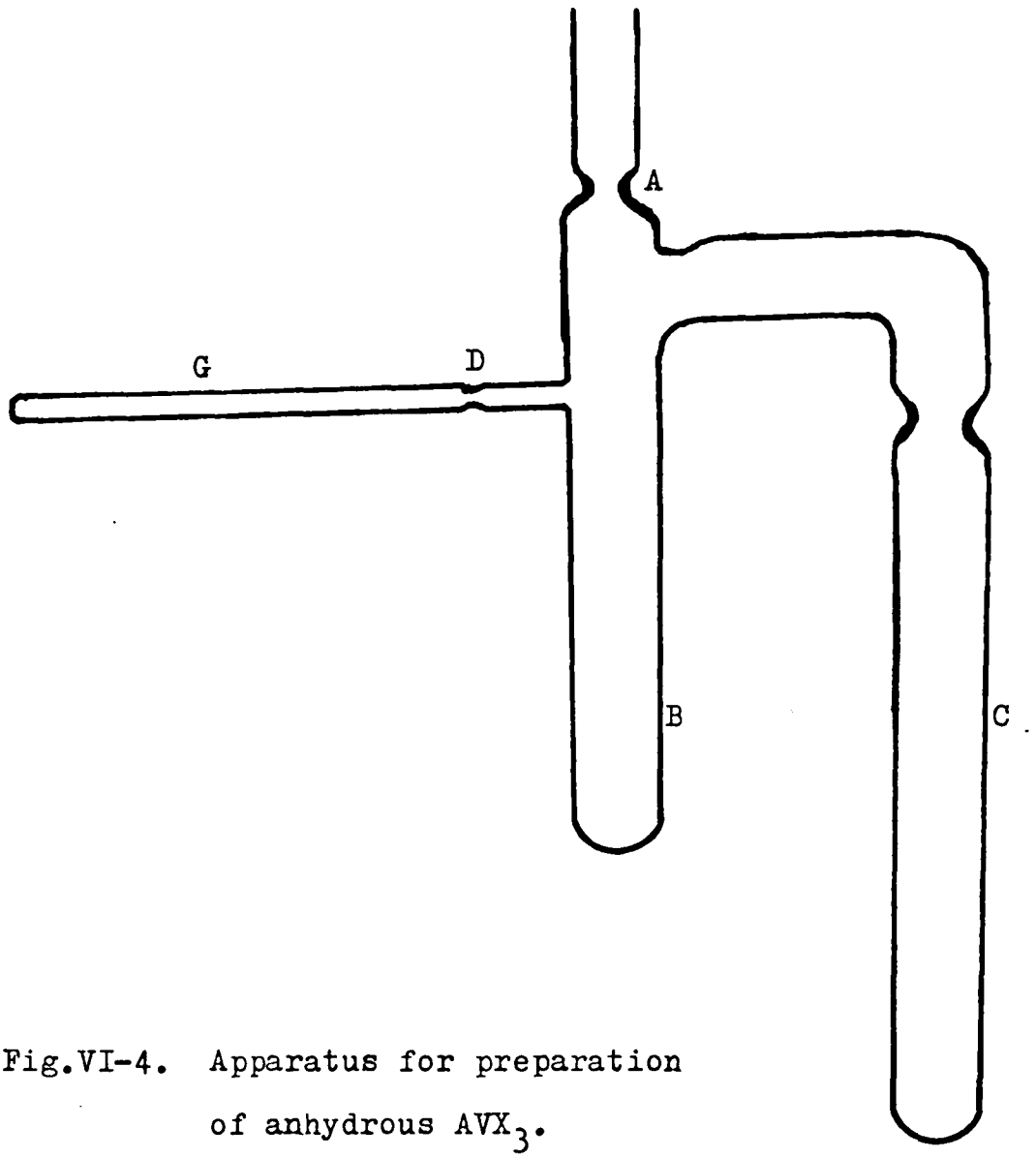

Fig.VI-4. Apparatus for preparation of anhydrous AVX_3.

Found: Cl, 43.2; Rb, 34.85; V, 20.77%.

$RbVCl_3$ requires: Cl, 43.8; Rb, 35.2; V, 20.98%.

The compound $NH_4.VCl_3$ was prepared in the same way. The product was slightly discoloured as a result of decomposition during the dehydration process. Hence for this compound only the spectral results, which are not as sensitive as the magnetic results to traces of oxidation, are reported.

Preparation of $RbVBr_3$:

This complex was prepared from the hydrated bromo-complex, $RbVBr_3.6H_2O$, as described above for $RbVCl_3$. The product obtained after dehydration was of a mustard colour. Single crystals, obtained from the powder at high temperatures formed as yellow-brown needles.

Found: Br, 63.2; V, 13.5%.

$RbVBr_3$ requires: Br, 63.7; V, 13.54%.

An infrared spectrum run on the anhydrous compound showed the presence of water even after prolonged dehydration. It was necessary to correct the magnetic susceptibilities for the presence of 1% paramagnetic impurity. (Calculated assuming the impurity is vanadium(II) hydrated species). All lines on the Debye-Scherrer powder photograph for $RbVBr_3$ could be indexed on a hexagonal cell very similar to that for the chloro-complex.

Analyses:

To determine total vanadium a sample of compound (0.2 g) was oxidized to the five valent state with concentrated nitric acid. Quantitative reduction to vanadium(IV) was effected by boiling with sodium sulphite. The reduced solution was titrated with potassium permanganate. Chlorine and bromine were analysed gravimetrically as the silver salts (77). Rubidium was estimated as the tetraphenyl boron compound (106).

X-ray diffraction studies:

Powder photographs were recorded on a Debye-Scherrer 57.5 mm. radius camera. Line positions were measured with a travelling microscope. The films were internally calibrated with silicon. Line intensities for $RbVCl_3$ were measured using a microdensitometer and values were averaged over four films. For the structure factor calculations, Lorentz-polarization corrections were applied to the measured intensities. Scattering curves for the ions Rb^+, V^{2+}, and Cl^- were obtained from the international Tables for Crystallography. No absorption corrections were applied.

Electronic spectra:

Reflectance spectra for the compounds were recorded on a Perkin Elmer "Spectracord" 4000A spectrophotometer.

Care was taken to ensure the compounds were very finely ground to minimize scattering. Reflectance measurements in the range 10,000 to 30,000 cm^{-1} were also made with a modified Unicam SP 500 Spectrophotometer fitted with an SP 540 diffuse reflectance attachment. Lithium fluoride and magnesium oxide were used as reference standards and samples were diluted with these compounds.

Far infrared spectra:

Infrared spectra were recorded in the range 200–400 cm^{-1} on a Beckman IR-12 spectrophotometer, using nujol mulls and polythene windows.

REFERENCES

1. J.H. Van Vleck, "Electric and Magnetic Susceptibilities", Oxford University Press, New York, 1932.
2. J.S. Griffith, "Theory of Transition Metal Ions", Cambridge University Press, London, 1961.
3. B.N. Figgis and J. Lewis, Progress in Inorganic Chemistry, 1964, 6, 37.
4. B.N. Figgis, "Introduction to Ligand Fields" Interscience Publishers, New York, 1966.
5. W. Heisenberg, Z. Physik, 1928, 49, 619.
6. P.A.M. Dirac, Proc. Roy. Soc., 1929, A123, 714.
7. W. Heitler and F. London, Z. Physik, 1927, 44, 455.
8. E.C. Stoner, J. phys. et radium, 1951, 12, 372.
9. J.C. Slater, Revs. Modern Phys., 1953, 25, 199.
10. E.P. Wohlfarth, Revs. Modern Phys., 1953, 25, 211.
11. T. Kasuya, "Magnetism", Volume IIB, 215, Academic Press, New York, 1966.
12. C. Zener, Phys. Rev., 1951, 81, 440; 82, 403; 83, 299.
13. J.S. Smart, "Magnetism", Volume III, 63, Academic Press, New York, 1963.
14. R.E. Behringer, J. Chem. Phys., 1958, 29, 537.
15. J.N. Van Niekerk and F.R.L. Schoening, Acta Cryst., 1953, 6, 227.
16. B.N. Figgis and R.L. Martin, J. Chem. Soc., 1956, 3837.

17. J.N. Van Niekerk, F.R.L. Schoening and J.F. de Wet, Acta Cryst., 1953, 6, 501.

18. D. Lawton and R. Mason, J.A.C.S., 1967, 87, 921.

19. M.A. Porai-Koshits and A.S. Antschishkina, Proc. Acad. Sci. USSR, Chem. Sect., 1962, 146, 902.

20. D.J.W. Ijdo and G.J. Wessel, Acta Cryst., 1957, 10, 466.

21. W.H. Watson and J. Waser, Acta Cryst., 1958, 11, 689.

22. G.A. Barclay, C.M. Harris, B.F. Hoskins, and E. Kokot, Proc. Chem. Soc., 1961, 264.

23. A. McL. Mathieson, D.P. Mellor, and N.C. Stephenson, Acta Cryst., 1952, 5, 185.

24. J. Lewis, F.E. Mabbs, M. Gerloch, and A. Richards, Nature, 1966, 212, 809.

25. F.A. Cotton and C.B. Harris, Inorg. Chem., 1965, 4, 330.

26. M.J. Bennett, K.G. Caulton, and F.A. Cotton, Inorg. Chem., 1969, 8, 1.

27. M.J. Bennett, W.K. Bratton, F.A. Cotton, and W.R. Robinson, Inorg. Chem., 1968, 7, 1570.

28. F.A. Cotton and B.M. Foxman, Inorg. Chem., 1968, 7, 2135.

29. G.J. Bullen, R. Mason, and P. Pauling, Inorg. Chem., 1965, 4, 456.

30. F.A. Cotton and R.C. Elder, Inorg. Chem., 1965, 4, 1145.

31. J.A. Bertrand, Inorg. Chem., 1967, 6, 495.

32. B.N. Figgis and G.B. Robertson, Nature, 1965, 205, 694.

33. A. Earnshaw, B.N. Figgis, and J. Lewis, J. Chem. Soc. (A), 1966, 1656.

34. R.L. Martin and H. Waterman, J. Chem. Soc., 1957, 2545.

35. A. Earnshaw and J. Lewis, J. Chem. Soc., 1961, 396.

36. M. Gerloch, J. Lewis, F.E. Mabbs, and A. Richards, J. Chem. Soc. (A), 1968, 112.

37. J. Lewis, F.E. Mabbs, and A. Richards, J. Chem. Soc.(A), 1967, 1014.

38. J. Lewis, Y.C. Lin, L.K. Royston, and R.C. Thompson, J. Chem. Soc., 1965, 6464.

39. A.P. Ginsberg, R.C. Sherwood, and E. Koubek, J. Inorg. Nucl. Chem., 1967, 29, 353.

40. W. Wojciechowski, Inorganica Chimica Acta, 1967, 1, 319, 324, 329.

41. G.A. Kakos and G. Winter, Aust. J. Chem., 1969, 22, 97.

42. J.B. Goodenough, "Magnetism and the Chemical Bond", Interscience Publishers, New York, 1963.

43. C.J. Ballhausen and L.S. Forster, Acta Chem. Scand., 1962, 16, 1385.

44. I.G. Ross, Trans. Far. Soc., 1959, 55, 1057.

45. E.A. Boudreaux, Inorg. Chem., 1964, 3, 506.

46. D.J. Royer, Inorg. Chem., 1965, 4, 1830.

47. W.E. Hatfield and J.S. Paschal, J.A.C.S., 1964, 86, 3888.

48. M. Kato, H.B. Jonassen, and J.C. Fanning, Chem. Revs., 1964, 64, 99.

49. A.P. Ginsberg, E. Koubek, and H.J. Williams, Inorg. Chem., 1966, 5, 1656.

50. P.W. Anderson, Phys. Rev., 1959, 115, 2.

51. R.L. Martin, "New Pathways in Inorganic Chemistry", Cambridge University Press, 1968.

52. R.K. Nesbet, Ann. Phys., 1958, 4, 87.

53. R.K. Nesbet, Phys. Rev., 1960, 119, 658.

54. G.W. Pratt, Phys. Rev., 1955, 97, 926.

55. J.B. Goodenough and A.L. Loeb, Phys. Rev., 1955, 98, 391.

56. P.W. Smith and A.D. Wadsley, unpublished results.

57. G.N. Tischenko, Tr. Inst. Kristallogr. Akad, Nauk. SSSR., 1955, 93.

58. A.W. Schlueter, R.A. Jacobson, and R.E. Rundle, Inorg. Chem., 1966, 5, 277.

59. A. Engberg and H. Soling, Acta Chem. Scand., 1967, 21, 168.

60. G. Stucky, S.D'Agostino and G. McPherson, J.A.C.S., 1966, 88, 4828.

61. H.J. Seifert and K. Klatyk, Z. anorg. allgem. Chem., 1964, 334, 113.

62. N.L. Huang, Phys. Rev., 1967, 157, 378.

63. N.L. Huang and R. Orbach, J. Appl. Phys., 1968, 39, 426.

64. A.G. Gossard, Phys. Rev., 1964, 135, 1051.

65. A.P. Ginsberg, R.L. Martin, and R.C. Sherwood, Inorg. Chem., 1968, 7, 932.

66. J. Kanamori, J. Phys. Chem. Solids, 1959, 10, 87.

67. B. Morosin and A. Nareth, J. Chem. Phys., 1964, 40, 1958.

68. D.J.W. Ijdo, Ph.D. Thesis, Leiden, 1960.

69. W. Klemm and H. Steinberg, Z. anorg. allg. Chem., 1936, 227, 193.

70. R. Saillant and R.A.D. Wentworth, Inorg. Chem., 1968, 7, 1606.

71. A.T. Casey and R.J.H. Clark, Inorg. Chem., 1968, 7, 1598.

72. A.P. Ginsberg and M.B. Robin, unpublished.

73. P.D.W. Boyd, P.W. Smith, and A.G. Wedd, Aust. J. Chem., 1969, 22, 653.

74. W.N. Hansen and M. Griffel, J. Chem. Phys., 1958, 28, 902.

75. W.N. Hansen and M. Griffel, J. Chem. Phys., 1959, 30, 913.

76. Vogel "A Textbook of Quantitative Inorganic Analysis", 1961, Longmans.

77. R.S. Nyholm, private communication.

78. B.N. Figgis and R.S. Nyholm, J. Chem. Soc., 1959, 331.

79. J. Lewis and R. Wilkins, "Modern Coordination Chemistry", Interscience, New York, 1960.

80. A.G. Wedd, Ph.D. Thesis, Hobart, 1968.

81. F.A. Cotton, Rev. Pure and Appl. Chem., 1967, 17, 25.

82. M.C. Baird, Progr. in Inorg. Chem., 1968, 9, 1.

83. P.W. Smith and A.G. Wedd, J. Chem. Soc.(A), 1969.

84. P.W. Smith, Ph.D. Thesis, London, 1963.

85. I.I. Kozhina and D.V. Korol'kov, Russ. J. Struct. Chem., 1965, 6, 84.

86. C. Herring and M. Flicker, Phys. Rev. 1964, 134, A362.

87. C.G. Barraclough and C.F. Ng, Trans. Farad. Soc., 1964, 60, 836.

88. H.J. Seifert and P. Ehrlich, Z. anorg. allgem. Chem., 1959, 301, 282.

89. R.W. Asmussen, Proc. symp. on coordination Chem., Copenhagen, 1953.

90. H.J. Seifert, H. Fink, and E. Just, Naturwissenschaften, 1968, 55, 297.

91. I.E. Grey and P.W. Smith, Aust. J. Chem., 1969, 22, 121.

92. K. Brodersen, H.K. Breitbach, and G. Thiele, Z. anorg. allgem. Chem., 1968, 357, 162.

93. L.F. Dahl and D.L. Wampler, Acta. Cryst., 1962, 15, 903.

94. A.F. Wells, J. Chem. Soc., 1947, 1670.

95. R.W. Adams, C.G. Barraclough, R.L. Martin, and G. Winter, Aust. J. Chem., 1967, 20, 2351.

96. D.M. Gruen and R.L. McBeth, J. Phys. Chem., 1962, 66, 57.

97. R.J.H. Clark, J. Chem. Soc., 1964, 417.

98. J.R. Perumareddi, J. Chem. Phys., 1967, 71, 3144, and references contained within.

99. D.M. Adams and P.J. Lock, J. Chem. Soc.(A), 1967, 620.

100. D.M.L. Goodgame, M. Goodgame, and M.J. Weeks, J. Chem. Soc., 1964, 5194.

101. A. Magneli and G. Andersson, Acta Chem. Scand., 1955, 9, 1378.

102. K. Brodersen, Angewandte Chemie, 1968, 4, 155.

103. M. Inove, M. Kishita, and M. Kubo, Inorg. Chem., 1967, 6, 900.

104. B. Bleaney and K.D. Bowers, Proc. Roy. Soc. (London), 1952, A214, 451.

105. H.J. Seifert and B. Gerstenberg, Z. anorg. allgem. Chem., 1962, 315, 56.

106. R. Belcher and C.L. Wilson, "New Methods in Analytical Chemistry", Chapman and Hall, 1955.

APPENDIX I

STUDIES OF METAL HALIDES. III.

Far-infrared Spectra of Chromium(III) and Molybdenum(III) Complex Halides of Formula $A_3M_2X_9$ and A_3MX_6.

Accepted for Publication in Aust. J. Chem.,
1969, 22, -.

Submitted for Examination

STUDIES OF METAL HALIDES. III.

Far-infrared Spectra of Chromium(III) and Molybdenum(III) Complex Halides of Formula $A_3M_2X_9$ and A_3MX_6.

by I.E. Grey* and P.W. Smith*

Summary

Far-infrared spectra are reported for compounds of formula $A_3M_2X_9$, with M = Cr, Mo; X = Cl, Br; A = univalent cations, for the region 400-200 cm^{-1}. Assignments for metal-terminal halogen and metal-bridging halogen stretching vibrations in the binuclear anion are proposed. Data on several related mononuclear hexahalo-complexes are included for comparison. An explanation is offered for differences in the spectral features of the series of compounds in terms of distortions of the binuclear anion which arise from cation-anion interaction in the crystal lattice.

We have discussed previously structural variations in the solid state between compounds of general formula $A_3M_2X_9$, with M = Cr(III), Mo(III), and W(III); X = Cl,

*Chemistry Department, University of Tasmania, P.O. Box 252C, Hobart, Tasmania, 7001.

Br, arising as the cation (A) is varied. These are manifested indirectly in changes in magnetic properties[12] and electronic spectra[3,4] of the binuclear anion $[M_2X_9]^{3-}$. A more direct measure of effects on molecular structure may be obtained from far-infrared spectra where the symmetry and bonding in the anion should be reflected in the relative and absolute band positions and number of terminal- and bridging-halogen stretching vibrations, $\nu(MX_t)$ and $\nu(MX_{br})$, respectively.

Far-infrared studies of bridged metal halide complexes reported so far, have included detailed investigations of planar $[M_2X_6]^{n-}$ [5,6] and "tetrahedral" M_2X_6 [7,8] species for which normal coordinate analyses and assignments for $\nu(MX_t)$ and $\nu(MX_{br})$ have been made. Data have been reported also for several M_2X_{10} species in which two octahedra share an edge; the complexity of the spectra has presented difficulties in interpretation[9,10] but recently a detailed analysis has been made[11].

Complexes of the type $[M_2X_9]^{3-}$ studied here, for which the structure comprises two face-sharing octahedra, have received little attention. The spectra of $(Et_4N)_3M_2Cl_9$ (M = Cr, V) have been reported[12]. Recently Beattie et. al. have presented complete spectral data for $Cs_3Tl_2Cl_9$[11]. From a detailed study of the Raman spectrum of a single crystal, together with a simple normal

coordinate treatment of the $[Tl_2Cl_9]^{3-}$ anion, assignments for all observed Raman and infrared frequencies were made.

In this investigation we have examined the infrared spectra of compounds of stoichiometry $A_3M_2X_9$ in the following instances:

(i) M = Cr; X = Cl; A = K, Rb, Cs, Et_4N.

(ii) M = Cr; X = Br; A = Cs, Et_4N.

(iii) M = Mo; X = Cl; A = K, NH_4, Cs, Me_4N, Et_3NH, Et_4N.

(iv) M = Mo; X = Br; A = Cs, Et_4N.

Assignments have been made for all observed bands in the infrared spectral region 400-200 cm^{-1}. The spectral band shifts observed for $\nu(MX_t)$ and $\nu(MX_{br})$ as the cation (A) is varied have been interpreted, on the basis of X-ray data, as indicating structural distortions of the anion and variations in metal-metal and metal -halogen separations.

Spectral data for the mononuclear complexes $(NH_4)_3MoCl_6$, K_3MoCl_6, K_3CrCl_6, and Cs_3CrCl_6 are given for comparative purposes.

Results:

For the binuclear chromium and molybdenum complexes considered, the bands observed in the region 400-200 cm^{-1} at room temperature are listed in Tables 1, and 2,

TABLE 1

BAND POSITIONS FOR CHROMIUM(III) BINUCLEAR COMPLEXES

(400-200 cm^{-1} region)

Complex	Band 1 $\nu(M\text{-}Cl_t)$ (a_2'')	Band 2 $\nu(M\text{-}Cl_t)$ (e')	Band 3 $\nu(M\text{-}Cl_{br})$ (a_2'')	Band 4 $\nu(M\text{-}Cl_{br})$ (e')
$K_3Cr_2Cl_9$	373 sh	358 s	268 m	244 m
$Rb_3Cr_2Cl_9$	372 sh 362 s	349 s	265 m	240 w-m
$Cs_3Cr_2Cl_9$	368 sh 357 s	339 vs	268 m	234 w-m
$(Et_4N)_3Cr_2Cl_9$	345 vs 338 sh	329 sh 325 sh 322 vs 315 sh	266 w-m	264?
$Cs_3Cr_2Br_9$	288 vs	273 s	*	*
$(Et_4N)_3Cr_2Br_9$	277 vs	259 s	*	*

* Not observed down to 200 cm^{-1}.

TABLE 2

BAND POSITIONS FOR MOLYBDENUM(III) BINUCLEAR COMPLEXES

(400-200 cm^{-1} region)

Complex	Band 1 $\nu(M\text{-}Cl_t)$ (a_2'')	Band 2 $\nu(M\text{-}Cl_t)$ (e')	Band 3 $\nu(M\text{-}Cl_{br})$ (a_2'')	Band 4 $\nu(M\text{-}Cl_{br})$ (e')
$K_3Mo_2Cl_9$	340 vs	327 sh 322 s	283 vw	236 m
$(NH_4)_3Mo_2Cl_9$	338 s	320 s	283 w	238 m
$Cs_3Mo_2Cl_9$	333 vs	318 s	277 w	238 m
$(Me_4N)_3Mo_2Cl_9$	325 s	308 ms	273 w	250 w
$(Et_3NH)_3Mo_2Cl_9$	328 vs	294 s	267 m	250 w
$(Et_4N)_3Mo_2Cl_9$	325 s 320 vs	304 s 298 vs	268 m	252 w
$Cs_3Mo_2Br_9$	253 vs	231 s	*	*
$(Et_4N)_3Mo_2Br_9$	247 vs	227 s	*	*

*Not observed down to 200 cm^{-1}.

TABLE 3

ν_3 BAND POSITIONS FOR MONONUCLEAR COMPLEXES

(400-200 cm^{-1} region)

K_3CrCl_6	328 vs, br 315 sh 292 m-s	$(NH_4)_3MoCl_6$	307 vs
		K_3MoCl_6	298 vs 285 s 269 m
Cs_3CrCl_6	330 sh 318 vs		

respectively, and for the mononuclear complexes in Table 3.

The spectra of both the chromium and molybdenum binuclear chloro- complexes are similar, showing in general two strong bands in the high wavenumber region above 300 cm^{-1} and two bands of medium to weak intensity below 300 cm^{-1}. The bromo- complexes, down to the experimental limit of 200 cm^{-1}, show two strong bands only. These lie approximately 60-80 cm^{-1} below the corresponding bands for the chloro- complexes. Calculation of the ratio of the related band positions for bromide/chloride gives values of about 0.75 for the molybdenum complexes and 0.8 for the chromium complexes.

The relative intensities of the four main bands are shown in Figure 1 for the two extremes in the molybdenum series, $K_3Mo_2Cl_9$ and $(Et_4N)_3Mo_2Cl_9$. Further intensity data are indicated in Figs.2 and 3 and in Tables 1,2, and 3.

Assignments:

The symmetry of the isolated $[M_2X_9]^{3-}$ molecular unit is D_{3h}. Of the total of twenty-seven modes, eighteen may be classified as vibrational and comprise the set ($4a_1' + a_1'' + a_2' + 3a_2'' + 5e' + 4e''$). Only the e' and a_2'' species are infrared active. The eight infrared active fundamentals may be separated into vibrations involving as

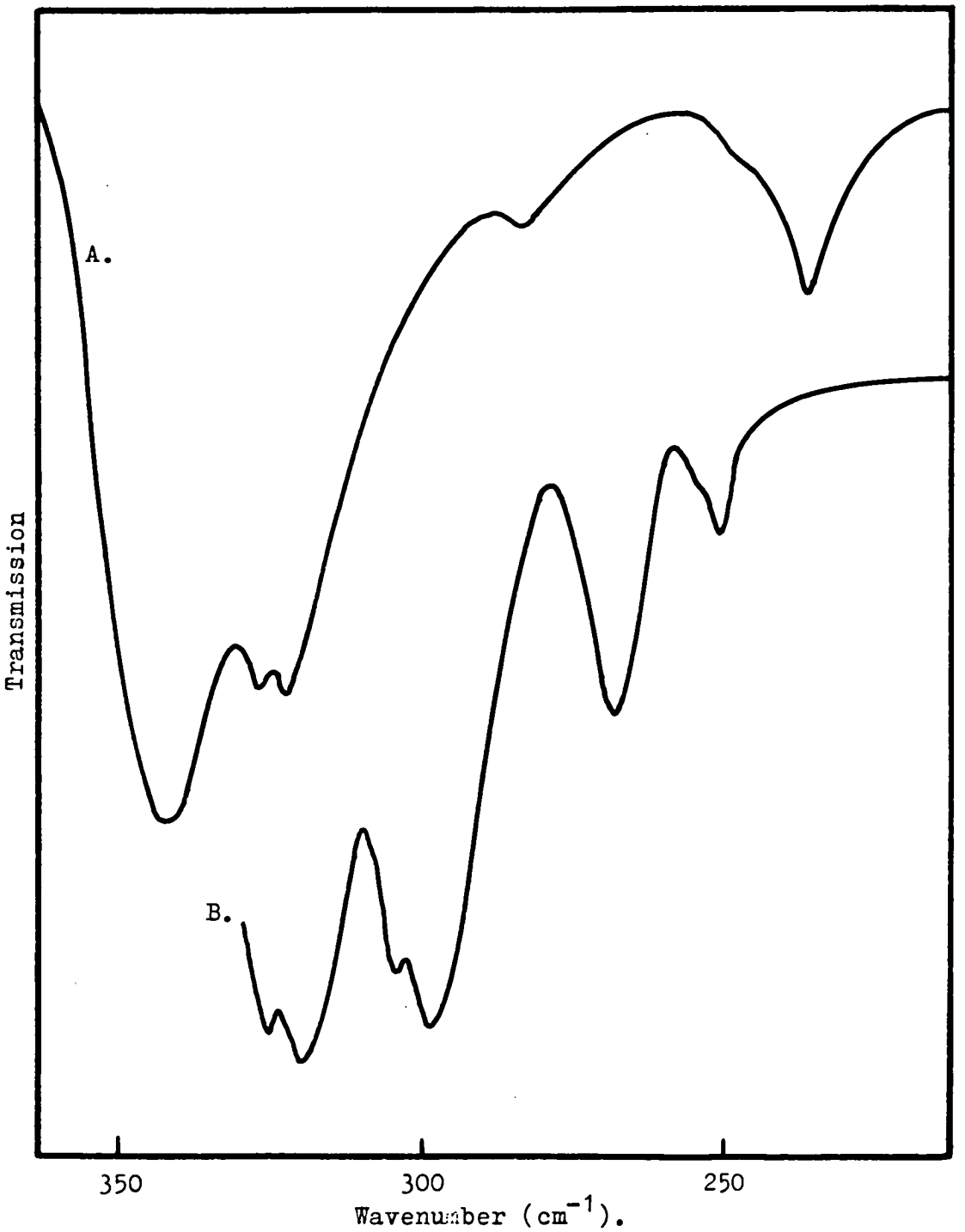

Fig. 1. - Far-infrared spectra: A. $K_3Mo_2Cl_9$;
B. $(Et_4N)_3Mo_2Cl_9$.
Curves displaced vertically for clarity.

an approximation, mainly:

Metal terminal-halogen stretching modes $(a_2'' + e')$

Metal bridging-halogen stretching modes $(a_2'' + e')$

Bending modes $(a_2'' + 3e')$

There should then be two bands in the infrared spectrum attributable predominantly to $\nu(MX_t)$, two bands mainly to $\nu(MX_{br})$ and four bands for the bending modes. Because each of the three types of infrared active fundamentals include the same symmetry representation, configuration mixing is to be expected, especially between the bridge stretching and the bending modes.

In $Cs_3Tl_2Cl_9$, two strong bands at 279 and 265 cm^{-1} have been assigned to $\nu(TlCl_t)$ and two bands of medium intensity at 222 and 180 cm^{-1} to $\nu(TlCl_{br})$; in each case the higher frequency band was assigned to the non-degenerate a_2'' mode[11]. For the complex $(Et_4N)Ti_2Cl_9$, believed to contain $[Ti_2Cl_9]^-$, two very strong bands at 416 and 379 cm^{-1} were classed as $\nu(TiCl_t)$ and two weak bands as 268 and 230 cm^{-1} as $\nu(TiCl_{br})$[13]. For both these compounds, bands associated with bending vibrations lie below 200 cm^{-1}.

Accordingly, for the chromium and molybdenum complexes examined here, the two strong bands in the wavenumber region above 300 cm^{-1} are assigned as $\nu(MCl_t)$

and the two bands of lower intensity below 300 cm^{-1} as $\nu(MCl_{br})$ vibrations, as shown in Tables 1 and 2. For the bromo-complexes, the two strong bands in the region 230-290 cm^{-1} (approximately) are assigned to $\nu(MBr_t)$. The specific assignments to a_2'' and e' modes proposed follow from the analysis for $Cs_3Tl_2Cl_9$.

From Tables 1 and 2 it is apparent that the bands for some complexes are not single peaks but are split or have shoulders. This is interpreted as indicating a lowering of the symmetry of the isolated binuclear anion in the solid state. In cases where the crystal structure of the complex is known, the number of infrared active vibrations may be determined from site symmetry analysis as given by Halford[14]. Thus, from our studies[15] $K_3Mo_2Cl_9$ has a bimolecular cell and belongs to space group $P6_3/m$, (C_{6h}^2); the site group for the $[Mo_2Cl_9]^{3-}$ ion is then C_{3h} (sub group of D_{3h}). With this reduced symmetry three infrared active terminal stretching modes ($a_2'' + 2e'$) are predicted. In agreement with this, three bands in the $\nu(MoCl_t)$ region are observed for $K_3Mo_2Cl_9$. The bridge stretching vibrations in this instance are too weak for splittings to be discerned. For the two tetraethylammonium binuclear chloro- compounds splittings appear as shoulders on the main bands (see Figs. 1 and 2). It can be shown that the maximum number of terminal and bridging halogen-metal stretching vibrations is six in each

case, when the site symmetry is lowered to C_s. For the complexes studied here, however, the splittings of the main bands are small and in analysing the spectra the symmetry of the binuclear anion in the crystal may be considered as effectively that of the isolated anion, D_{3h}.

It can be seen from the Tables that for the binuclear chromium chloro- complexes the bands assigned to $\nu(MX_t)$ and $\nu(MX_{br})$ lie in the ranges 370-315 cm^{-1} and 270-230 cm^{-1}, respectively. For the molybdenum analogues the corresponding ranges are 345-290 cm^{-1} and 285-235 cm^{-1}. Hence in the latter instance the two sets of bands almost overlap but they are well separated for the chromium complexes. If the wavenumber difference $\Delta\nu$ between the average of the two $\nu(MX_t)$ and the two $\nu(MX_{br})$ bands is examined, then for $A_3Cr_2Cl_9$, $\Delta\nu$ is 67-110 cm^{-1} while for $A_3Mo_2Cl_9$, $\Delta\nu$ is 52-74 cm^{-1}. Similar results have been observed for the complexes $A_2Pd_2X_6$ and $A_2Pt_2X_6$: here $\Delta\nu$ is 68-83 cm^{-1} for the palladium compounds whereas it is only 36-40 cm^{-1} for the platinum series[5].

The large values of $\Delta\nu$ for the chromium complexes are attributable to extensive coupling between terminal and bridging stretching modes belonging to the same representation, vis. to a_2'' or e'. This interaction,

which causes $\nu(MX_t)$ and $\nu(MX_{br})$ to diverge, is expected to be less important in the molybdenum series than for chromium because of the greater atomic mass of the molybdenum. The smaller values of $\Delta\nu$ are in accordance with this view.

The spectra of the several mononuclear complexes of chromium and molybdenum listed in Table 3 show one main band system only. For both Cs_3CrCl_6 and $(NH_4)_3MoCl_6$ a very strong band is observed with a maximum at 318 and 307 cm^{-1}, respectively. The band for the chromium complex displays a shoulder at 330 cm^{-1} but the peak position agrees well with the value 315 cm^{-1} reported for $Copn_3CrCl_6$[16]. These bands are assigned to the infrared active metal-chlorine stretching vibration ν_3 for an anion of symmetry O_h.

The potassium salts K_3CrCl_6 and K_3MoCl_6 each display three distinct peaks. The splitting is such here that the octahedra must be considerably distorted, and in fact it has been reported that K_3MoCl_6 has a monoclinic space group - $P2_1/a$[17]. The only possible site for the $[MoCl_6]^{3-}$ ion has C_i symmetry and on this basis three infrared active stretching modes are predicted.

Discussion:

For convenience, discussion of the structural implications of the spectra is restricted to those binuclear chloro- complexes of molybdenum and chromium for which powder x-ray photographs indicate that they are isostructural with $Cs_3Cr_2Cl_9$ and $K_3Mo_2Cl_9$. These comprise the compounds in the series $A_3Cr_2Cl_9$ with A = K, Rb, Cs, Et_4N and the series $A_3Mo_2Cl_9$ with A = K, NH_4, Cs, Me_4N, Et_4N. To facilitate further interpretation of spectra, reference will be made to the correlation diagrams given in Figures 2 and 3.

From Fig.2 the main changes in spectra to be noted in passing from $Cs_3Cr_2Cl_9$ to $Cs_3Mo_2Cl_9$ are:

(a) The mean of the two $\nu(MCl_t)$ modes shifts to a lower wavenumber; that for the two $\nu(MCl_{br})$ modes shifts slightly to a higher wavenumber.

(b) The separation between the two $\nu(MCl_t)$ bands ($a_2'' + e$) is almost unchanged.

(c) The two $\nu(MCl_{br})$ bands diverge.

The shifting of the absolute positions of the band systems described in (a) is a result of the mass change from chromium to molybdenum together with coupling of the terminal and bridge stretching modes as described above. It is proposed, however, that the observations (b) and (c)

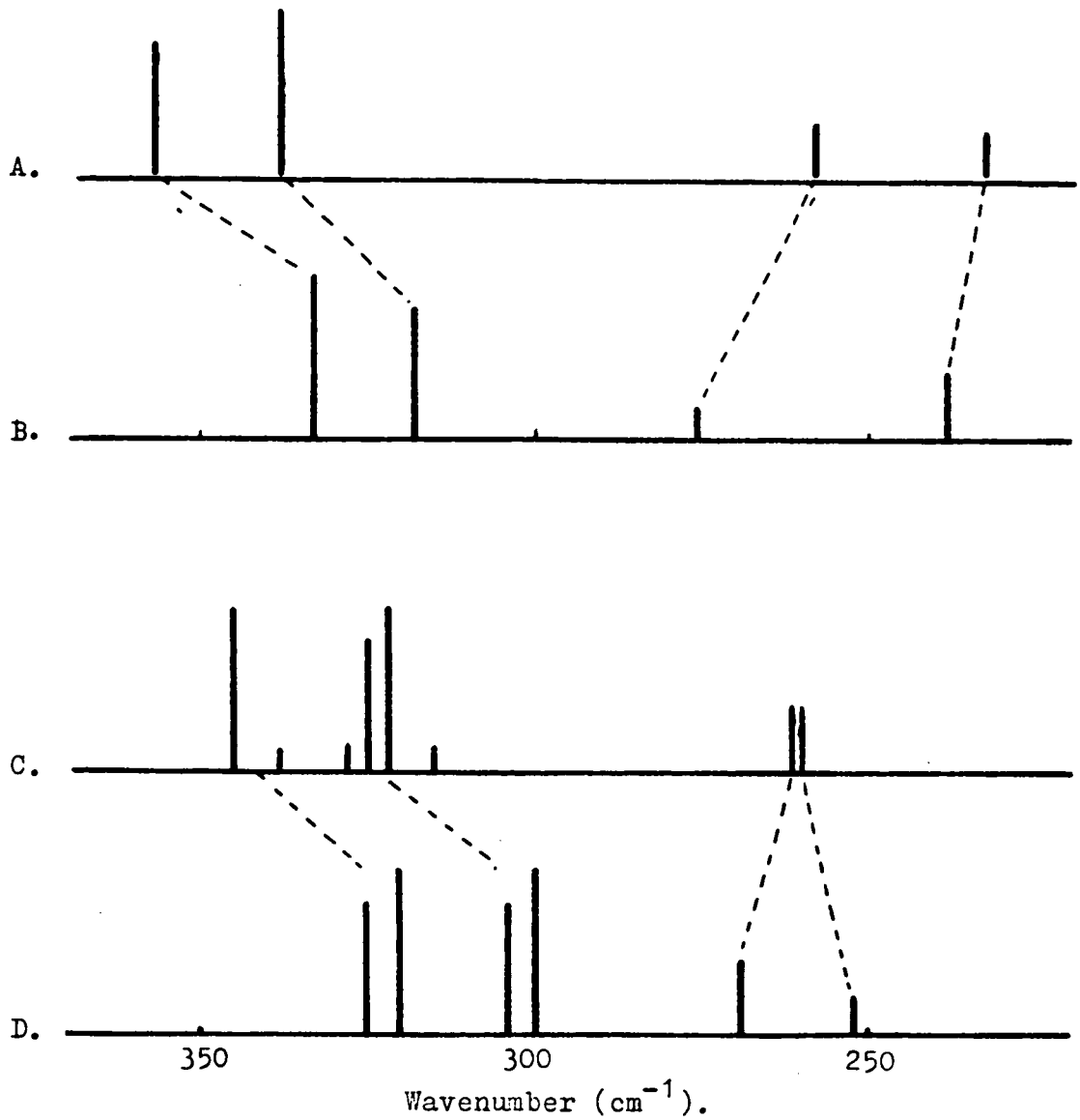

Fig. 2. - Correlation diagrams showing band positions and relative intensities:

A. $Cs_3Cr_2Cl_9$; B. $Cs_3Mo_2Cl_9$; C. $(Et_4N)_3Cr_2Cl_9$; D. $(Et_4N)_3Mo_2Cl_9$.

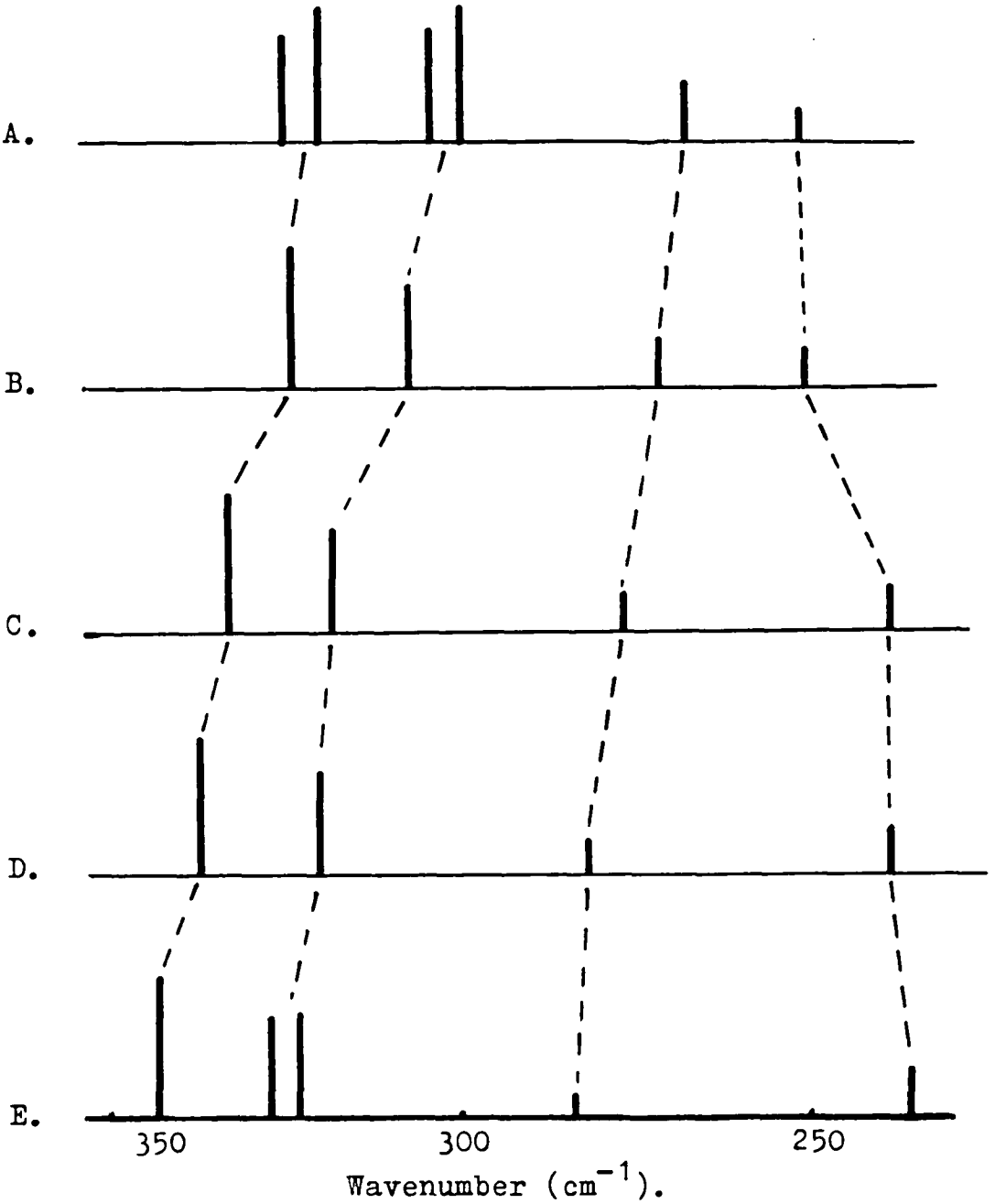

Fig. 3. - Correlation diagram for:

A. $(Et_4N)_3Mo_2Cl_9$; B. $(Me_4N)_3Mo_2Cl_9$;
C. $Cs_3Mo_2Cl_9$; D. $(NH_4)_3Mo_2Cl_9$;
E. $K_3Mo_2Cl_9$.

can be directly related to changes in the structure of the binuclear anion.

If it is accepted that a distortion of the Cl-M-Cl angle affects the non-degenerate (a_2'') and doubly degenerate (e') modes differently and hence that the frequencies of the two modes will converge or diverge, then the spectra may be readily understood as follows.

From the x-ray data of Table 4, it is seen that the angle between the terminal chlorine-metal bonds, (Cl_t-M-Cl_t) is only slightly decreased in passing from $Cs_3Cr_2Cl_9$ to $Cs_3Mo_2Cl_9$. In accord with this the separation between the a_2'' and e' modes is found to decrease slightly. The angles between the bridging chlorine-metal bonds, (Cl_{br}-M-Cl_{br}) and (M-Cl_{br}-M), change markedly and this is reflected in the trend noted under (c) above. Hence, corresponding to an axial compression of the (MX_3M) structure in passing from the chromium to the molybdenum complex the non-degenerate and doubly degenerate $\nu(MCl_{br})$ modes, a_2'' and e', diverge.

The validity of this simple approach may now be checked by considering the spectral changes in the isostructural series $A_3Mo_2Cl_9$. Here the spectra should be quite sensitive to distortions of the anion as the situation is not complicated by mass effects resulting

TABLE 4

Complex	$Cs_3Cr_2Cl_9$ (a)	$Cs_3Mo_2Cl_9$ (b)	$K_3Mo_2Cl_9$ (c)
M-M (Å)	3.12	2.68	2.53
$M-Cl_t$ (Å)	2.34	2.40	2.41
$M-Cl_{br}$ (Å)	2.52	2.52	2.50
Angle Cl_t-M-Cl_t	93°	91.0	91.5°
Angle $Cl_{br}-M-Cl_{br}$	85°	95°	97°
Angle $M-Cl_{br}-M$	76°	64°	60.5°

(a) Reference 18.

(b) Reference 17.

(c) Reference 15.

from the change of metal (M), and the coupling between vibrations of the same symmetry should be small for the heavy molybdenum atom. We have recently determined the structure of both $K_3Mo_2Cl_9$[15] and $Cs_3Mo_2Cl_9$[18] using single-crystal x-ray diffraction techniques. The relevant structural parameters for the binuclear anion in each of these compounds are compared in Table 4. It can be seen that decrease in the size of the cation from Cs to K has resulted in a compression of the complex anion with the bridging angle decreasing from 64° to 60°. There is, however, a negligible increase in the terminal chlorine-molybdenum angle, Cl_t-Mo-Cl_t and little change in the Mo-Cl_t and Mo-Cl_{br} bond lengths. On this basis, as the cation size is decreased in such a series the main spectral change should be a progressive separation of the a_2'' and e' $\nu(MoCl_{br})$ modes. On the other hand little or no change should occur either for the splitting of the $\nu(MoCl_t)$ modes or in the mean positions for the $\nu(MoCl_{br})$ and $\nu(MoCl_t)$ band systems.

Inspection of Figure 3 shows that these predictions are largely borne out in the spectra for the compounds. From $(Et_4N)_3Mo_2Cl_9$ to $K_3Mo_2Cl_9$, the separation of the $\nu(MoCl_{br})$ bands increases from 16 to 47 cm^{-1} whereas for $\nu(MoCl_t)$ the corresponding change is from approximately 22 to 28 cm^{-1}. The mean position of the two $\nu(MoCl_t)$

bands does not change. The mean for the ($MoCl_t$) bands, however, shows some change from approximately 311 to 331 cm^{-1}. This reamins to be explained although it might be expected to indicate a change in Mo-Cl_t bond length. Additional x-ray and Raman data are being sought on these compounds.

We conclude that in the $A_3M_2X_9$ series the absolute and relative values for the metal-halogen stretching frequencies are sensitive to structural changes within the binuclear complex anion. In particular, elongation on compression of the anion with change of cation is reflected in the convergence or divergence, respectively, of the metal-bridging halogen stretching modes.

Acknowledgements:

One of us (I.E.G.) acknowledges receipt of a Commonwealth Post-Graduate Scholarship. We thank the Division of Mineral Chemistry, C.S.I.R.O., and Drs. A.F. Reid and D.E. Scaife for the use of the infrared spectrophotometer.

Experimental:

Samples of $(NH_4)_3MoCl_6$, $(NH_4)_3Mo_2Cl_9$, K_3MoCl_6 and $Cs_3Mo_2X_9$ (X=Cl,Br) were supplied by Dr. A.G. Wedd.

The preparations and analyses for the compounds $(Et_3NH)_3Mo_2Cl_9$ and $(Et_4N)_3Mo_2X_9$ (X=Cl,Br) are described elsewhere[1].

$K_3Mo_2Cl_9$ - Acid molybdenum(III) chloride[4] solution (30 ml) was evaporated to dryness. The resulting solid residue was transferred to a nitrogen filled glovebox where it was added in four portions to finely powdered KCl (half stoichiometric quantity). After each addition the mixture was intimately ground. The extremely hygroscopic solid mixture absorbed traces of moisture and the mixture gradually was ground to a paste. It was then vacuum-dried. After all the acid solid residue had been added, the mixture was finally dried and 'superdry' ethanol (50 ml) added. The insoluble compound was filtered, washed with ethanol and vacuum dried to light orange-brown powder.

Found: Cl, 50.7; Mo, 30.2, 30.3%. $K_3Mo_2Cl_9$ requires: Cl, 50.78; Mo, 30.54%.

$(Me_4N)_3Mo_2Cl_9$ - This was prepared by the same method as for the tetraethylammonium salt[1], involving addition of a solution of tetramethylammonium chloride in dry ethanol to an evaporated molybdenum(III) acid solution. The light orange complex precipitated immediately.

Found: C, 19.60; H, 5.01; Cl, 43.1; Mo, 26.2; N, 5.60%.

$C_{12}H_{36}N_3Mo_2Cl_9$ requires C, 19.68; H, 4.95; Cl, 43.51; Mo, 26.16; N, 5.73%.

$A_3Cr_2Cl_9$ (A = K, Rb, Cs) - Exact stoichiometric quantities of $CrCl_3$ and the alkali metal chloride previously dried in vacuo at 200° were weighed accurately and transferred to a nitrogen filled glovebox where they were intimately ground. The mixtures were sealed in small silica tubes under high vacuum. The tubes were heated with careful temperature control, a few degrees above the melting point of the compound[20,21] for 2-3 days, then cooled slowly. The cooled melts consisted of large aggregates of purple hexagonal plates. All lines on Debye-Scherrer powder photographs could be indexed on a bimolecular hexagonal cell analogous to that for $Cs_3Cr_2Cl_9$.

A_3CrCl_6 (A = K, Cs) - The mononuclear complexes[20,21] were prepared by the above method, using 1:3 mixtures of $CrCl_3$:ACl. The melts were ground to a light pink powder.

$Cs_3Cr_2Br_9$ - A bromine-nitrogen mixture was passed over a 3:2 mixture of CsBr and $CrBr_3$ contained in a silica tube. A temperature gradient was maintained along the length of the tube and large hexagonal green crystals of the complex deposited at the cool end. Found: Br, 58.5%;

$Cs_3Cr_2Br_9$ requires: Br, 58.85%. The Debye-Scherrer powder picture of $Cs_3Cr_2Br_9$ indicated it was isostructural with $Cs_3Cr_2Cl_9$ and all observed lines could be indexed on this basis.

$(Et_4N)_3Cr_2Br_9$ - Tetramethyl ammonium bromide and chromium tribromide ("active $CrBr_3$") were refluxed in acetyl bromide for one hour and then cooled in ice. The green complex crystallized as large hexagonal prisms. These were filtered, washed with acetyl bromide and dried in vacuo. Found: C, 23.6; H, 5.0; Br, 58.6; Cr, 8.45; N, 3.6%; $C_{24}H_{60}N_3Cr_2Br_9$ requires: C, 23.75; H, 5.0; Br, 59.2; Cr, 8.55; N, 3.5%.

Spectra were obtained on a Beckman IR-12 spectrophotometer using nujol mulls and polythene windows.

X-ray powder photographs on moisture sensitive compounds were obtained as described previously[22].

REFERENCES

1. I.E. Grey and P.W. Smith, Aust. J. Chem., 1969, 22,121.
2. P.D.W. Boyd, P.W. Smith and A.G. Wedd, Aust. J. Chem., 1969, 22, 653.
3. P.W. Smith and A.G. Wedd, unpublished.
4. J. Lewis, R.S. Nyholm, and P.W. Smith, J.C.S.(A), 1969, 57.
5. D.M. Adams, P.J. Chandler, and R.G. Churchill, J.C.S.(A), 1967, 1272.
6. R.J. Goodfellow, P.L. Goggin, and L.M. Venanzi, J.C.S.(A), 1967, 1897.
7. T. Onishi and T. Shimanouchi, Spectrochim Acta, 1964, 20, 325.
8. I.R. Beattie, T. Gilson, and G.A. Ozin, J.C.S.(A), 1968, 813.
9. G.L. Carlson, Spectrochim Acta, 1963, 19, 1291.
10. B.J. Brisdon and R.A. Walton, Spectrochim Acta, 1967, 23A, 2489.
11. I.R. Beattie, T.R. Gilson, and G.A. Ozin, (J.C.S.(A), 1968, 2765.
12. D.M. Adams, J. Chatt, J.M. Davidson, and J.Cerratt, J.C.S., 1963, 2189.
13. J.A. Creighton and J.H.S. Green, J.C.S.(A), 1968, 808.
14. R.S. Halford, J. Chem. Phys., 1946, 14, 8.
15. I.E. Grey and P.W. Smith, unpublished.

REFERENCES

(continued)

16. D.M. Adams and D.M. Morris, J. Chem. Soc. 1968(A), 694.

17. B. Van Laar and R.C.N. Petten, quoted in Physica, 1967, 36, 269.

18. P.W. Smith and A.D. Wadsley, unpublished.

19. D.J.W. Ijdo and G.J. Wessel, Acta Cryst, 1957, 10, 466.

20. S.A. Shchukarev, I.V. Vasil'kova, A.I. Efimov, and B.Z. Pitirimov, Russ. J. Inorg. Chem., 1966, 11, 268.

21. C.M. Cook, J. Inorg. Nucl. Chem., 1963, 25, 123.

22. I.E. Grey and P.W. Smith, J. Sci. Inst. 1968, 2, 1, 693.

APPENDIX II

PAPERS PUBLISHED DURING COURSE OF STUDY

Submitted for Examination

Journal of Scientific Instruments (Journal of Physics E)
1968 Series 2 Volume 1

Accurate determination of lattice parameters on air-sensitive compounds

I E Grey and P W Smith
Chemistry Department, University of Tasmania, Hobart, Tasmania, Australia
MS *received 21 February 1968*

Abstract A simple method of sample preparation for examination of air-sensitive compounds with the Hägg–Guinier focusing x-ray camera is described.

The advantages of the Hägg–Guinier x-ray camera for accurate determination of lattice parameters on powder samples are now well known. However, with air-sensitive compounds difficulty arises both in preparing the mixture of sample and internal calibrant and in protecting the sample during exposure (8–48 h). A precision sample holder in which the powder is hermetically sealed between two thin metal foils has been described recently (Scaife and Watts 1964). This requires construction to fine tolerances and in use must be loaded in an efficient evacuable glove box.

The alternative method of sample preparation described here needs standard vacuum line equipment only. Small portions of the sample powder are loaded *in vacuo* into a series of Lindemann glass capillaries (0·3 mm in diameter) which are then sealed off at a suitable length (10–15 mm). The capillaries (five or more) are taped on the standard sample holder as shown in figure 1. As in the normal method, an internal standard is required to obtain accurate line positions; suitable standards are potassium chloride and silicon metal.

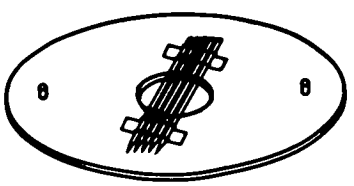

Figure 1

We have established that any errors arising as a result of displacement from the normal sample plane position can be corrected with an internal standard. The precision of the method is illustrated by typical results obtained with potassium chloride as calibrant (see table 1).

Table 1

	ASTM value (Å)	This method (Å)	Stand. dev. (Å)
$Pb(NO_3)_2$ (cubic)	7·8568	7·855	0·002 (9 lines)
K_2PtCl_6 (cubic)	9·755	9·756	0·003 (9 lines)

The method has been applied successfully to the determination of cell parameters of several series of air-sensitive uranium and transition element complexes.

In the event of a solid state reaction between calibrant and compound, these may be sealed in separate capillaries and alternated on the sample holder, with small loss in precision.

We thank Dr A D Wadsley, CSIRO Division of Mineral Chemistry, for helpful discussions on the use of the camera. One of us (IEG) acknowledges the award of University Honours and Commonwealth Post-graduate Scholarships. The camera employed was constructed in the Science Equipment Centre of the Education Department of Tasmania, Hobart.

References

Scaife D E and Watts J A 1964 *J. Sci. Instrum.* **41** 569–70

Reprinted from

Chemical Communications

NUMBER 23/1968 4 DECEMBER

Co-ordination Isomerism in Hydrated Vanadium(II) Double Chlorides and Evidence for Binuclear Structure in $RbVCl_3$

By I. E. Grey and P. W. Smith*

(*Chemistry Department, University of Tasmania, Hobart, Australia*)

Recently the first vanadium(II) complex chlorides to be isolated from aqueous solution were reported.[1] They comprise the red-violet hexahydrates $A^{I}VCl_3,6H_2O$ (A = Rb, NH_4) and the green dihydrate $CsVCl_3,2H_2O$. We have examined the spectral and magnetic properties of these compounds and their dehydrated forms and find unexpected structural effects.

The hydrated compounds exhibit the electronic spectra of d^3 ions in octahedral symmetry (see Table 1). However, comparison with the band positions reported[2,3] for vanadium(II) compounds of known structure, such as $VSO_4,7H_2O$ and VCl_2, leads to the conclusion that the co-ordination entity in the rubidium and ammonium salts is $[V(H_2O)^6]^{2+}$ whereas in the case of the caesium salt it is $[VCl_6]^{4-}$, with water being bound as hydrate water in the crystal lattice. In the latter

The Chemical Society

Burlington House London W1V OBN

TABLE 1

Reflectance spectra at room temperature

Complex	Observed bands and assignments ($^4A_{2g} \rightarrow$)			
	^2E, $^2T_{1g}$	$^4T_{2g}$	$^4T_{1g}$ (F)	$^4T_{1g}$ (P)
$[V(H_2O)]_6^{2+}$ in $VSO_4,7H_2O$[2]	—	12,000	17,800	27,800
$RbVCl_3,6H_2O$	11,000	12,000	18,000	27,200
$NH_4VCl_3,6H_2O$	11,000	12,200	18,000	27,600
$[VCl_6]^{4-}$ in VCl_2[3]	—	9000	14,000	21,500
$CsVCl_3,2H_2O$	10,900	9000	14,600	22,700
$RbVCl_3$	—	7300	13,200	21,900
		8900	14,000	24,200
		9700	14,900	25,600

instance the broadness and asymmetry of the spin-allowed absorption bands suggests that the symmetry is lower than octahedral. The influence of the cation on the nature of the species crystallizing from aqueous solution is thus very marked in this series.

The green, anhydrous compound $RbVCl_3$ was prepared by careful dehydration of $RbVCl_3,6H_2O$ at 100° under reduced pressure. The compound so prepared is identical with $RbVCl_3$ prepared by high-temperature methods. From Debye–Scherrer photographs the symmetry is hexagonal with $a = 7{\cdot}04 \pm 0{\cdot}01$ and $c = 6{\cdot}0 \pm 0{\cdot}01$ Å. The compound is formally isostructural with $CsNiCl_3$ ($a = 7{\cdot}18$, $c = 5{\cdot}95$ Å)[4] and hence a similar linear chain structure, with vanadium atoms symmetrically spaced and essentially octahedrally co-ordinated by chlorines but with a small trigonal distortion, could be inferred.

However, $RbVCl_3$ displays unusual spectral and magnetic properties which cannot be reconciled with this model. In the reflectance spectrum (Table 1 and Figure 1) each of the three spin-allowed bands is clearly split into three components. These splittings are quite large, of the order of 1000—2000 cm.$^{-1}$. This would appear to be the first reported instance in which such splittings have been observed in a d^3 complex. Small trigonal distortions in the related compounds

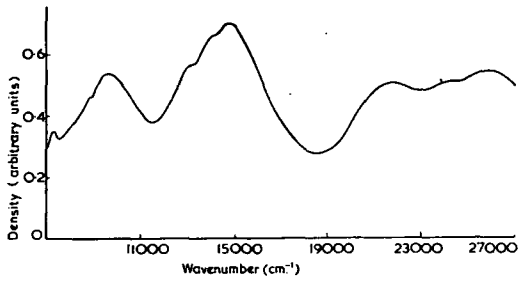

FIGURE 1. *Reflectance spectrum of* $RbVCl_3$ *(dehydrated).*

$(Me_4N)NiBr_3$[5] and $(Me_4N)NiCl_3$[6] have been reported to produce no measurable spectral effects.

Furthermore, in contrast to the hydrated compounds with normal paramagnetic behaviour (see Table 2), anhydrous $RbVCl_3$ is strongly antiferro-

TABLE 2

	μ_{eff} (300° K)	θ (° K)	J/k (° K)
$NH_4VCl_3,6H_2O$ ..	3·82	0	—
$RbVCl_3,6H_2O$ ..	3·82	0	—
$CsVCl_3,2H_2O$ ..	3·86	−11[a]	—
$RbVCl_3$	1·85	AFM	−151

[a] From $\chi'_A = c/(T + \theta)$.

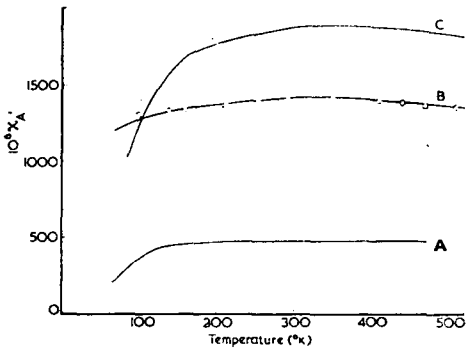

FIGURE 2. *Temperature dependence of magnetic susceptibility for* $RbVCl_3$ *(dehydrated).*
○ *Experimental points;* —— *theoretical curves for* (A) $N = 10$, $\theta = 0°$, $T_N = 330°$, (B) $N = 2$, $\theta = 136°$, $T_N = 350°$, (C) $N = 2$, $\theta = 0°$, $T_N = 350°$.

magnetic. As shown in Figure 2, the susceptibility passes through a maximum at approximately 330° K. Similar behaviour has been reported for $CsVCl_3$.[7] Our susceptibility data show wide divergences from theoretical values for simple linear chains[8] with a large number ($n = 10$) of interacting atoms [Figure 2 (A)]. On the other hand we have obtained excellent agreement [Figure 2 (B)] on the basis of a model which assumes dominant spin interaction between pairs of

atoms ($n = 2$) with secondary interaction between adjacent binuclear units. The latter effect is taken into account by modifying the susceptibility equation for interaction between pairs[9] to include the Weiss constant θ. This approach has been applied successfully in the case of $KCuBr_3$[10] which contains binuclear $[Cu_2Br_6]^{2-}$ units.

Finally, in the far-infrared two strong absorption bands centred at 310 and 260 cm.$^{-1}$ are exhibited. The bands are asymmetric and the higher-energy band has a shoulder at 317 cm.$^{-1}$. Very similar spectra have been observed for $CsCuCl_3$[11] and for the binuclear complexes $Al_3Mo_2Cl_9$,[12] where these absorptions are attributed to stretching vibrations of the metal–chlorine bonds associated with terminal and bridging chlorines, respectively.

Accordingly, we believe that the apparent anomalies in the properties of $RbVCl_3$ can be explained in terms of a linear-chain model in which the vanadium atoms are paired. The *X*-ray results quoted earlier are not in conflict with this since structure-factor calculations, taking trial values for the V–V distances of 2·75 and 3·25 Å (as compared with the symmetrical value of 3·0 Å), show that the effects on the positions and intensities of the 22 observed lines would be negligible. Single-crystal *X*-ray studies are in progress.

One of us (I.E.G.) acknowledges receipt of a Commonwealth Post-Graduate Scholarship.

(*Received, September 30th*, 1968; *Com.* 1341.)

[1] H. J. Seifert and B. Gerstenberg, *Z. anorg. Chem.*, 1962, **315**, 56.
[2] R. M. Bennett and O. G. Holmes, *Canad. J. Chem.*, 1960, **38**, 2319.
[3] R. J. H. Clark, *J. Chem. Soc.*, 1964, 417.
[4] G. N. Tishchenko, *Trudy Inst. Krist., Akad. Nauk S.S.S.R.*, 1955, **11**, 93.
[5] G. Stucky, S. D'Agostino, and G. McPherson, *J. Amer. Chem. Soc.*, 1966, **88**, 4828.
[6] D. M. L. Goodgame, M. Goodgame, and M. J. Weeks, *J. Chem. Soc.*, 1964, 5194.
[7] D. J. W. Ijdo, Thesis, Leiden, 1960.
[8] A. Earnshaw, B. N. Figgis, and J. Lewis, *J. Chem. Soc.* (*A*), 1966, 1656.
[9] A. Earnshaw and J. Lewis, *J. Chem. Soc.*, 1961, 396.
[10] M. Inove, M. Kishita, and K. Kubo, *Inorg. Chem.*, 1967, **6**, 900.
[11] D. M. Adams and P. J. Lock, *J. Chem. Soc.* (*A*), 1967, 620.
[12] I. E. Grey and P. W. Smith, unpublished.

Reprinted from the
AUSTRALIAN JOURNAL OF CHEMISTRY

STUDIES OF METAL HALIDES. MAGNETIC PROPERTIES OF SOME MOLYBDENUM(III) BINUCLEAR COMPLEX HALIDES

By I. E. GREY* and P. W. SMITH*

[Manuscript received July 29, 1968]

Summary

The variation of magnetic susceptibility with temperature for a number of binuclear halide complexes of molybdenum of formula $A_3^{I}Mo_2X_9$ (A = Cs, Et_4N, Et_3NH; X = Cl, Br) has been studied over the range 90–400°K. The magnetic behaviour is consistent with that expected for magnetically isolated exchange-coupled pairs of molybdenum atoms. The coupling is interpreted as occurring mainly by direct metal–metal interaction rather than superexchange.

Studies of the magnetic behaviour of binuclear complexes of the transition elements have been restricted almost exclusively to bivalent copper[1–3] and tervalent chromium and iron,[4–6] with oxygen or hydroxyl as the bridging ligand. Little is known of the mechanism by which the spins of the isolated pairs of metal atoms couple to give rise to the typical antiferromagnetic behaviour. Magnetic exchange has been variously attributed to predominantly direct metal–metal interaction or to superexchange through the bridging ligands.

A convenient system in which the mechanisms of spin–spin coupling can be investigated is one comprising binuclear complexes of formula $A_3^{I}M_2^{III}X_9$ (M = Cr, Mo, W; X = halogen). In these, pairs of $[MX_6]^{3-}$ octahedra share a face, allowing close approach of the two metal atoms with the possibility of direct metal–metal bonding.

The variation of magnetic susceptibility, χ'_A, with temperature for this type of complex has been given by Earnshaw and Lewis[4] as:

$$\chi'_A = \frac{K}{T}\left[\frac{42+15\exp(6x)+3\exp(10x)}{7+5\exp(6x)+3\exp(10x)+\exp(12x)}\right]+N(\alpha) \qquad (1)$$

where $K = g^2N\beta^2/3\mathbf{k}$ and $x = -J/\mathbf{k}T$.

The interaction between the two metal ions is represented by the exchange integral $-J$, $2J$ being the separation between the singlet and triplet states.

Only a few complexes of this series have been studied previously. The compound $(Et_4N)_3Cr_2Cl_9$ has a very small J value of $-5°$.[4] Although interatomic distances in

* Chemistry Department, University of Tasmania, P.O. Box 252C, Hobart, Tas. 7001.

[1] Kato, M., Jonassen, H. B., and Fanning, J. C., *Chem. Rev.*, 1964, **64**, 99.
[2] Lewis, J., Lin, Y. C., Royston, L. J., and Thompson, R. C., *J. chem. Soc.*, 1965, 6464.
[3] Ginsberg, A. P., Sherwood, R. C., and Koubek, E., *J. inorg. nucl. Chem.*, 1967, **29**, 353.
[4] Earnshaw, A., and Lewis, J., *J. chem. Soc.*, 1961, 396.
[5] Lewis, J., Mabbs, F. E., and Richards, A., *J. chem. Soc.* (*A*), 1967, 1014.
[6] Khedekar, A. V., Lewis, J., Mabbs, F. E., and Weigold, H., *J. chem. Soc.* (*A*), 1967, 1561.

this instance are not known, X-ray diffraction studies of the corresponding caesium salt show that the chromium atoms are displaced from the centres of the octahedra to give a relatively large Cr–Cr separation of 3·12 Å (compare 2·5 Å in the metal).[7] In $K_3W_2Cl_9$, however, in which the tungsten atoms are displaced towards each other to give a very short W–W distance of 2·409 Å[8] (cf. 2·741 Å in the metal), diamagnetism is observed.[9]

We report here the magnetic data on related tervalent molybdenum complexes[10] in which intermediate behaviour is observed.

Results

The experimental results from temperature-dependence studies on compounds of formula $A_3^{I}Mo_2^{III}X_9$ (A = Cs, Et_4N, Et_3NH, and X = Cl, Br) are listed in Table 1.

The effective moments at each temperature were calculated from the equation

$$\mu_{eff} = 2{\cdot}839\{[\chi'_A - N(\alpha)]T\}^{1/2} \qquad (2)$$

Interpretation of the data proved to be quite straightforward for the salts with organic cations, but for the two caesium salts it was not possible to prepare the complex completely free from paramagnetic impurity (the corresponding mononuclear complex[10]). The effect of the impurity on the susceptibility curve is shown by the increase in χ'_A with decreasing temperature below 150°K in the case of $Cs_3Mo_2Cl_9$ (Fig. 1). In this instance the calculated percentage impurity is 0·2%. However, it

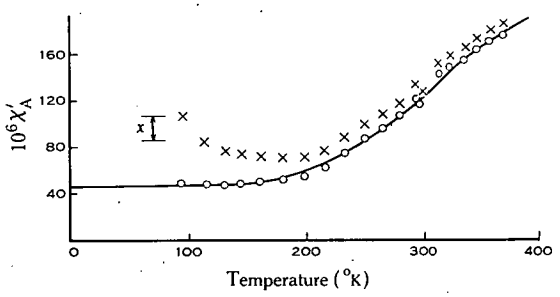

Fig. 1.—Temperature dependence of susceptibility for $Cs_3Mo_2Cl_9$.
× χ'_A (uncorr.);
○ χ'_A (corr.).
Curve calculated for
$J = -610$°K, $g = 1{\cdot}951$,
$N(\alpha) = 45 \times 10^{-6}$.

proved quite simple to correct for the paramagnetism. A theoretical curve derived from equation (1) using a reasonable value of $N(\alpha)$ and a value of $-J$ obtained from the high-temperature section of the experimental curve (where paramagnetic contribution is small) was found to be constant in χ'_A ($\pm 1 \times 10^{-6}$) below 130°K. Hence below this temperature the experimental susceptibilities could be treated as the resultant of the paramagnetic contribution plus a constant antiferromagnetic contribution.

Three simultaneous equations of the form

$$\chi_{T'} = \chi_T - x^* = C/(T' + \theta) \qquad (3)$$

[7] Wessel, G. J., and Ijdo, D. J. W., *Acta crystallogr.*, 1957, **10**, 466.
[8] Watson, W. H., and Waser, J., *Acta crystallogr.*, 1958, **11**, 689.
[9] Klemm, W., and Steinberg, H., *Z. anorg. allg. Chem.*, 1936, **227**, 193.
[10] Lewis, J., Nyholm, R. S., and Smith, P. W., unpublished data.

TABLE 1

MAGNETIC DATA

(χ in CGS units)

T (°K)	$10^6\chi'_A$ (uncorr.)	$10^6\chi'_A$ (corr.)	μ_{eff} (B.M.)
	$Cs_3Mo_2Cl_9$		
368·3	183·9	176·9	0·62
357·2	178·0	170·7	0·60
347·5	172·0	164·5	0·58
337·0	162·6	154·8	0·545
323·1	156·8	148·6	0·52
312·8	151·5	143·0	0·50
295·5	126·3	117·0	0·415
293·3	130·9	121·7	0·43
277·8	117·5	101·6	0·375
263·6	107·0	96·5	0·33
249·0	98·2	86·9	0·29
232·5	87·7	75·3	0·24
215·3	76·0	62·3	0·17
198·0	70·2	54·8	0·125
179·6	70·2	52·5	0·10
161·5	71·9	51·2	0·09
143·0	73·7	48·6	0·06
129·8	77·2	47·6	0·05
113·4	86·0	48·0	0·05
93·3	107·0	48·7	0·05
	$Cs_3Mo_2Br_9$		
295·8	285·7	264·5	0·52
277·8	267·2	244·2	0·46
263·5	252·5	227·9	0·42
249·1	246·9	220·4	0·375
232·5	226·7	197·6	0·30
215·3	215·6	183·3	0·24
198·0	206·3	169·8	0·18
179·4	200·8	158·5	0·11
159·8	204·6	153·7	0·07
147·0	208·2	149·6	0·00
129·8	226·7	153·2	0·06
113·4	248·8	151·5	0·04
97·0	294·9	155·0	0·03

T (°K)	$10^6\chi'_A$	μ_{eff} (B.M.)
	$(Et_3NH)_3Mo_2Cl_9$	
296·3	304·2	0·80
271·3	276·5	0·73
264·2	253·7	0·68
249·8	230·9	0·63
232·8	200·4	0·56
215·4	167·2	0·48
198·3	138·8	0·41
179·6	110·0	0·33
163·5	88·3	0·265
147·0	70·6	0·205
129·6	56·2	0·15
115·2	51·2	0·12
100·0	44·1	0·085
	$(Et_4N)_3Mo_2Cl_9$	
291·7	430·5	0·96
271·3	383·5	0·865
251·0	349·5	0·79
230·5	306·2	0·70
210·2	263·0	0·615
193·0	212·9	0·52
173·0	167·5	0·42
162·5	158·2	0·39
152·8	126·5	0·325
136·5	99·0	0·255
120·3	71·5	0·175
110·4	67·0	0·155
98·0	67·0	0·15
	$(Et_4N)_3Mo_2Br_9$	
293·3	728·4	1·09
277·8	711·4	1·04
260·2	674·6	0·965
249·9	653·4	0·92
226·0	604·4	0·83
200·5	541·9	0·71
182·3	496·1	0·625
163·3	442·1	0·53
153·7	396·6	0·455
146·7	388·4	0·43
131·8	322·0	0·31
119·5	305·5	0·27
114·5	284·7	0·225
98·0	264·0	0·16
90·5	255·8	0·14

where $\chi_{T'}$, the susceptibility of the paramagnetic species at temperature T' ($< 130°K$) and x^*, the susceptibility difference (see Fig. 1), were solved for C and θ. The values of C and θ were then used in equation (3) to calculate the susceptibility of the paramagnetic impurity at temperatures over the range 90–300°K, and the experimental susceptibility was corrected by subtracting the impurity susceptibility. The corrected susceptibilities, χ' (corr.), are given in Table 1. The values of C and θ for the caesium salts are listed in Table 2, together with the estimated percentage of paramagnetic impurity.

TABLE 2

VALUES OF C, θ, AND PARAMAGNETIC IMPURITY IN CAESIUM SALTS

Compound	10^6C	θ (°K)	Impurity (%)*
$Cs_3Mo_2Cl_9$	2191	−56	0·2
$Cs_3Mo_2Br_9$	4938	−63	0·4

* This was estimated at 95°K on the assumption of a Curie law behaviour with μ_{eff} 3·87 B.M.

This correction procedure was not required for the tetraethylammonium salts, which could be prepared free from impurity as demonstrated by the close agreement between experimental and calculated susceptibility values shown in Figure 2.

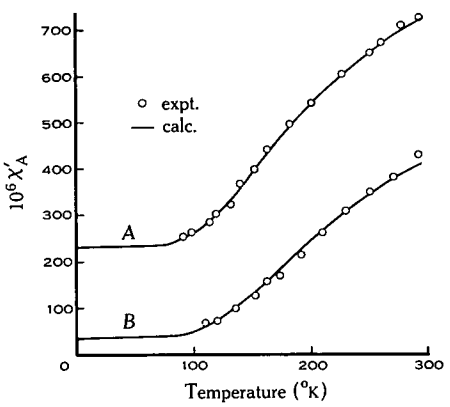

Fig. 2.—Temperature dependence of susceptibility.
A, $(Et_4N)_3Mo_2Br_9$, calculated curve for $J = -310°K$, $g = 2·10$, $N(\alpha) = 230\times10^{-6}$;
B, $(Et_4N)_3Mo_2Cl_9$, calculated curve for $J = -345°K$, $g = 1·956$, $N(\alpha) = 40\times10^{-6}$.

The calculation of the theoretical susceptibility curves using equation (1) was simplified by substituting g values available from powder e.s.r. measurements on the complexes.[11] The problem reduced to a least-squares fit including two variables, J and $N(\alpha)$. Approximate values of $N(\alpha)$ were obtained from extrapolation of the experimental curves to $T = 0°K$. These initial values were then adjusted in steps of 5×10^{-6}, recalculating J until the best fit of equation (1) to the experimental results was achieved.

[11] Boyd, P. D. W., Smith, P. W., and Wedd, A. G., unpublished data.

In Table 3 final values of g, $-J$ (actually $-J/\mathbf{k}$, in °K), $N(\alpha)$, and T_{max} ($= -J/0{\cdot}324$) are listed. The limits of error are calculated on the basis of a precision of measurement of weight change of $\pm 0{\cdot}01$ mg, an average change being about 2 mg. Due allowance was made for packing errors as estimated from duplicate determinations.

TABLE 3
MAGNETIC PARAMETERS
($N(\alpha)$ in CGS units)

Complex	$-J$ (°K)	g	$10^6 N(\alpha)$	T_{max} (°K)
$Cs_3Mo_2Cl_9$	605 ± 10	1·951	45	1867
$(Et_3NH)_3Mo_2Cl_9$	415 ± 10	2·010	35	1281
$(Et_4N)_3Mo_2Cl_9$	345 ± 9	1·956	40	1065
$Cs_3Mo_2Br_9$	555 ± 10	1·995	150	1713
$(Et_4N)_3Mo_2Br_9$	310 ± 8	2·011	230	957

DISCUSSION

Two trends are apparent from a study of the data in Table 3, namely (i) the magnitude of the exchange integral, $-J$, increases as the size of the cation decreases, and (ii) $-J$ increases as the size of the ligand decreases (bromide to chloride).

In order to examine further the first trend it is necessary to refer to the crystal structure of these compounds. The three-dimensional structure of $Cs_3Mo_2Cl_9$ has been investigated[12] and the molecular structure of the binuclear entity has been established as being more closely related to the tungsten than to the chromium analogous species. X-ray powder photographs of $Cs_3Mo_2Br_9$ and $(Et_4N)_3Mo_2X_9$ (X = Cl, Br) show that these compounds are isostructural with the caesium salt and have hexagonal unit cells. The unit cell parameters for these compounds are given in Table 4. The remaining compound studied, $(Et_3NH)_3Mo_2Cl_9$, has a powder photograph which cannot be indexed simply on a hexagonal cell and hence this compound is not considered in the following discussion.

TABLE 4
UNIT CELL PARAMETERS FOR COMPLEXES $A_3Mo_2X_9$

Compound	a (Å)	c (Å)
$Cs_3Mo_2Cl_9$	$7{\cdot}346 \pm 0{\cdot}003$*	$17{\cdot}506 \pm 0{\cdot}014$
$(Et_4N)_3Mo_2Cl_9$	$10{\cdot}085 \pm 0{\cdot}008$	$22{\cdot}45 \pm 0{\cdot}03$
$Cs_3Mo_2Br_9$	$7{\cdot}644 \pm 0{\cdot}005$	$18{\cdot}350 \pm 0{\cdot}02$
$(Et_4N)_3Mo_2Br_9$	$10{\cdot}298 \pm 0{\cdot}008$	$23{\cdot}13 \pm 0{\cdot}03$

* Uncertainties to two standard deviations.

The packing of the cations around the $M_2X_9^{3-}$ units as found in $Mo_2Cl_9^{3-}$, $Cr_2Cl_9^{3-}$, and $W_2Cl_9^{3-}$ is illustrated in Figure 3. It can be seen that an increase in the size of cations B, which pack between the metal pairs in the plane of the bridging halogens, should result in a forcing apart of the metal atoms with consequent decreased magnetic interaction. One cannot make any assumptions on the nature of the

[12] Smith, P. W., and Wadsley, A. D., unpublished data.

exchange from this observation, as an increased M–M distance may or may not result in an increased M–X–M distance.

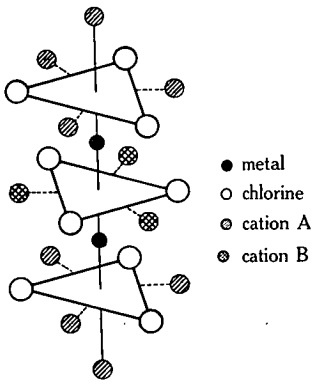

Fig. 3.—Packing of cations around the $[Mo_2X_9^{3-}]$ unit.

However, it is found also that increasing the size of the ligand decreases the exchange integral $-J$. For complexes in which magnetic exchange takes place by a superexchange mechanism it has been observed that the bromides have lower moments than the corresponding chlorides. For example, the Curie–Weiss constant increases from $CsNiCl_3$ to $CsNiBr_3$,[13] indicating greater antiferromagnetic interaction for the latter, even though the Ni–Ni distance also increases (2·97 Å to 3·12 Å). For the complexes studied, the decrease of $-J$ from the chloride to the bromide is evidence which is suggestive of direct metal–metal bonding. This is further supported by the short Mo–Mo distance, *c.* 2·7 Å found for $Cs_3Mo_2Cl_9$,[12] which is comparable with that observed in the metal (2·73 Å). In $[Mo(OPh)_3Cl_2]_2$, which contains binuclear Mo^V–Cl_2–Mo^V groups, the Mo–Mo distance is 2·8 Å and a direct metal–metal bond is postulated, the compound being virtually diamagnetic.[14] However, in the dimeric molecule Mo_2Cl_{10} which also has Mo^V–Cl_2–Mo^V bonding, the Mo–Mo distance is much larger, 3·84 Å,[15] and the susceptibility is of the order of 20 times greater than that for the phenoxide.

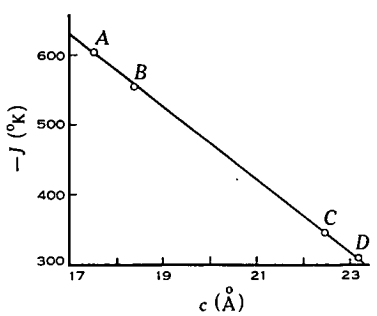

Fig. 4.—Lattice parameter *c* against exchange integral.
A, $Cs_3Mo_2Cl_9$;
B, $Cs_3Mo_2Br_9$;
C, $(Et_4N)_3Mo_2Cl_9$;
D, $(Et_4N)_3Mo_2Br_9$.

In the isostructural compounds, the $Mo_2X_9^{3-}$ units are aligned parallel to the *c* axis of the unit cell. It could be thus argued that the Mo–Mo distance would be

[13] Stucky, G., D'Agostino, S., and McPherson, G., *J. Am. chem. Soc.*, 1966, **88**, 4828.
[14] Mitchell, P. C. H., and Williams, R. J. P., *J. chem. Soc.*, 1962, 4570.
[15] Sands, D. E., and Zalkin, Z., *Acta crystallogr.*, 1959, **12**, 723.

approximately proportional to the length of the *c* axis. With this approximation duly considered, Figure 4 indicates a linear relationship between the *c* parameter and the magnetic exchange interaction, for the four isostructural complexes. This relationship is further evidence for direct metal–metal interaction being the major mechanism for spin coupling. For a superexchange mechanism it would be expected that the points for the bromides and chlorides be non-collinear. However, the preceding discussion does not rule out the possibility of superexchange occurring.

Further information on some of these points may be obtained from an extension of a theoretical treatment[16] now in progress.

Experimental

Preparations

All preparative operations were conducted either under vacuum or under an inert (nitrogen) atmosphere. The caesium salts were prepared as described elsewhere.[10]

$(Et_4N)_3Mo_2Cl_9$.—Addition of half the required amount of Et_4NCl,H_2O in dry ethanol to a viscous molybdenum(III) chloride solution precipitated the complex immediately. It was washed with ethanol and dried to give an orange powder (Found: C, 31·7; H, 6·95; Cl, 35·4; Mo, 21·6; N, 4·5. $C_{24}H_{60}Cl_9Mo_2N_3$ requires C, 32·0; H, 6·7; Cl, 35·4; Mo, 21·3; N, 4·7%).

$(Et_4N)_3Mo_2Br_9$.—Acid molybdenum(III) chloride solution (35 ml; 10% w/v) was evaporated to dryness and hydrobromic acid solution (15 ml; 50% w/w) added. The solution was stirred for 4 hr and then evaporated. This process was repeated a number of times. The solution, now a deep purple-red, was evaporated almost to dryness and the cation added as for the corresponding chloride. The dried compound was light brown in colour (Found: C, 22·2; H, 4·7; Br, 55·0; Mo, 14·9; N, 2·55. $C_{24}H_{60}Br_9Mo_2N_3$ requires C, 22·2; H, 4·65; Br, 55·25; Mo, 14·7; N, 3·2%).

$(Et_3NH)_3Mo_2Cl_9$.—This salt was prepared by the addition of approximately half the required amount of Et_3NHCl, dissolved in a small volume of concentrated hydrochloric acid, to a concentrated molybdenum(III) chloride solution. After evaporation to near dryness, ethanol was added. Dark red-brown crystals of the complex precipitated. These were washed repeatedly with ethanol and dried under vacuum (Found: C, 25·75; H, 6·0; Cl, 38·95; Mo, 23·65; N, 5·1. $C_{18}H_{48}Cl_9Mo_2N_3$ requires C, 26·45; H, 5·9; Cl, 39·0; Mo, 23·6; N, 5·15%).

Magnetic Measurements

Magnetic susceptibilities were measured between 90° and 400°K by the Gouy method. The general design of the apparatus employed closely follows that of Figgis and Nyholm.[17] A 4-in. Newport Type A magnet was employed in conjunction with a Stanton centre-zero Type SM12 balance. The equipment was calibrated with $CoHg(SCN)_4$ and temperatures were measured with a calibrated copper–constantan thermocouple. The dependence of susceptibility on magnetic field strength was checked at 3300 and 5770 oersteds; all measurements reported were made at 5770 oersteds. Diamagnetic corrections were made in accordance with standard values.[18]

X-ray Measurements

A Hägg–Guinier focusing powder camera was employed, with potassium chloride as an internal calibrant, using the procedure described elsewhere.[19]

Acknowledgment

One of us (I.E.G.) acknowledges receipt of a Commonwealth Postgraduate Scholarship.

[16] Smith, P. W., Stoessiger, R., and Wedd, A. G., *Theor. chim. Acta*, 1968, **11**, 81.

[17] Figgis, B. N., and Nyholm, R. S., *J. chem. Soc.*, 1959, 331.

[18] Lewis, J., and Wilkins, R., "Modern Coordination Chemistry." (Interscience: New York 1960.)

[19] Grey, I. E., and Smith, P. W., *J. scient. Instrum.*, 1968, [2] **1**, 693.